The Pennsylvania State University

The Graduate School

Department of Energy and Mineral Engineering

NUMERICAL MODEL REPRESENTATION OF MULTI-STAGE HYDRAULICALLY FRACTURED HORIZONTAL WELLS LOCATED IN SHALE GAS RESERVOIRS USING NEURAL NETWORKS

A Thesis in

Energy and Mineral Engineering

by

Kanin Bodipat

Submitted in Partial Fulfillment
of the Requirements
for the Degree of

Master of Science

May 2012

The thesis of Kanin Bodipat was reviewed and approved* by the following:

Turgay Ertekin
Professor of Petroleum and Natural Gas Engineering
Thesis Advisor

Ronald J. Briggs
Assistant Professor of Energy and Environmental Economics

Li Li
Assistant Professor of Petroleum and Natural Gas Engineering

Larry R. Grayson
Professor of Energy and Mineral Engineering
Graduate Program Officer of Energy and Mineral Engineering

*Signatures are on file in the Graduate School

ABSTRACT

Numerical representation of hydrocarbon reservoirs has seen increase usage and sophistication due to recent surge in demands for unconventional hydrocarbon resources. Unlike the conventional fields most oil companies are familiar with; these unconventional fields often require special recovery techniques that significantly elevate the project size and funds required.

One of the popular recovery method used that has proven highly successful is hydraulic fracturing combined with horizontal wells. Sometimes referred to as “frac job”, this process has seen extensive use in US shale gas reservoirs that were in the past regarded as non-recoverable sources.

Due to the effectiveness of fracturing shale combined with horizontal wellbore, several reservoir models have been proposed to represent how these techniques would affect the characteristics of the reservoir. The particular model used in this thesis is the “crushed zone” model that represents the effect of multiple stages of hydraulic fracturing as an elliptical shape around the horizontal well that sees an increased in fracture permeability and smaller fracture spacing.

To study the validity of this particular reservoir representation an artificial neural-network (ANN) is created using production data generated from a commercial simulator. This first network is then used to predict production performances over a period of 50 years. A second network is then required to establish a quantitative relationship between the crushed zone model and another hydraulic fracturing model called the “transverse fracture” model. In addition, an error filter neural network has been created to improve upon the predictions of the second network.

The results of the network were all within the expected ranges and the ANN can then be used to predict new gas rates and equivalent transverse fracture representations for any reservoir that has its characteristics within the range of the training data

.

TABLE OF CONTENTS

LIST OF FIGURES

LIST OF TABLES

Nomenclature

Artifical Neural Network	ANN
Computer Modelling Group Commercial Simulator	CMG
US Energy Information Administration	EIA
Millidarcy	mD
Langmuir Volume	V_L
Langmuir Pressure	p_L
Linear Transfer Function	*purelin*
Log-Sigmoid Transfer Function	*logsig*
Hyperbolic Tangent Sigmoid Transfer Function	*tansig*
Scaled conjugate gradient backpropagation	*trainscg*
conjugate gradient backpropagation with Fletcher-Reeves updates	*traincgf*
Constant specified pressure	p_{sf}
Reservoir edge length	edge_l
Thickness	h
Depth	D
Compressibility of Formation	cf
Matrix Permeability	k_m
Fracture Permeability	kf
Natural Fracture Spacing	nfsp
Reservoir Temperature	Ti
Initial Reservoir Pressure	pi
Block Size	B
Horizontal Wellbore Length	HWl

Crushed Zone Minor Axis Length	a_{minor}
Crushed Zone Permeability	$k_{f,cz}$
Gas flow rate at specified time x	q_x
Eigen-value	λ
Cumulative Gas Production	CGP
Hydraulic Fracture Spacing	HFsp
Fracture Half Length	xf
Hydraulic Fracture Permeability	k_{hf}
Gas flow rate from commercial simulator	$\mathrm{q_{com}}$
Gas flow rate predicted by ANN	$\mathrm{q_{ANN}}$
Cumulative Gas Production in Percentage	CGP_{error}
Cumulative Gas Production predicted by ANN	CGP_{ANN}

ACKNOWLEDGEMENTS

First and foremost I would like to thank my professor and advisor Dr. Turgay Ertekin for his intellectual weekly meetings and the invaluable advices and knowledge I obtained from his classes. I also deeply appreciate the efforts of Nithiwat Siripatrachai who provided some sample data for my research as well as plenty of knowledge sharing during the meetings with Dr. Ertekin. In addition, I would also like to thank my colleague from Thailand, Pichit Vardcharagosad who was like a mentor in many of the classes I took at Penn State. Finally, thanks must also go to the department and Penn State for the facilities and resources as well as my sponsor, PTT Exploration and Production PLC for providing me with the financial support and this unique opportunity to pursue a graduate degree at this prestigious university.

Chapter 1

Introduction

As we enter the second decade in the new millennium, the global demand in energy has reached a record high. With the rapid economic expansions in China and India, combined with the nuclear debacle in Japan, the Petroleum industry is burdened with the responsibility to provide both sufficient and green energy to the masses.

One solution that has proven especially popular in North America is the exploration and production of shale gas. Previously thought to be uneconomical and not commercially feasible source of hydrocarbons, recent technological developments in drilling and well-stimulations have seen some media sources like the Calgary Herald predicting that shale gas could power half the US's natural gas supply by 2020.

A critical stage in the development of a shale gas field is the reservoir simulation process. This is where numerical models are used to predict production and plan how the field is developed. The numerical representation of a hydrocarbon reservoir (Reservoir Simulation) has seen increase usage and sophistication due to recent surge in demands for unconventional hydrocarbon resources. Unlike the conventional fields most oil companies are familiar with; these unconventional fields often require special recovery techniques that significantly elevates the project size and funds required. Decisions such as the number of wells, their locations, optimal completions and needs to stimulations and artificial lifts are made throughout the field's life using simulation as a guide.

During this decision making process, questions such as "What type of reservoir will produce this particular amount of gas" will arise. This is where Artificial Neural Networks (ANN) come into play; they help speed up the long arduous task of simulating for many different scenarios. Instead of having to make 100 different simulation runs, with each run taking from anywhere as long as 1 minute to a few days (depending on the number of blocks), a “trained” ANN can predict the 100 simulation run results in fraction of a second.

Chapter 2 and chapter 3 aim to acclimatize the readers with the problem statement and fundamental materials involving reservoir simulation, shale gas reservoir, hydraulic fracturing and artificial neural networks. In chapter 4 the methods of approached used in generating data and training the neural networks will be discussed step-by-step. Chapter 5 discusses the results and findings of this research. Finally, chapter 6 includes a conclusion and summary of all chapters.

Chapter 2

Problem Statement

In the industry, there is a need for oil companies to obtain information before investing in a gas field. For an unconventional field such as a shale gas field, it is especially critical that some expected performance information on the hydraulic fracturing job is obtained beforehand. Questions such as “How many hydraulic fracturing stages are needed?”, “How deep is the penetration?”, “How large is the spacing between each hydraulic fractures?” These questions are easily answered if the oil company has a transverse fracture model in their simulators. Unfortunately, many companies utilize the crushed zone model instead, which brings about the needs to form an equivalency between the two models.

It would also be of great convenience if the gas rate of the crushed zone model can be acquired instantly without having to create a new simulation run using a commercial simulator every time a new set of data is obtained. This is because each run by a commercial simulator may take up to hours or days to create and compiled, a whole batch of runs would take up quite a lot of time, while a trained neural network would be able to predict a similar set of results in a fraction of a second.

Based on the two problems stated above, the objective of this thesis is to create two Artificial Neural Networks (ANN) based on the Crushed Zone Model:

1) Production Performance ANN

   This ANN needs to be able to receive any input that contains reservoir parameters along with crushed zone design characteristics and return an output in predicted gas production rate over the period of 50 years

2) Equivalency ANN

The equivalency network predicts an equivalent transverse model design characteristics based on the given reservoir characteristics and crushed zone design parameters.

List of inputs and outputs for the two ANNs will be discussed in chapter 4.

Chapter 3

Literature Review

Unconventional Reservoir& Shale Gas

The term ‘unconventional resources’ is a dynamic term that refers to resources, or in this case, reservoirs that are difficult to produce from. As technology and energy prices change, the difficulty of extracting resources from these unconventional reservoirs may change as well. These resources are of great interest to the industry due to its vast amount of reserves and diminishing production of conventional resources. The US Energy Information Administration (EIA) estimates that by the year 2030 unconventional sources will make up 56% of total domestic production and shale gas alone already accounts for 47% of US natural as production.

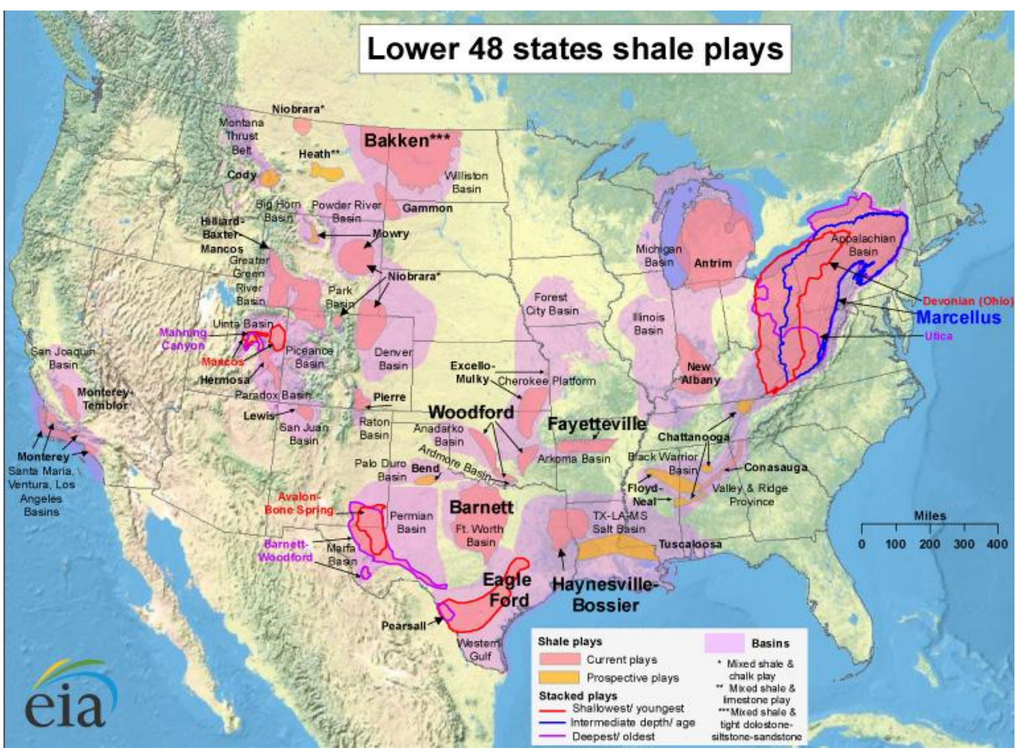

Figure 3-1: Shale Gas Plays in Lower 48 States of the USA

(U.S. Energy Information Administration, 2011)

Figure 3-1 shows that there is a substantial amount of shale gas plays in the US scattered across most regions outside the coastlines.

Shale gas is basically natural gas recovered from shale reservoirs previously thought to be uneconomical to recover.

Figure 3-2: Shale Rock (Westbroek, G. Utah State Office of Education, 2005)

Figure 3-2 portrays a shale rock, a sedimentary rock composed mostly of consolidated clay-sized particles, hence the description "Organic-rich and fine-grained" by Bustin, 2006. Shale was previously thought of as merely source rocks and seals due to the extremely low permeability on the order of 0.1 to 0.00001 mD. In addition, the structurally sheet-like and laminated layers results in even lower vertical permeability. Shale matrix consists of clay minerals, quartz, pyrite, and organic matter. Most of the gas is then adsorbed into these organic matters and trapped within the pore spaces of the fine-grained clays. However, in addition to being stored as free gas in the matrix pore, gas can also be stored as free gas in the natural fractures and as adsorbed gas on the rock surface. The adsorption and desorption in shale is governed by a curve called the Langmuir Isotherm. This isotherm can be described by two parameters: Langmuir Volume (V_L), the maximum gas content at infinite pressure and the Langmuir Pressure (p_L), the pressure at which half that gas exists within the shale. p_L and $V_L$are intrinsic properties of the rock and varies from shale to shale. From Figure 3-3, it is clear that as pressure decreases due to production, more gas content is desorbed (ΔV_L - shown as green line) from the shale. It is also observed that the lower the pressure the more gas is released.

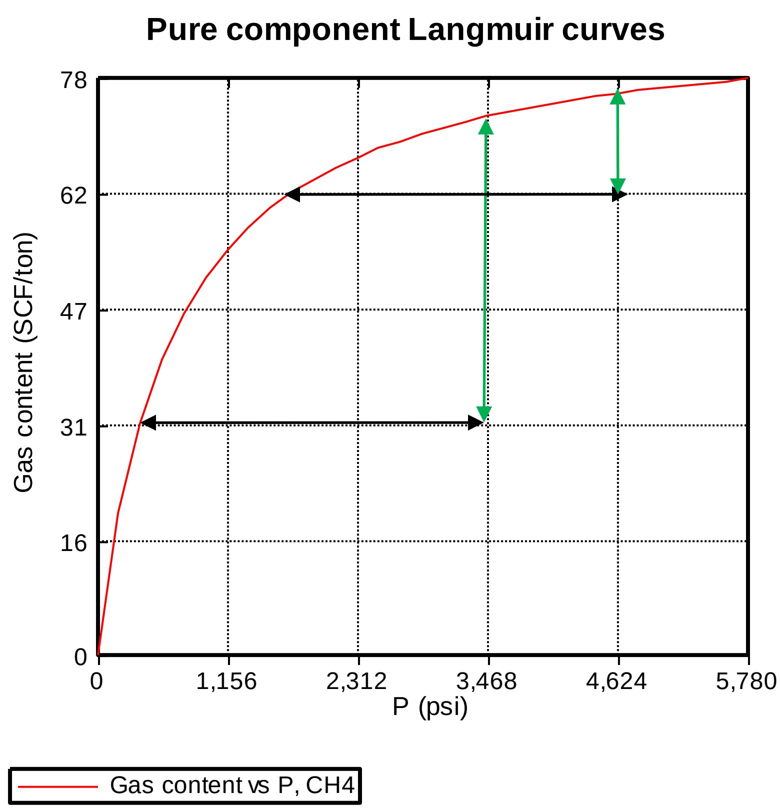

Figure 3-3: Langmuir curve showing increased desorption as pressure decreases.

Due to its dual-porosity nature, shale has a unique production mechanism:

Two step process shown in Figure 3-4:

1.) As pressure decreases, gas is released from the surface of the primary-porosity (fine pores) => diffuses through the matrices to the fractures
2.) Gas from fractures are then transported via Darcy flow to the wells

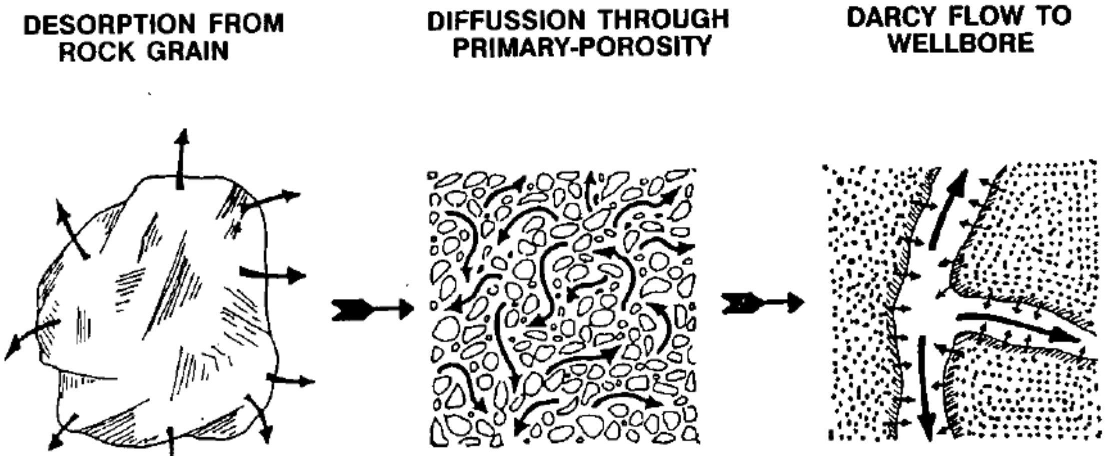

Figure 3-4 - Diagrams illustrating transport of gas through coal seam/shale gas reservoirs (Remner, D. J., T. Ertekin, W. Sung, G. R. King, November 1986)

Shale also has a dual-porosity nature with values ranging from 2 to 15% according to SPE-124253-MS by F.P. Wang and R.M. Reed, 2009. Chemically, most shale gas (90%) are methane, some are wet gas.

Due to the extremely low vertical permeability and sheet-like structure of shale, horizontal wells and hydraulic fracturing techniques are required to extract gas efficiently from shale reservoirs. These topics are discussed in the next two sections.

Horizontal Wells

A horizontal well, as shown in Figure 3-5,is a well that has been drilled vertically at first, but after reaching a certain point the direction is changed to horizontal. The EIA has established the definition of directional drilling as follows:

“Horizontal drilling is the process of drilling and completing, for production, a well that begins as a vertical or inclined linear bore which extends from the surface to a subsurface location just above the target oil or gas reservoir called the "kickoff point," then bears off on an arc to intersect the reservoir at the "entry point," and, thereafter, continues at a near-horizontal attitude tangent to the arc, to substantially or entirely remain within the reservoir until the desired bottom hole location is reached”

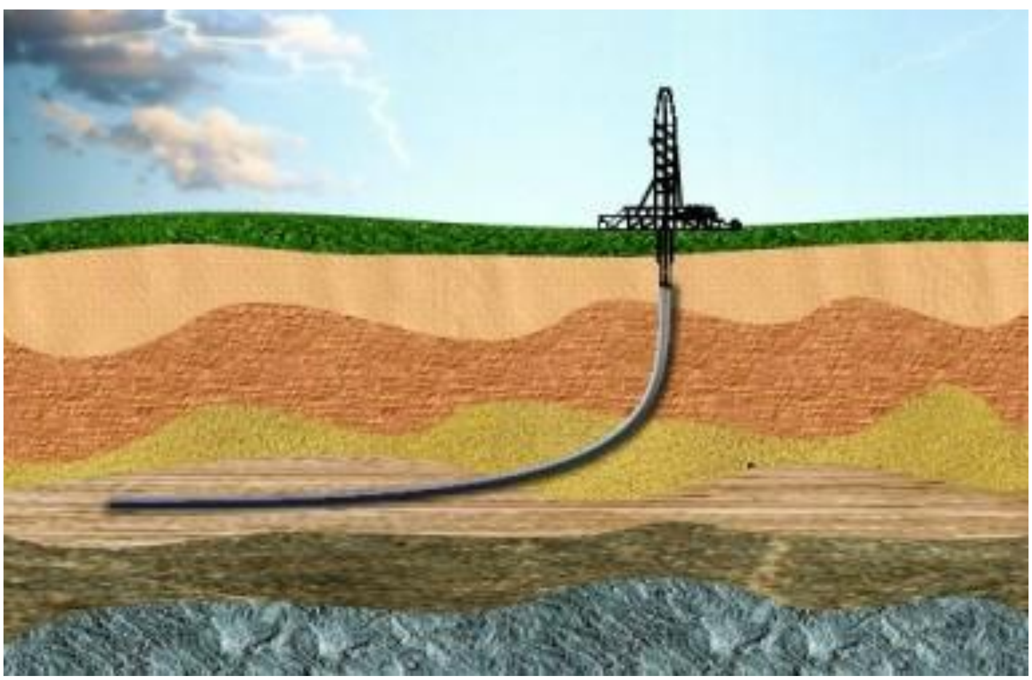

Figure 3-5–Horizontal Well (Oil and Gas Evaluation Report, 2011)

Due to the nature of shale which exhibits very low vertical permeability and the ability of a horizontal well to cover a larger section of the pay-zone, horizontal well is one of the two break-through techniques that allow shale gas to be economically recovered.

Horizontal wells also have the following benefits:

- Crucial for areas where number of wells are limited (protected forestry, cities)
- Allows greater reach, up to 8,000 feet of lateral length.
- Allows greater flexibility and coverage, as shown in Figure 3-6
- Old vertical wells can be modified to become horizontal wells
- Intersects natural fractures, thus providing extra pathways for gas flow

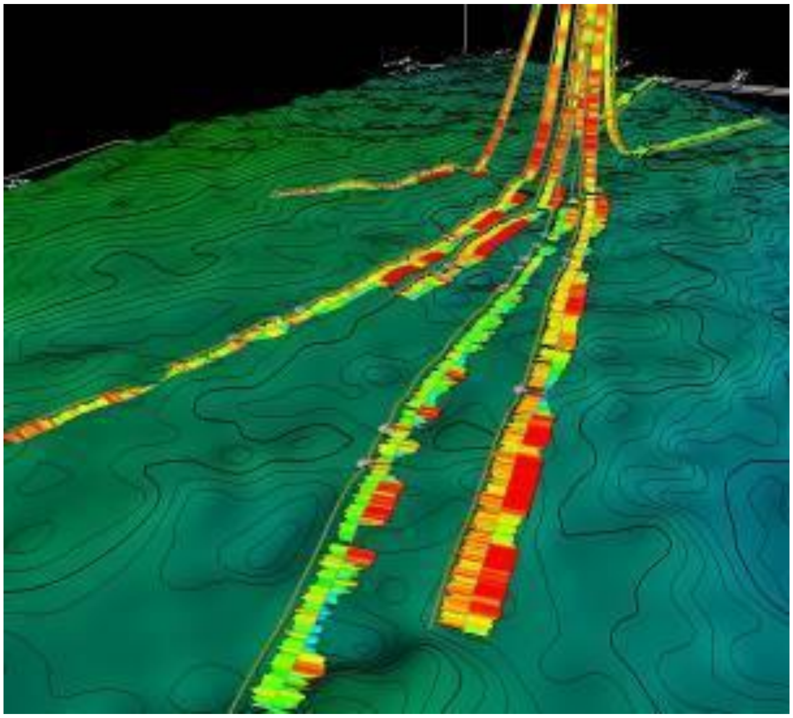

Figure 3-6–Horizontal Wells shown in 3D to display greater reach and coverage of the reservoir (AGM Inc., 2010)

Hydraulic Fracturing

Hydraulic fracturing is a well stimulation technique that involves injecting high pressured chemically-enhanced water/sand slurry into the formation in order to create artificial fractures in the target area. The Figure 3-7 shows a simplistic view of which part of the well is targeted for fracturing.

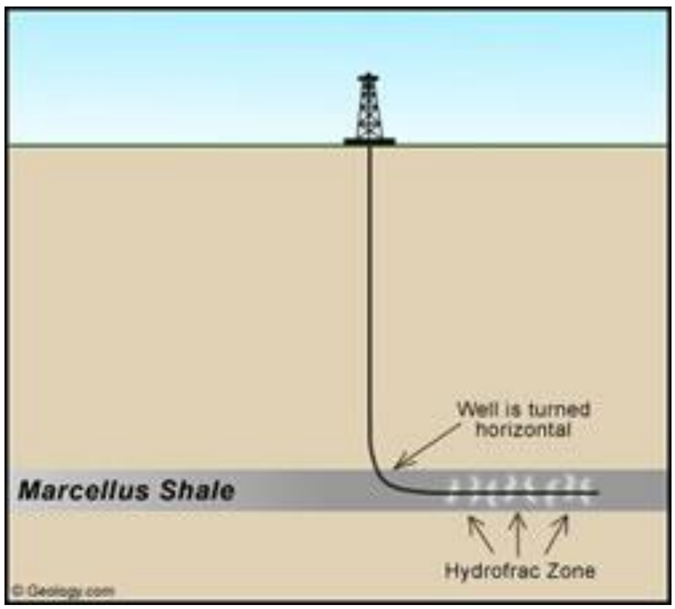

Figure 3-7–Hydrofrac (hydraulic fracturing) Zone (Brad Cole, Geology.com)

The processes involved in hydraulic fracturing are as follows:

- Pumper trucks transports water to the site
- Water is mixed with components such as proppants – particles mixed into water to hold fractures open after hydraulic fracturing has been applied.

- Fracture fluid is then injected at high pressure into the formation at the targeted zones
- This increases the size of fractures and may also create more fractures and may also crush the rocks within the target area
- Geophones are used to measure the effectiveness of the job by listening to micro seismic events occurring near targeted hydrofrac zones

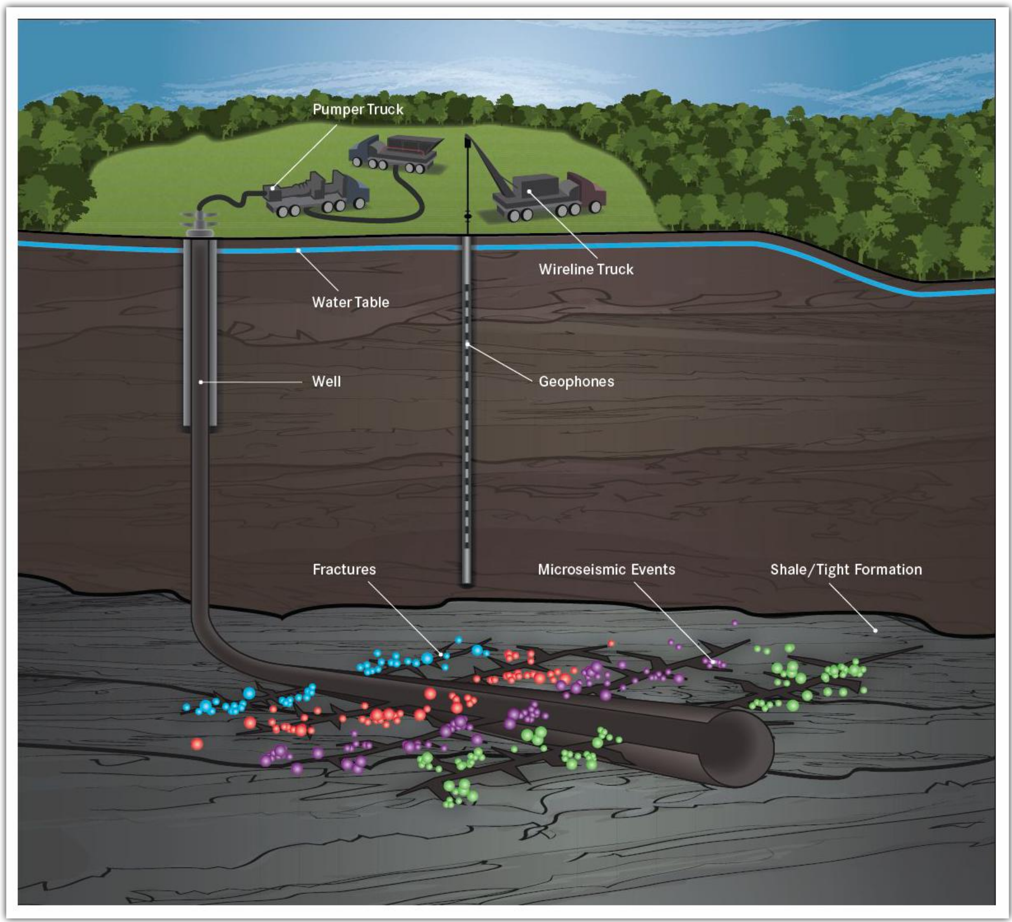

Figure 3-8–Events and Components of a Hydraulic Fracturing Job (ESG Solutions, 2011)

Modeling Hydraulic Fracturing

Hydraulic Fracturing is done in stages and is usually visually represented as fractured planes perpendicular to the horizontal well. Numerical models that contain these fracture planes are called the "transverse fracture" model. Figure 3-9 shows microseismic monitoring data that gauges the seismic activities near the sensors, allowing us to clearly see strips of highly fractured rocks in the blue and purple bubbles. However, in the same figure, the yellow bubbles show that the effects of some fracture may be more extensive than just a simple plane and seems to form a somewhat elliptical-shaped zone around the wellbore.

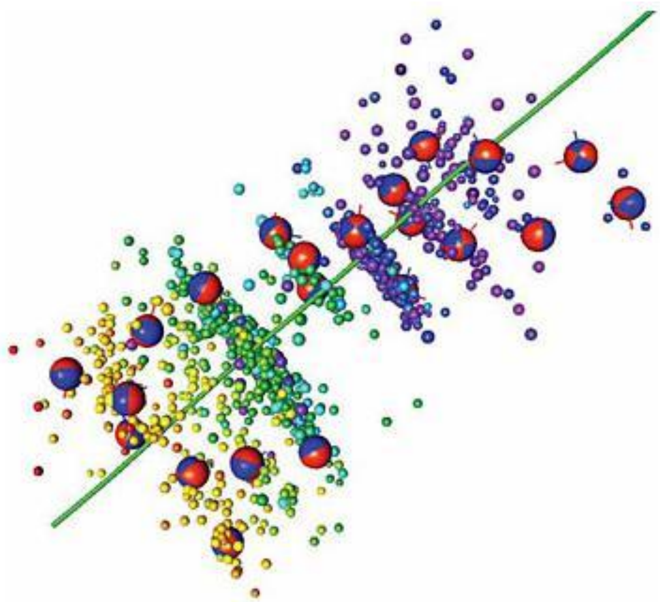

Figure 3-9–Microseimic Data – Transverse Fracture (CGGVeritas)

As more microseismic data are collected, it became clear that a highly fractured zone of rock bearing an elliptical shape is also a valid representation of the reservoir after it has been hydraulically fractured. Figure 3-10 provides further evidence of this so-called "crushed zone".

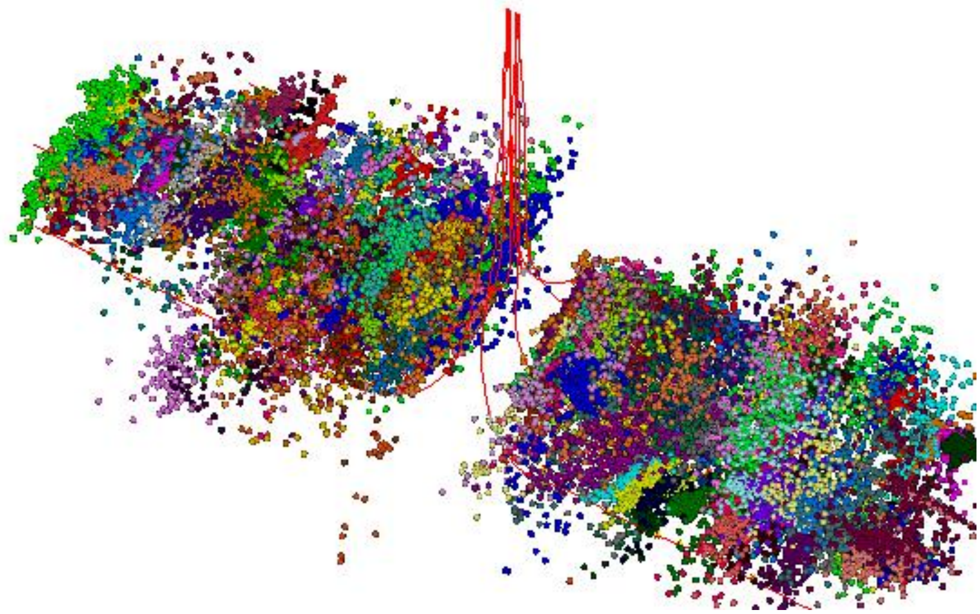

Figure 3-10–Microseimic Data – Crushed Zone (ESG solutions)

Artificial Neural Network

Artificial Neural Network (ANN) is a non-linear statistical modeling tool that is based on real-life biological neural networks like the human brain. An ANN can be compared directly with biological networks that consist of synapses, soma and axon as input, transfer function and output respectively. The ANN toolbox chosen for this project is the MathWork's MATLAB Neural Network Toolbox.

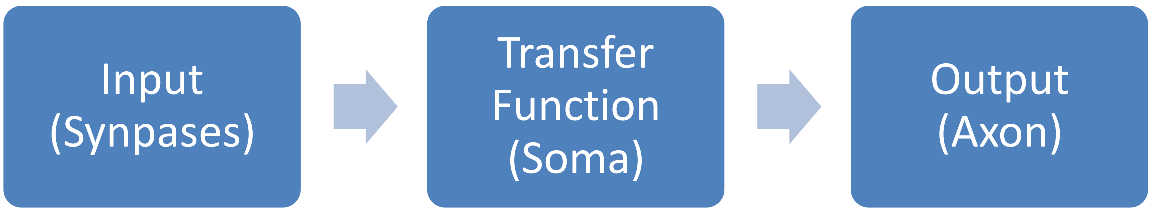

Figure 3-11–Simplified Overview of the ANN

Figure 3-10 shows a simplified overview, process-by-process diagram of an artificial neural network that will be used in this thesis. In the following section we will go into detail on what the input, transfer function and output in an ANN will contain.

Input

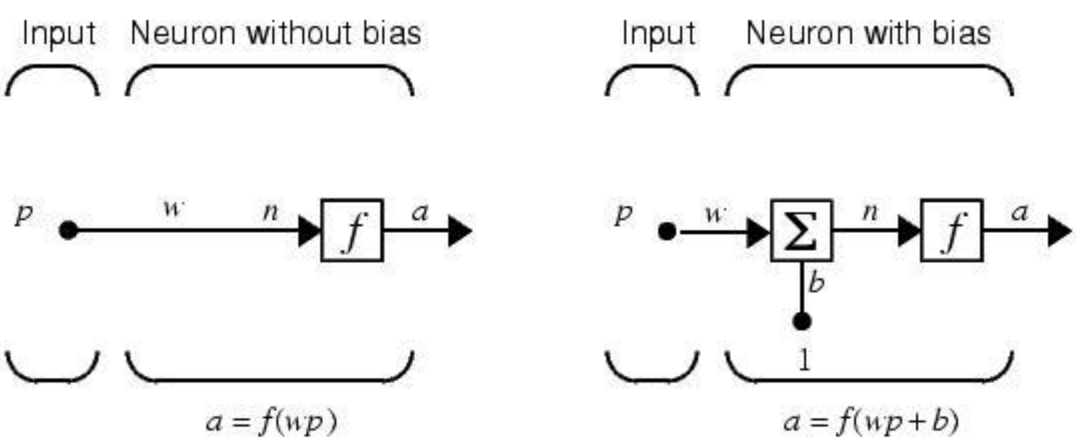

Figure 3-12–Simple Neuron: without bias & with bias (MATLAB Neural Network User Guide, 2011)

Inputs in MATLAB's ANN toolbox are not just simply passed through straight into the transfer function, they are "weighted" and "biased" through the training process and/or controlled by user. The weight is multiplied by the scalar *w*, representing the importance of that particular input, while the bias *b* is also similar but it always has an input of 1. After these weights and biases are established through rigorous training, the network will become much more capable of identifying key inputs.

Transfer Function

Transfer functions, also called activation functions, adjust the input using the specified type of function and then sends it to the output. Although 14 transfer functions exist within MATLAB's ANN toolbox, through past experiences with ANN, only the three most effective for this type of project were chosen:

- Linear Transfer Function (*purelin*)

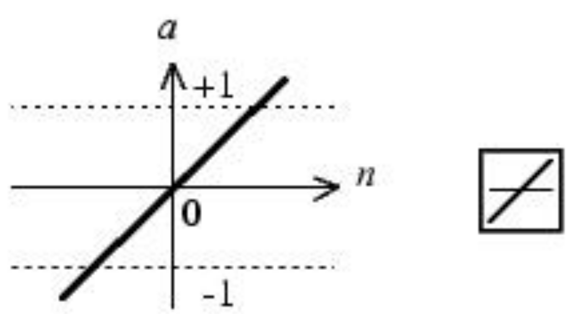

Figure 3-13–Linear Transfer Function (MATLAB Neural Network User Guide, 2011)

One of the most simple transfer function represented by $f(y) = k * y$ (k is a constant)

- Log-Sigmoid Transfer Function (*logsig*)

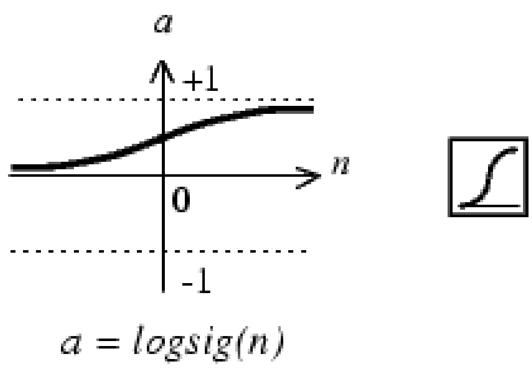

Figure 3-14–Log-Sigmoid Transfer Function (MATLAB Neural Network User Guide, 2011)

The log-sigmoid function can be represented by $f(y) = \frac{1}{1+e^{y}}$. It basically takes any input and compresses the output within the range of 0 to 1.

- Hyperbolic Tangent Sigmoid Transfer Function (*tansig*)

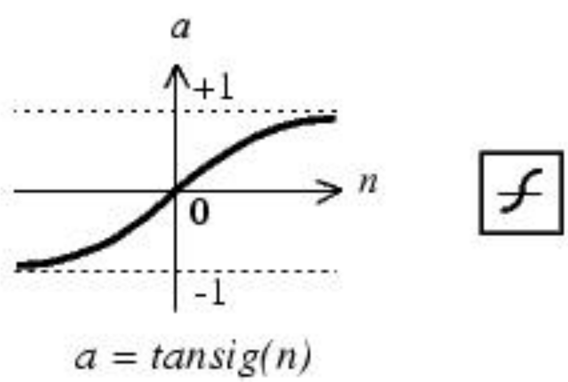

Figure 3-15–Tan-Sigmoid Transfer Function (MATLAB Neural Network User Guide, 2011)

The tan-sigmoid transfer function can be represented by $(y) = \frac{e^{y} - e^{-y}}{e^{y} + e^{-y}}$. This function has an output range between -1 and 1.

Feed-Forward Networks and Training Algorithms

The network used in training all the ANN in this thesis is the feed-forward backpropagation network. This network adjusts its weight and biases as data is sent through and the error is propagated back. According to MATLAB these networks have one-way connections from input to output layers. They are most commonly used for prediction, pattern recognition, and nonlinear function fitting. The two network training function used in this thesis are the scaled conjugate gradient backpropagation (trainscg) and the conjugate gradient backpropagation with Fletcher-Reeves updates (traincgf). The trainscg updates its weight and biases based on the conjugate gradient method while the traincgf also uses the conjugate gradient method but with Fletcher-Reeves updates.

Over learning and the Early Stopping Method

Over learning or memorization is the process where the network begins to memorize the instead of generalizing. This makes the network inflexible and may struggle to adapt to new data sets. The early stopping method is designed to alleviate this problem by dividing the data set randomly into three parts: 1) Training 2) Validation 3) Testing. Once the training has started, the validation curve has to be monitored carefully, and as soon as it begins to increase, the training should be stopped.

Note that the validation curve may incur some local minima where the curve increases temporarily. Therefore user must pay attention not to stop the run at this stage and wait for the curve to increase permanently or in other words: at the global minima. These concepts are shown in Figure 3-15, with orange circles showing local minima and purple circles showing the global minima.

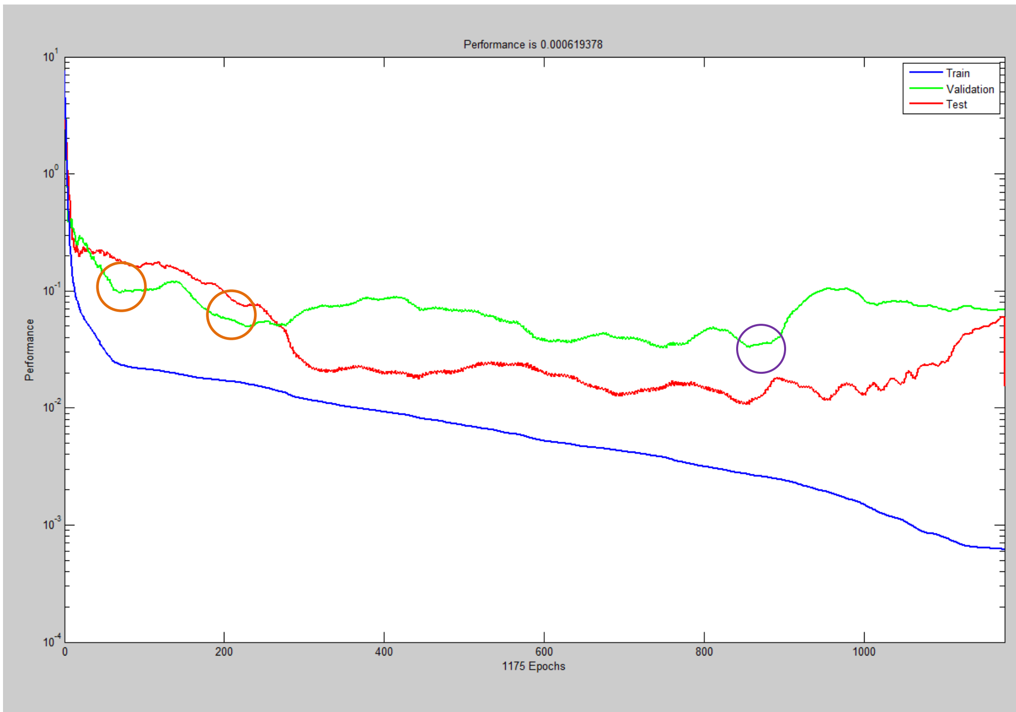

Figure 3-16–Sample ANN Training Record showing local and global minima

training early at the first or second orange circle, however, this is too early and better network performance can be achieved if the user waits until the validation curve rises permanently first. This is because at the end of those two points, the validation curve only increases momentarily and the global minima is yet to come. At the purple circle, it is clear that this is the global minima because the validation curve does not decrease significantly after that point.

Chapter 4

Methods of Approach

Using all the concepts introduced in the literature review from Chapter 3, this chapter discusses the development of the three artificial neural networks: production performance network, equivalency network and the equivalency error-filter network. However, before the data sets, reservoir models and network structures can be formed, we must first establish common reservoir parameters, conditions and constraints for all models:

Reservoir Characteristics for all models:

- Homogeneous and isotropic
- Square shape
- Variable grid size and shape
- Methane only with minimal residual water
- One horizontal well with fixed length of 60% of reservoir length
- Well located at the center of the reservoir
- Constant specified pressure (p_{sf})
- Dual-porosity, single permeability
- Fracture permeability > matrix Permeability
- Fracture porosity < matrix porosity
- Production period of 50 years

Generating data sets for the production performance ANN

This section describes the methods of approach used in generating the data sets used in training the production performance artificial neural network. A MATLAB script is written to automatically make batch-runs of the crushed zone model that will be described in the following section.

Crushed Zone Model

The crushed zone model is created based on the equation of the ellipse, shown along with a diagram in Figure 4-1. The major axis is set to equal the well length, while the minor axis is variable.

$$\frac{x^2}{{a_{major}}^2} + \frac{y^2}{{a_{minor}}^2} = 1$$

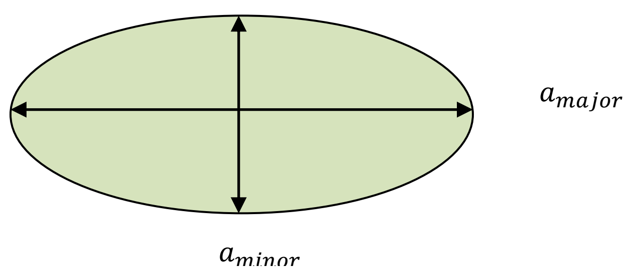

Figure 4-1–Ellipse equation and model

In order to create a numerical model using the commercial simulator as shown in Figure 4-2, the ellipse equation in Figure 4-1 had to be applied to control the shapes of the crushed zone. In this study, the major axis is fixed at 60% of the reservoir length, which, as mentioned above, is the same length as the horizontal wellbore. The minor axis, however, has a flexible range as indicated in Table 4-1.

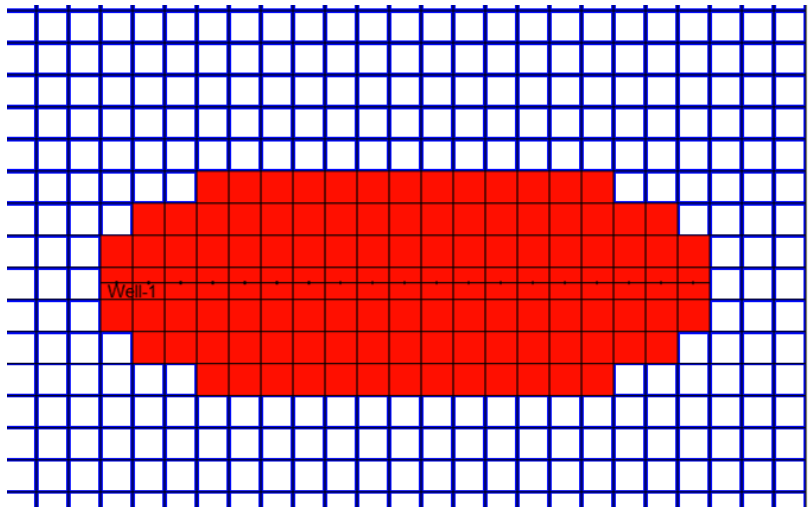

Figure 4-2–Crushed Zone Representation in numerical model used

Table 4-1–Reservoir Characteristics and Crushed Zone Design Parameters

Parameter	**Minimum Value**	**Maximum Value**	**Unit**
Reservoir edge length (edge_l)	1475	3614	ft
Thickness (h)	50	300	ft
Depth (D)	1000	15000	ft
Compressibility of Formation (cf)	5×10-6	8×10-6	1/psi
Matrix Permeability (k_m)	10-7	0.01	md
Fracture Permeability (kf)	0.0001	0.2	md
Matrix Porosity (m)	2	16	%
Fracture Porosity (f)	0.1	3	%
Natural Fracture Spacing (nfsp)	1	40	ft
Reservoir Temperature (Ti)	130	300	˚F
Initial Reservoir Pressure (Pi)	3,000	8,000	psi
Langmuir Pressure (PL)	200	800	psi
Langmuir Volume (VL)	50	200	scf/ton
Block Size(B)	59	144	ft

Horizontal Wellbore Length (HWl)	900	2168	ft
Crushed Zone Minor Axis Length (aminor)	361	1192	ft
Crushed Zone Permeability (kf,cz)	0.1	10	md
Specified Pressure (P_{sf})	14.7	4014.7	psi

Since the crushed zone is an elliptical area that is extensively fractured, the properties within that are is also altered. In this study, the parameters that are assumed to have been altered are the crushed zone permeability ($k_{f_{cz}}$) and the crushed zone minor axis length (a_{minor}).

Collecting & Filtering Results

In order to quantitatively collect crushed zone numerical model run results, 19 gas rates are collected as outputs for the production performance ANN. This is done using the numerical simulator's report program which saves the results as a text file. Another code is then written to export these text files into an excel worksheet. In addition, the data must be filtered so that realistic results are ensured. In order for the network to predict realistic results, realistic must be used to train the network, therefore gas rate maximums were established as follows:

1.) Initial gas rate at t = 1 day must not exceed 15MMSCF
2.) Final cumulative production must not exceed 15BCF

Work Flow

All inputs and outputs are generated using a generalized procedure and can be summarized as shown in figure 4-3:

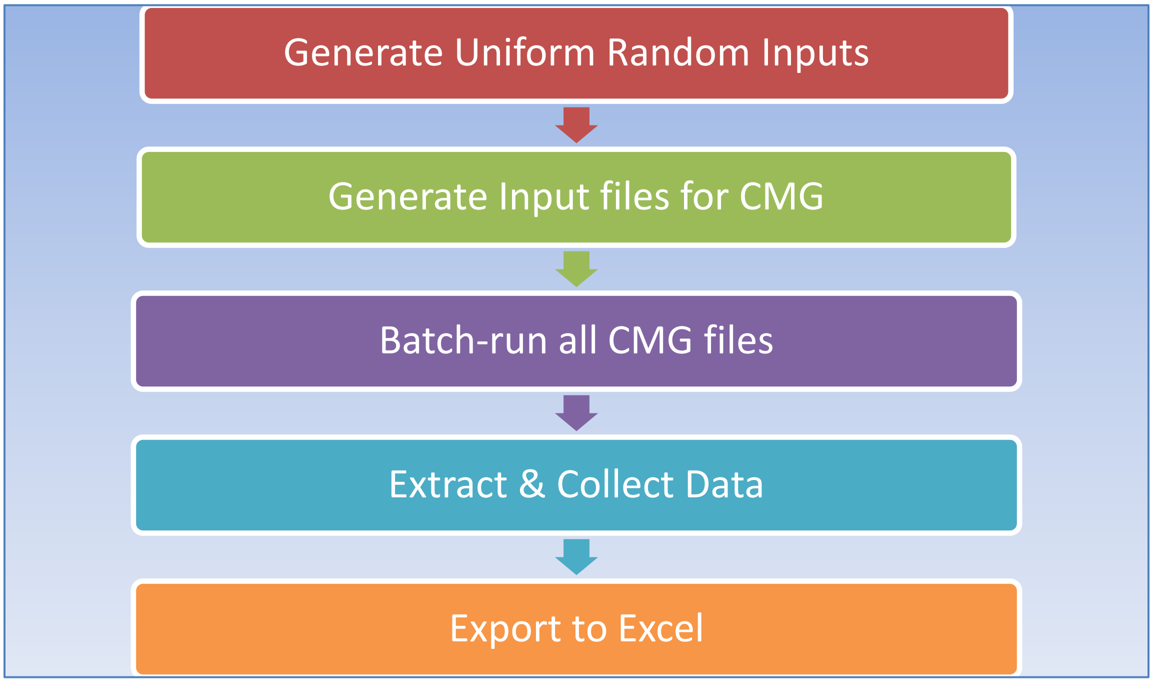

Figure 4-3–Procedure for Generating Data Sets

Training the ANN

In the development of the neural network, the training process, also known as learning process is the first step towards the success of the network. The network will ever only be as accurate as the data set it was trained it. Therefore, extra effort must be made to generate data that are accurate, realistic and varied. All the data generated are located in appendix B.

First ANN - Production Performance ANN

In the previous section we have established the range of reservoir characteristics, crushed zone design parameters and 19 gas rates as in the inputs and outputs for the network. After having acquired 597 realistic runs using the simulator, the data were then exported to excel where two text files were generated called “Input.txt” and “Output.txt”. The Input.txt file is then fed into the

ANN as input while the Output.txt will serve as the output of the network. Figure 4-4 shown below is used to familiarize the reader with the structure of the ANN and the concept of nodes and layers. In this example, the network contains 2 input nodes, 2 hidden layers with 4 and 3 neurons respectively and 1 output node. Since the complexity of the network is directly proportional to the complexity of the system it tries to predict, the network used in this study will require several more components than is shown in this figure

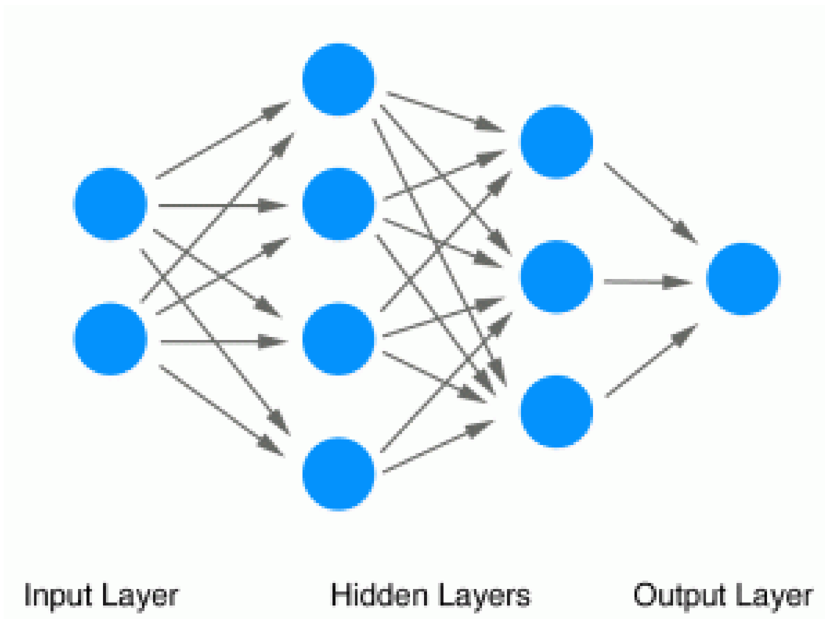

Figure 4-4–Example configuration of the neural network (Morten M., 2009)

It is evident from previous studies at the Pennsylvania State University (Nithiwat S., 2011, Ihsan K., 2010) that a neural network of a petroleum reservoir with as many as 20-30 inputs and outputs respectively, would almost certainly require a more complex neural network than what was shown in Figure 4-4. In those studies, one of the key components is the functional links which have proved to be exceptional in improving the accuracy of the network. This is especially true if the links are physically meaningful in terms of petroleum engineering like permeability-thickness (k-h). The Tables 4-2 and 4-3 below gives an initial configuration as we start the network:

Table 4-2– Initial input parameters used in the production performance ANN

Inputs	
Reservoir characteristics:	edge_l,h, c_f, k_m, k_f, $_m$, $_f$, nf_{sp}, T_i, P_i, P_L, V_L,
Crushed zone design parameters:	a_{major}, $k_{f,cz}$, p_{sf}

Table 4-3– Initial output parameters used in the production performance ANN

Outputs	
Gas Rates:	q_1, q_{180}, q_{360}, q_{540}, q_{720}, q_{900}, q_{1080}, q_{1440}, q_{1800}, q_{2160}, q_{2520}, q_{2880}, q_{3240}, q_{3600}, q_{5400}, q_{7200},q_{10800}, q_{14400}, and q_{18000}

Gas Rate Selection

Gas rates at specific times within the period of 50 years were picked as q1, q180, q360, q540, q720, q900, q1080, q1440, q1800, q2160, q2520, q2880, q3240, q3600, q5400, q7200, q10800, q14400, and q18000. The subscripts refer to the number of days since the first day of production, while the q refers to gas rate. Previous study at the Pennsylvania State University (Nithiwat S., 2011) has shown that early gas rates are difficult for the ANN to predict, therefore more gas rates were extracted during this period. More information on predicting early gas rates will be discussed in the results section in Chapter 5.

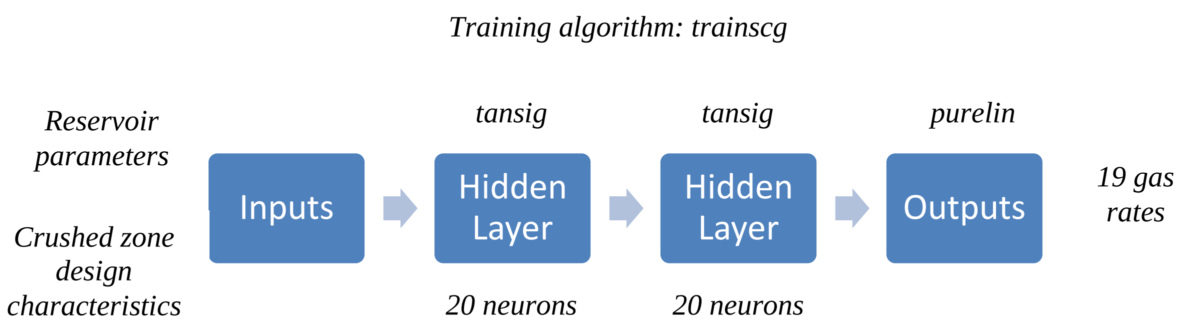

Figure 4-5– Initial configuration of the production performance ANN

Using the inputs from Table 4-2 and outputs from Table 4-3 and the network configuration in Figure 4-5, the first ANN was trained. After just several hundreds of epochs, it was clear that this small network could not handle the complexity of predicting such a complicated system. The following guideline serves to aid users in the process of training an ANN:

The nature of training the ANN is a heuristic process, there are rule of thumbs such as the formula Neuroshell (1998) proposed:

$$No.of\ Hidden\ Neurons = \frac{No.of\ Inputs + No.of\ Outputs}{2} + \sqrt{No.of\ Sets}$$

Starting with this rule of thumb, the network can be adjusted in the following ways in order to try to improve its performances:

1.) Adjust network type

2.) Adjust training and learning algorithm

3.) Adjust number of hidden layers

4.) Adjust number of neurons in each hidden layers

5.) Add or remove functional links

6.) Switch functional links from input to output and vice versa

In general, for a complex system such as gas rate predictions and model equivalencies, a relatively higher number of hidden layers and number of neurons are required. According to Ramgulam et al. (2006), functional links may prove essential in improving performances as well. These functional links varies from products or ratios of a few inputs to maximum eigen-values (λ), special scalars that are directly associated with the parameters in their corresponding matrix. In the MATLAB code the eigen-value function was used to calculate the two eigen-values of a two by two matrix. Then the “max” function was used to identify one maximum value out of those two eigen-values. The maximum eigen-values used in the production performance ANN are the following:

λ_1 is the maximum eigen-value calculated from the following matrix

$$\begin{bmatrix} kf_{cz} & \mathrm{a_{minor}} \\ \mathrm{Psf} & \mathrm{kf} \end{bmatrix}$$

λ_2 is the maximum eigen-value calculated from the following matrix

$$\begin{bmatrix} q_1 & \mathrm{CGP} \\ \mathrm{P_i} & \mathrm{k_f} \end{bmatrix}$$

λ_3 is the maximum eigen-value calculated from the following matrix

$$\begin{bmatrix} q_1 & \mathrm{kf_{cz}} \\ \mathrm{a_{minor}} & \mathrm{CGP} \end{bmatrix}$$

λ_4 is the maximum eigen-value calculated from the following matrix

$$\begin{bmatrix} T_i & \mathrm{P_i} \\ \mathrm{P_L} & \mathrm{V_L} \end{bmatrix}$$

Note that CGP stands for Cumulative Gas Production.

Based on the above guideline, further attempts were made to improve the capabilities of the network. The Tables 4-4 and 4-5 lists the inputs and outputs of this new network:

Table 4-4– New input parameters used in the production performance ANN

Inputs	
Reservoir characteristics:	B,h, c_f, k_m, k_f, ϕ_m, ϕ_f, nf_{sp}, T_i, P_i, P_L, V_L,
Crushed zone design parameters:	a_{minor}, k_{fcz}, p_{sf}
Functional links	λ_1, B/h, k_{m*h},k_{f*h}, B*h*D, CGP

Table 4-5– New output parameters used in the production performance ANN

Outputs	
Gas Rates:	q_1, q_{180}, q_{360}, q_{540}, q_{720}, q_{900}, q_{1080}, q_{1440}, q_{1800}, q_{2160}, q_{2520}, q_{2880}, q_{3240}, q_{3600}, q_{5400}, q_{7200},q_{10800}, q_{14400}, and q_{18000}
Functional links:	λ_2 , λ_3, λ_4, D/psf, a_{minor}*B,

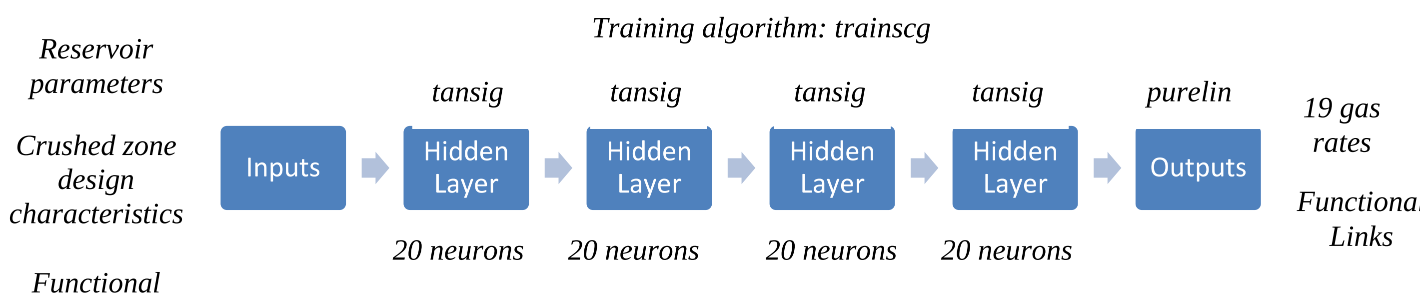

Figure 4-6– New configuration of the production performance ANN

More information on the how to measure and analyze the results will be discussed in the next chapter. However, even with this new configuration and the additional of several functional links, the result of 24% overall average accuracy were still not within the acceptable range of 10%, therefore the network must be tweaked even further.

Table 4-6 shows the final production performance ANN inputs; an additional maximum eigen-value λ_5 was also added:

$\lambda_5$is the maximum eigen-value calculated from the following matrix

$$\begin{bmatrix} kf_{cz} & a_{minor} \\ P_L & V_L \end{bmatrix}$$

Table 4-6 – Final input parameters used in the production performance ANN

Inputs	
Reservoir characteristics:	B, h, c_f, k_m, k_f, ϕ_m, ϕ_f, nf_{sp}, T_i, P_i, P_L, V_L,
Crushed zone design parameters:	a_{minor}, k_{fcz}, P_{sf}
Functional links:	λ_1, λ_4, λ_5, B/h, k_m*h, k_f*h, B*h*D, CGP, D/Psf, a_{minor}*B

Table 4-7 – Final output parameters used in the production performance ANN

Outputs	
Gas Rates:	q_1, q_{180}, q_{360}, q_{540}, q_{720}, q_{900}, q_{1080}, q_{1440}, q_{1800}, q_{2160}, q_{2520}, q_{2880}, q_{3240}, q_{3600}, q_{5400}, q_{7200},q_{10800}, q_{14400}, and q_{18000}
Functional links:	λ_2 , λ_3

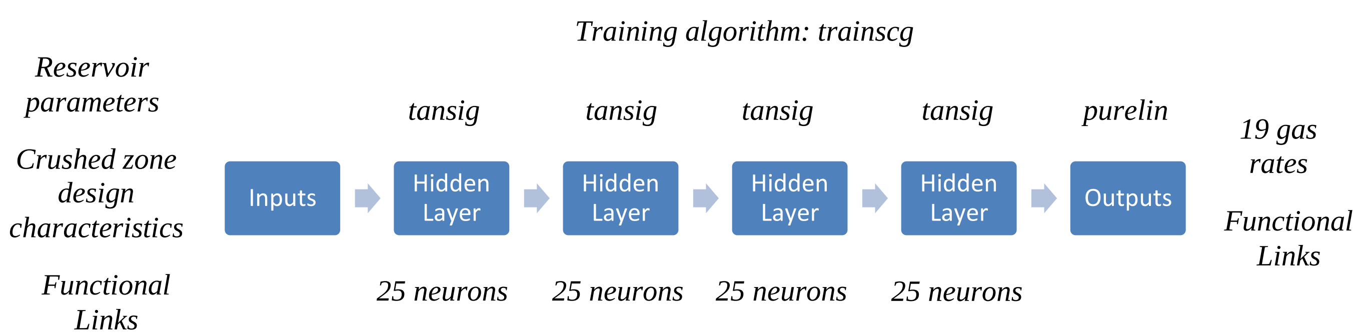

Figure 4-7– Final configuration of the production performance ANN

In the final configuration of the production performance ANN that achieved a 12% overall average accuracy, several tweaks were made to the input shown in Table 4-6. First all the regular functional links plus λ_4 were moved from output to input. In addition λ_5 was added to link the relationship between crushed zone design characteristics and the Langmuir constants. With these extra functional links, 5 more neurons were added to each hidden layer as shown in Figure 4-6.

Second ANN - Equivalency ANN

The equivalency ANN differs from the production performance ANN because its objective is to predict an equivalent transverse fracture representation as oppose to gas flow rates. In order to train the second ANN, a transverse fracture model was created using the same procedure as the crushed zone model with the list of reservoir parameters shown in Table 4-1. However, the crushed zone design characteristics are now replaced by the transverse fracture design characteristics listed in Table 4-8 below:

Table 4-8–Design Characteristics of the Transverse Fracture Model

Parameter	Minimum Value	Maximum Value	Unit
Hydraulic Fracture Spacing (HFsp)	100	300	ft
Fracture Half Length (xf)	100	850	ft
Hydraulic Fracture Permeability (khf)	10	106	md

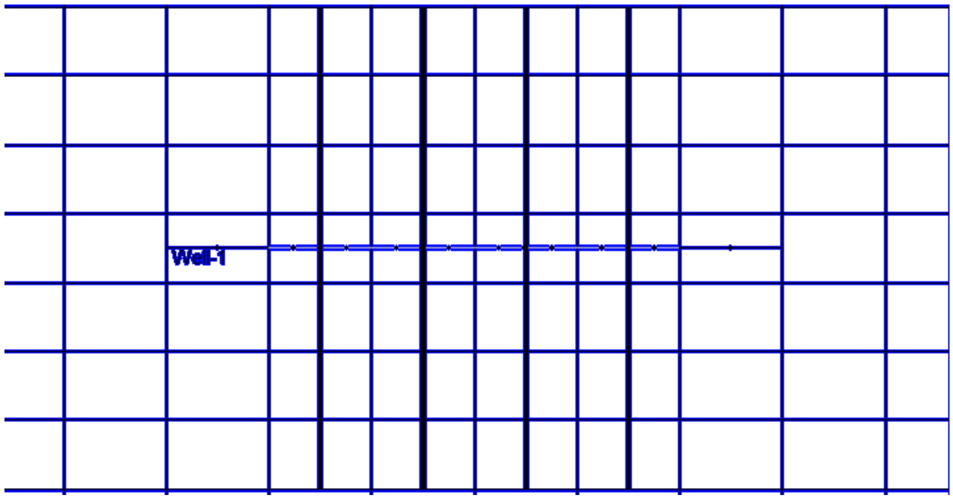

Figure 4-8–Transverse Fracture Representation using the commercial simulator

Figure 4-5 shows how a transverse fracture model looks like in the numerical simulator; the bold vertical lines are tiny strips of high permeability pathways of width 0.05 ft. Each strip represents one stage of hydraulic fracturing.

In order to generate a match, the reservoir characteristics of the previous crushed zone runs are used and a MATLAB script is written to make 20 Transverse Fracture Model runs per 1 Crushed Zone runs. The twenty runs are then compared with the crushed zone run using “Results” CMG program as shown in Figure 6-5 below. In the case that none of the 20 runs match, a new batch of 20 new runs are made. This process is repeated until a match is obtained, giving us a total of 317 matches.

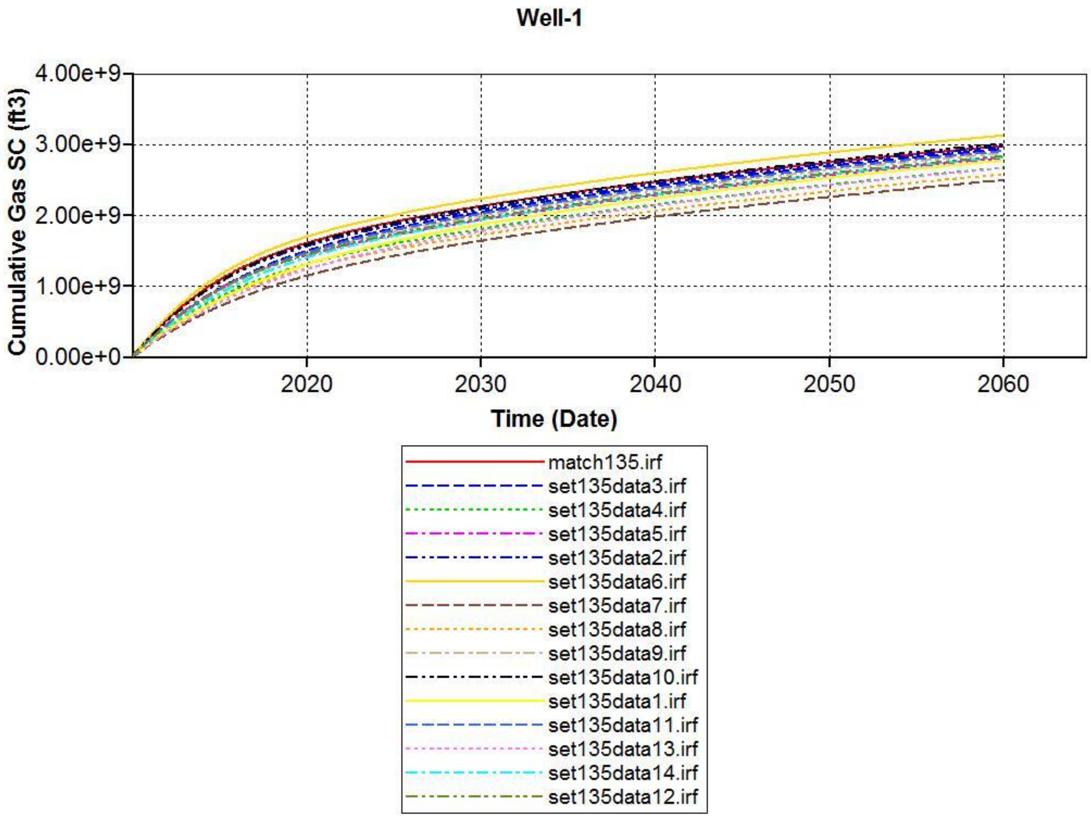

Figure 4-9–Example of Matching using the commercial simulator's graphical display program

In Figure 4-6the crushed zone cumulative production is shown, and 20 transverse fracture cumulative production profiles were juxtaposed for comparison purposes. The closest one is then picked qualitatively using a 10% tolerance, and the process is repeated until all the runs have been matched. Note that Cumulative production profiles are used instead of gas rate profiles because they are less sensitive and easier to match.

Figure 4-7 shows an ideal match where both gas rate and cumulative production match each other almost perfectly (< 1% error). Note that approximately 10% error tolerance is used when matching.

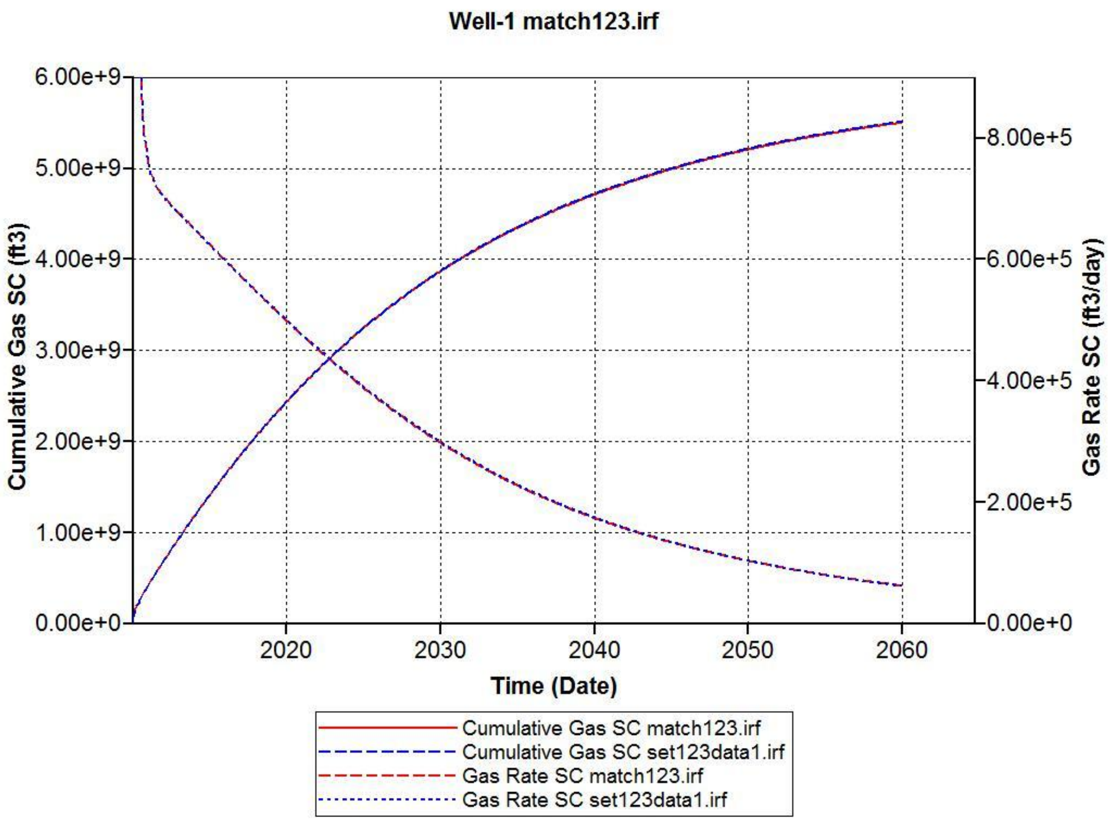

Figure 4-10– Ideal Match from data 'set123data1'

As noted from the development of the production performance ANN, in order to predict the output of such a complex system a larger and more sophisticated network will be required. Therefore, our initial configuration of the equivalency ANN will include several functional links along with 2 more hidden layers as shown in Table 4-9 and Table 4-10.

Table 4-9 – Initial input parameters used in the equivalency ANN

Inputs	
Reservoir characteristics:	edge_l, B, h, c_f, k_m, k_f, ϕ_m, ϕ_f, nf_{sp}, T_i, p_i, p_L, V_L,
Crushed zone design parameters:	a_{minor}, k_{fcz}, p_{sf}
Functional links	p_i/p_{sf}, a_{minor}*k_{fcz}

Table 4-10 – Initial output parameters used in the equivalency ANN

Outputs	
Transverse design parameters:	HF_{sp}, xf, k_{hf}
Functional links:	λ_6 , $\lambda_7, \lambda_8, \lambda_9, HF_{sp}$*xf*$k_{hf}$, p_{sf}*k_{hf}

The maximum eigen-values used in the outputs are:

$\lambda_6$is the maximum eigen-value calculated from the following matrix

$$\begin{bmatrix} kf_{cz} & \mathrm{a_{minor}} \\ \mathrm{psf} & \mathrm{kf} \end{bmatrix}$$

$\lambda_7$is the maximum eigen-value calculated from the following matrix

$$\begin{bmatrix} HF_S & \mathrm{xf} \\ \mathrm{k_{hf}} & \mathrm{p_{sf}} \end{bmatrix}$$

$\lambda_8$is the maximum eigen-value calculated from the following matrix

$$\begin{bmatrix} edge\_l & h \\ \mathrm{k_m} & \mathrm{k_f} \end{bmatrix}$$

$\lambda_9$is the maximum eigen-value calculated from the following matrix

$$\begin{bmatrix} T_i & \mathrm{P_i} \\ \mathrm{P_L} & \mathrm{V_L} \end{bmatrix}$$

Note that $\lambda_6$and $\lambda_9$is the same as $\lambda_1$and λ_4 respectively. $\lambda_1$and $\lambda_4$was used in the production performance ANN but is renamed here to avoid confusion.

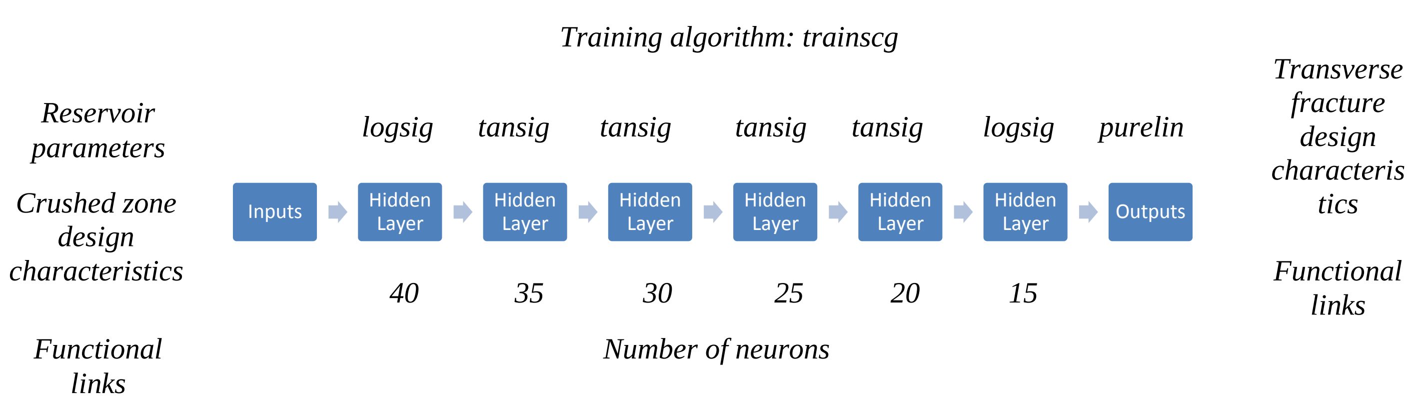

Figure 4-11– Initial configuration of the equivalency ANN

The network configuration shown in Figure 4-10 was trained with 317 data sets and had the logsig transfer function attached to the first and last hidden layers. The number of neurons decreases as we move towards the output in a funnel shape due to the larger number of parameters in the input layer. Overall, this configuration yielded decent results, but judging from the final configuration of the production performance ANN, adding more functional links and eigen-values should improve the network even further.

In this final inputs and outputs for the equivalency ANN shown below in Table 4-11 and Table 4-12, a fifth eigen-value λ_{10} has been added to the output layer along with various other functional links in the input layer.

Table 4-11 – Final input parameters used in the equivalency ANN

Inputs	
Reservoir characteristics:	edge_l, B, h, c_f, k_m, k_f, ϕ_m, ϕ_f, nf_{sp}, T_i, p_i, p_L, V_L,
Crushed zone design parameters:	a_{minor}, k_{fcz}, p_{sf}
Functional links:	p_i/p_{sf}, a_{minor}*k_{fcz}, k_{fcz}*p_{sf}

Table 4-12 – Final output parameters used in the equivalency ANN

Outputs	
Transverse design parameters:	HF_{sp}, xf, k_{hf}
Functional links:	λ_6 , λ_7,λ_8, λ_9,$\lambda_{10}$$HF_{sp}$*xf*$k_{hf}$, p_{sf}*k_{hf}

$\lambda_{10}$is the maximum eigen-value calculated from the following matrix

$$\begin{bmatrix} edge\_l & \mathrm{h} \\ \phi_m & \phi_f \end{bmatrix}$$

The training algorithm was also changed from the scaled conjugate gradient backpropogation (trainscg) to the conjugate gradient backpropogation with Fletcher-Reeves updates (traincgf) as shown in Figure 4-11 below which describes the final configuration of the equivalency ANN.

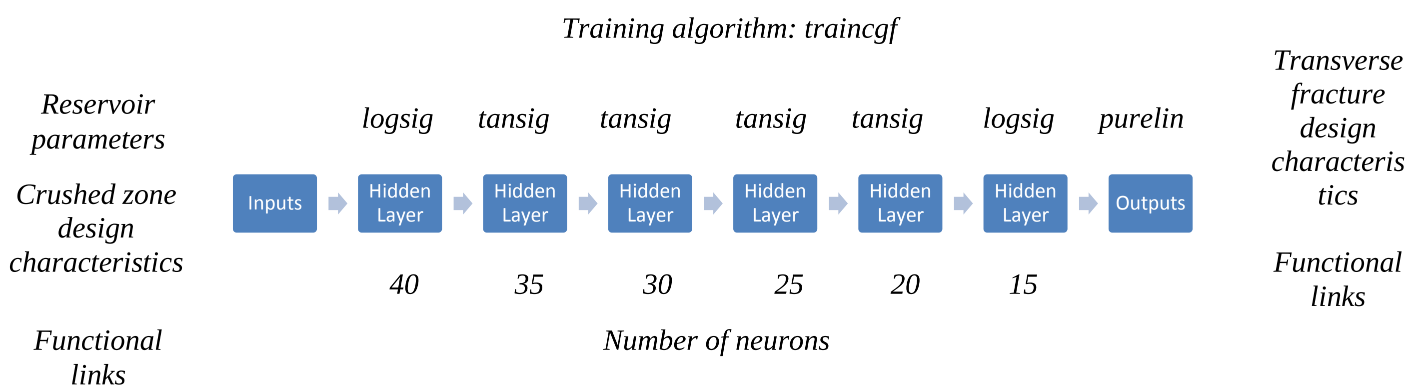

Figure 4-12– Final configuration of the equivalency ANN

Even though the equivalency ANN yielded acceptable results within the 15%-20% range, there is a possibility of improving the accuracy even further by introducing an equivalency error-filter

Equivalency error-filter ANN

The final configuration shown in Figure 4-10 in the previous section is pushing the equivalency ANN to its limits, and even though the results were within the acceptable accuracy range of 15%-20%, there is a desire to improve the results even further. This scenario resulted in the creation of an experimental third neural network called the equivalency error- filter ANN. Given that this network was trained with only 16 training sets, further network improvements and optimization is recommended as a future study.

When analyzing the results of the equivalency ANN, the predicted transverse fracture design parameters from the ANN is simulated using the commercial simulator and a gas rate production profile is generated. These ANN-predicted transverse fracture gas rates are then compared to the gas rate generated from the commercial simulator matches. Figure 4-11 gives a graphical overview of this procedure.

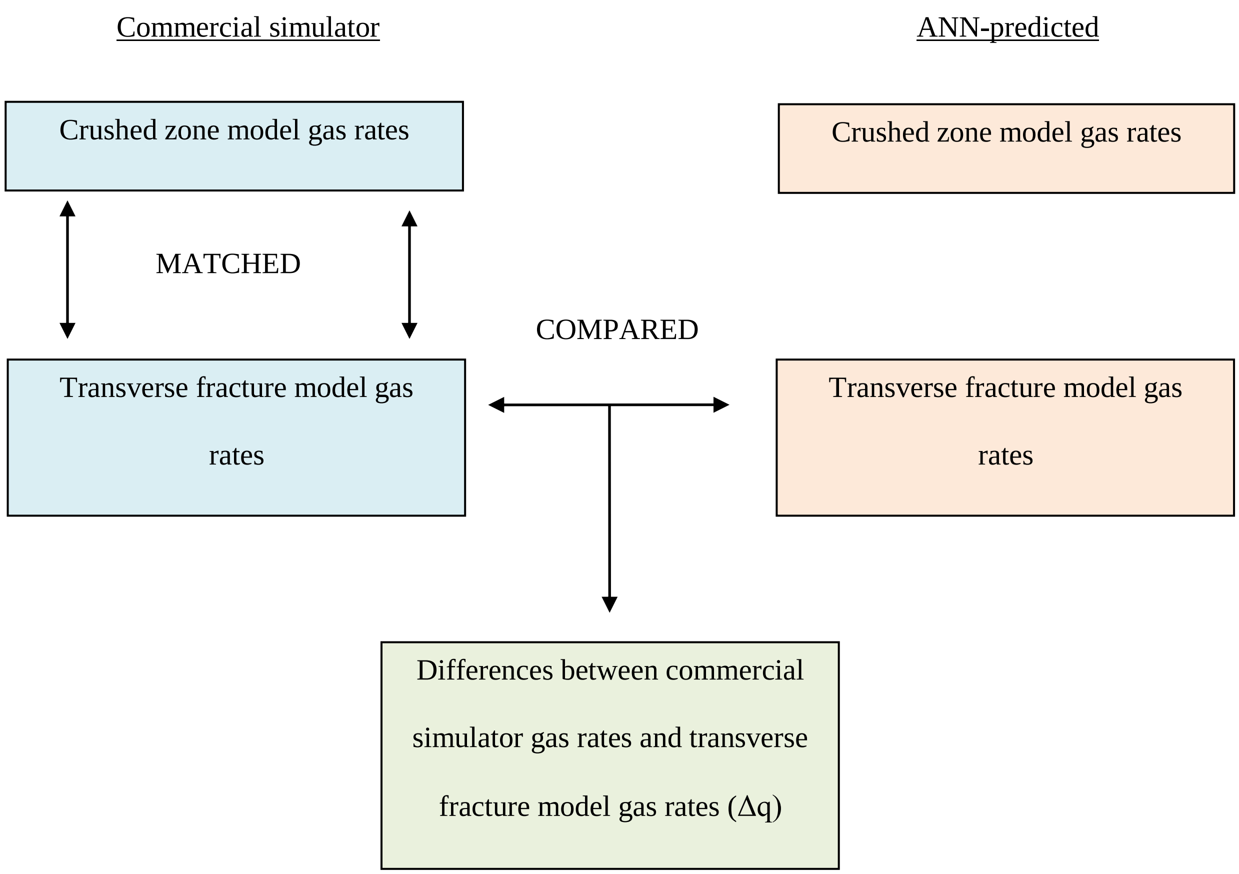

Figure 4-13– Process for obtaining the data for equivalency error-filter ANN

In Figure-11 our focus lies in comparing the two transverse fracture model gas rates from the commercial simulator and the ANN. Each gas rate difference is calculated the following way:

$$\Delta q = q_{com} - q_{ANN}$$

With q_{com} referring to the gas rate from the commercial simulator and q_{ANN} is the gas rate predicted by the ANN.

To summarize, this error-filter network's purpose is to learn what magnitude of error can be expected when a set of reservoir characteristics, crushed zone design parameters and transverse design parameters are combined. The inputs and outputs of this network are listed in Table 4-13 and Table 4-14.

Table 4-13 – Input parameters used in the equivalency error-filter ANN

Inputs	
Reservoir characteristics:	edge_l, B, h, c_f, k_m, k_f, ϕ_m, ϕ_f, nf_{sp}, T_i, p_i, p_L, V_L,
Crushed zone design parameters:	a_{minor}, k_{fcz}, p_{sf}
Transverse design parameters:	HF_{sp}, xf, k_{hf}

Table 4-14 – Output parameters used in the equivalency error-filter ANN

Outputs	
Differences in gas rates	Δq_1, Δq_{180}, Δq_{360}, Δq_{540}, Δq_{720}, Δq_{900}, Δq_{1080}, Δq_{1440}, Δq_{1800}, Δq_{2160}, Δq_{2520}, Δq_{2880}, Δq_{3240}, Δq_{3600}, Δq_{5400}, Δq_{7200},Δq_{10800}, Δq_{14400}, and Δq_{18000}

The following configuration shown in Figure 4-12 is used to train the network. A total of 16 data sets are used to train the network. Note that a smaller number of hidden layers are used because the number of data sets is small.

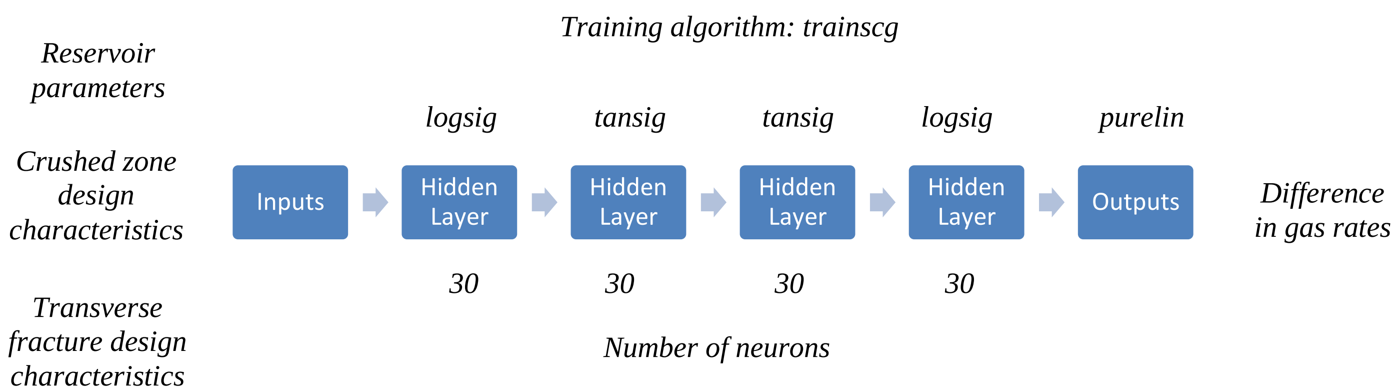

Figure 4-14– Final configuration of the equivalency error-filter ANN

This concludes the methods of approach used in generating data and training all three artificial neural networks. In Chapter 5 we will discuss the results and findings of all three networks.

Chapter 5

Results& Analysis

In this chapter, the results and findings for all three ANNs will be discussed and analyzed. Results for each ANNs are based on their accuracy when tested against an entirely new set of data that were not used in training. These data are called "testing sets"; for the purpose of this thesis 5% of the input data is used for testing.

Production Performance ANN

Establishing Production Performance ANN Analysis

For this ANN, 597 data sets were used as inputs and outputs, 5% were allocated for testing and validation purposes respectively. This gives us 30 test runs to evaluate the capability of the network.

To calculate the performance of each ANN predicted gas rate, the following equation was applied:

$$q_{t,error} = \frac{|q_t - q_{t,ANN}|}{q_t} \times 100$$

Where $q_{t,error}$ is the gas rate error at that time, q_t is the gas rate from CMG at that time and $q_{t,ANN}$ is the gas rate as predicted by ANN.

Overall gas rate error is calculated as follows:

$$q_{ave,error} = \frac{\sum q_{t,error}}{N}$$

Where $q_{ave,error}$ is the average of all the gas rate errors

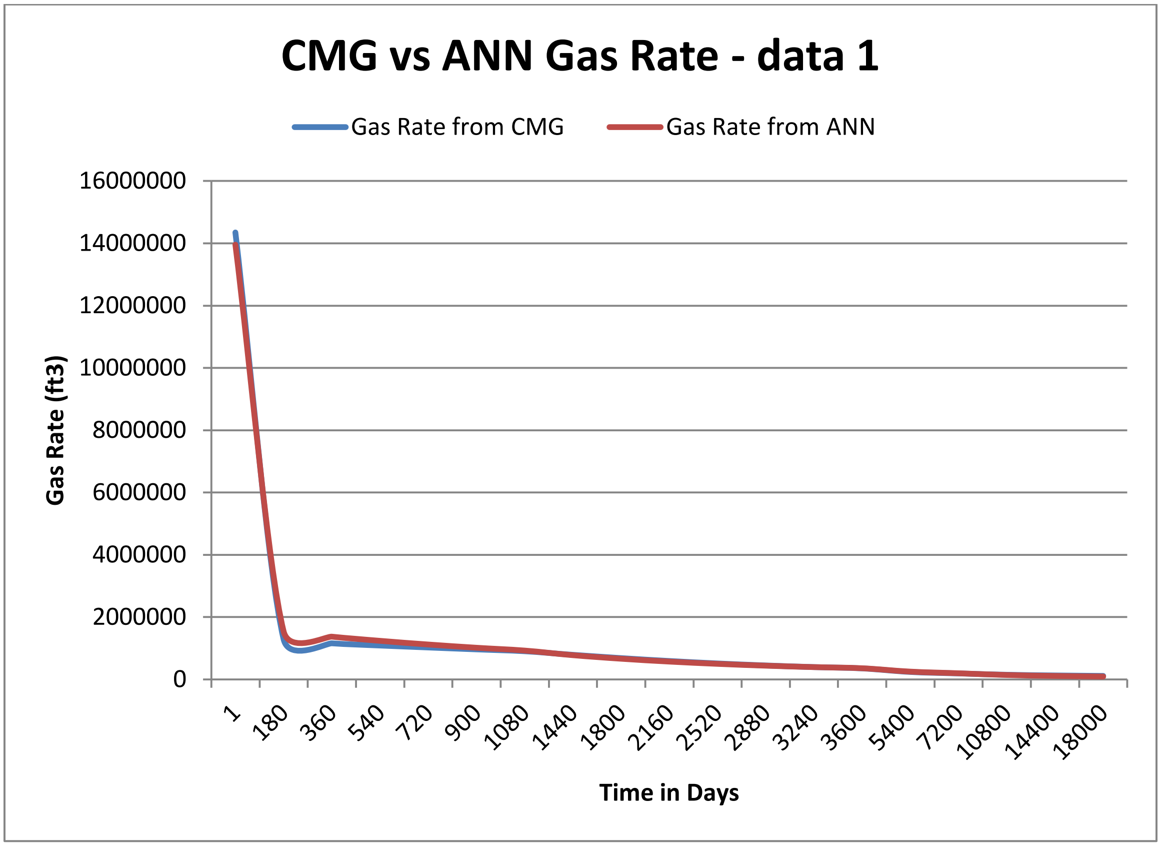

Figure 5-1– Commercial simulator vs. ANN gas rate results from data 1

Comparison of gas rates between CMG and ANN at various times throughout the 50 years of production for data is shown in Figure 5-1. As we can see, the gas rates data are almost on top of each other; this particular run had an average error of 7.07%. Notice that greatest error in this run is in the early gas rates. To investigate whether the ANN is better at predicting late time gases, we analyze several more data sets below.

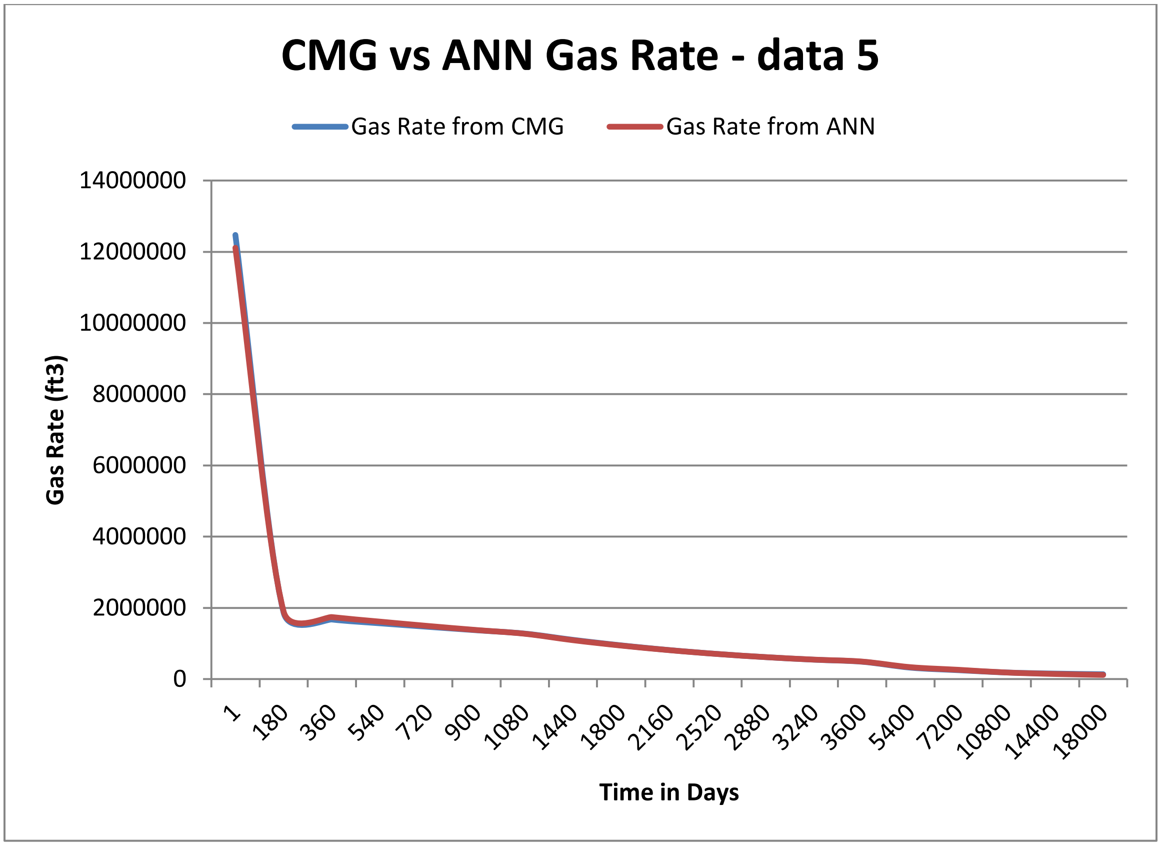

Figure 5-2–Commercial simulator vs. ANN gas rate results from data 5

This particular data in Figure 5-2 suggests an almost impeccable performance by the ANN and results in an average gas rate error as low as 2.56%. Similar to data 1 earlier, even with such a low average error, the very first gas rates still indicate some slight discrepancies as seen in Figure 5-3. Figure 5-3 is a sub-set of data 5 showing only the first 3 gas rates collected (1, 180, 360 days).

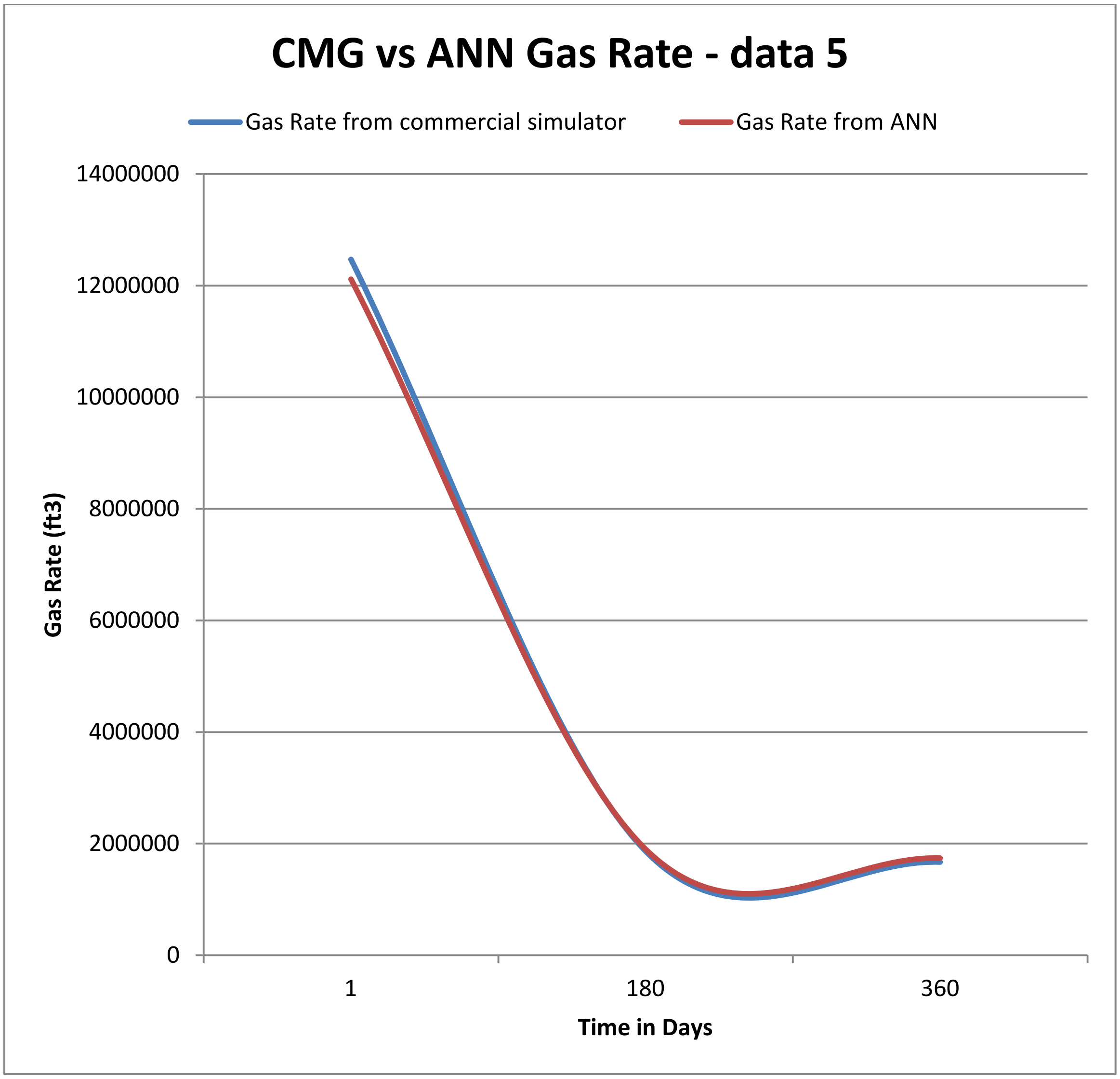

Figure 5-3–Commercial simulator vs. ANN gas rate results from data 5 (1-360 days)

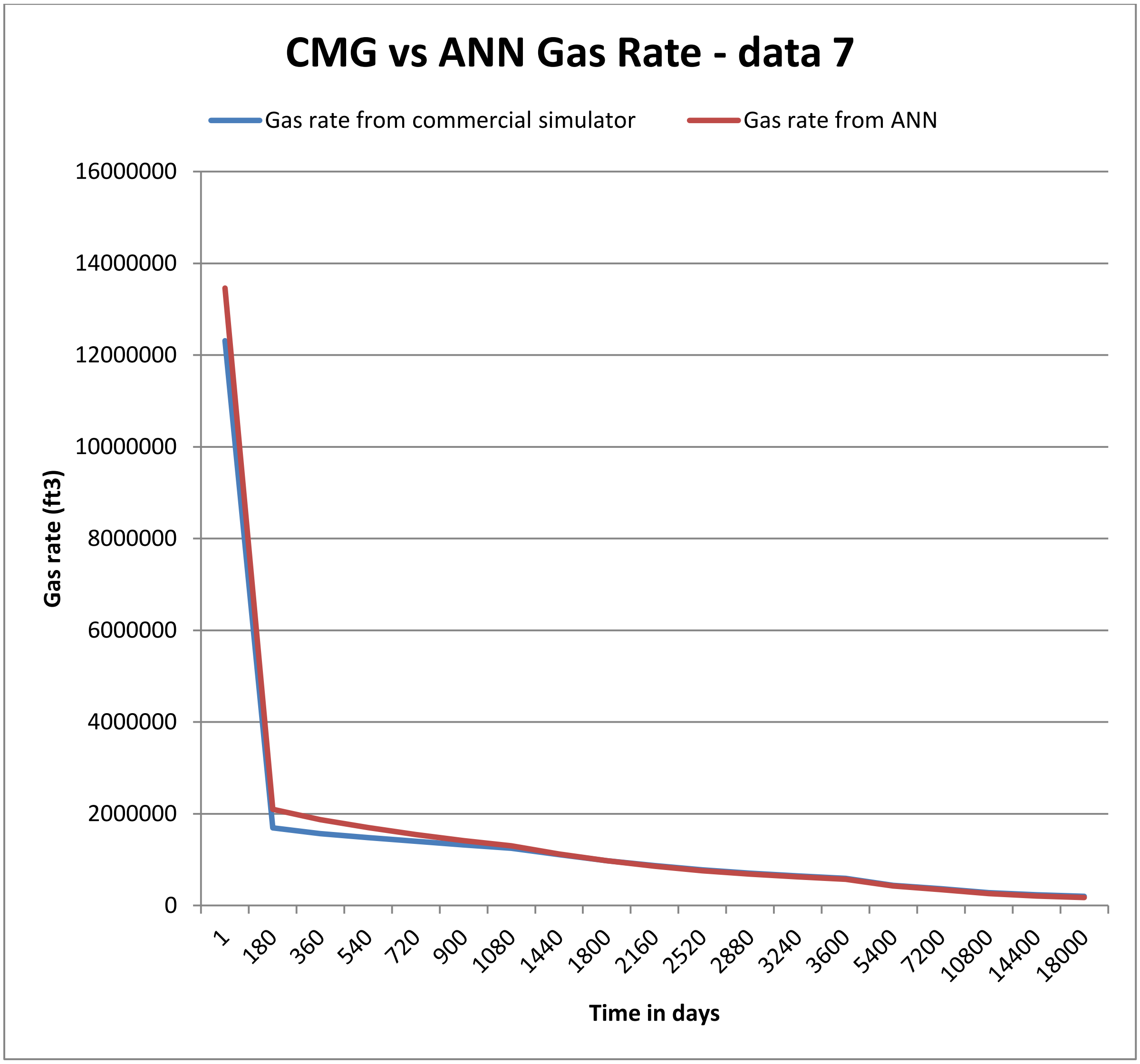

Figure 5-4–Commercial simulator vs. ANN gas rate results from data 7

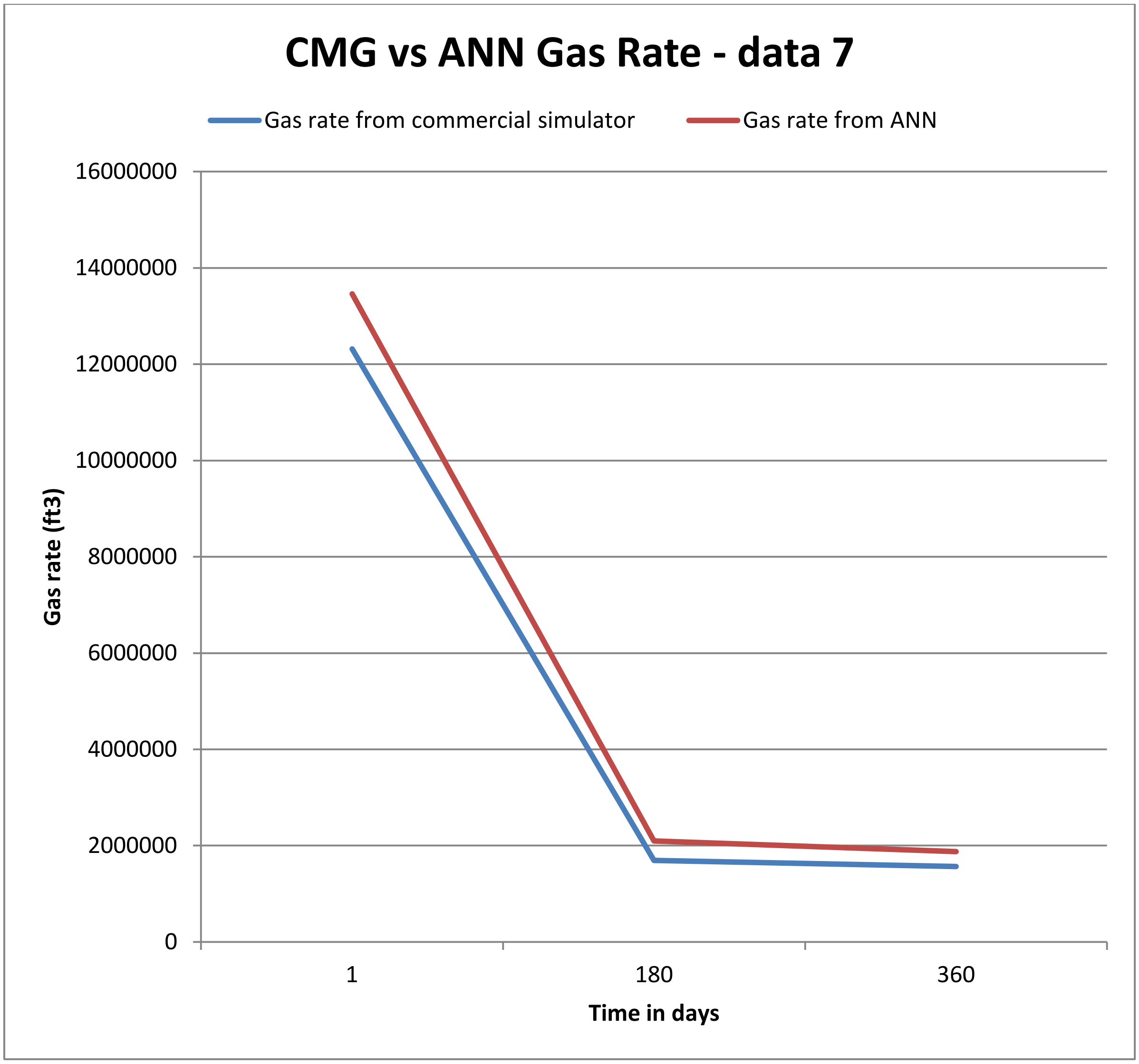

Figure 5-5–Commercial simulator vs. ANN gas rate results from data 7 (1-360 days)

Results from data 1 (Figure 5-1), data 5 (Figure 5-2 and 5-3) and data 7 (Figure 5-4 and 5-5)suggests that the ANN has the most trouble predicting q1 (gas rate at day 1), q2 (at day 180) and q3 (at day 360) and is increasingly accurate as the number of days increase. However, many other data sets reveal that this is not always the case. Figure 5-6 and 5-7 shows that even if early time predictions are good, late time prediction can still be poor.

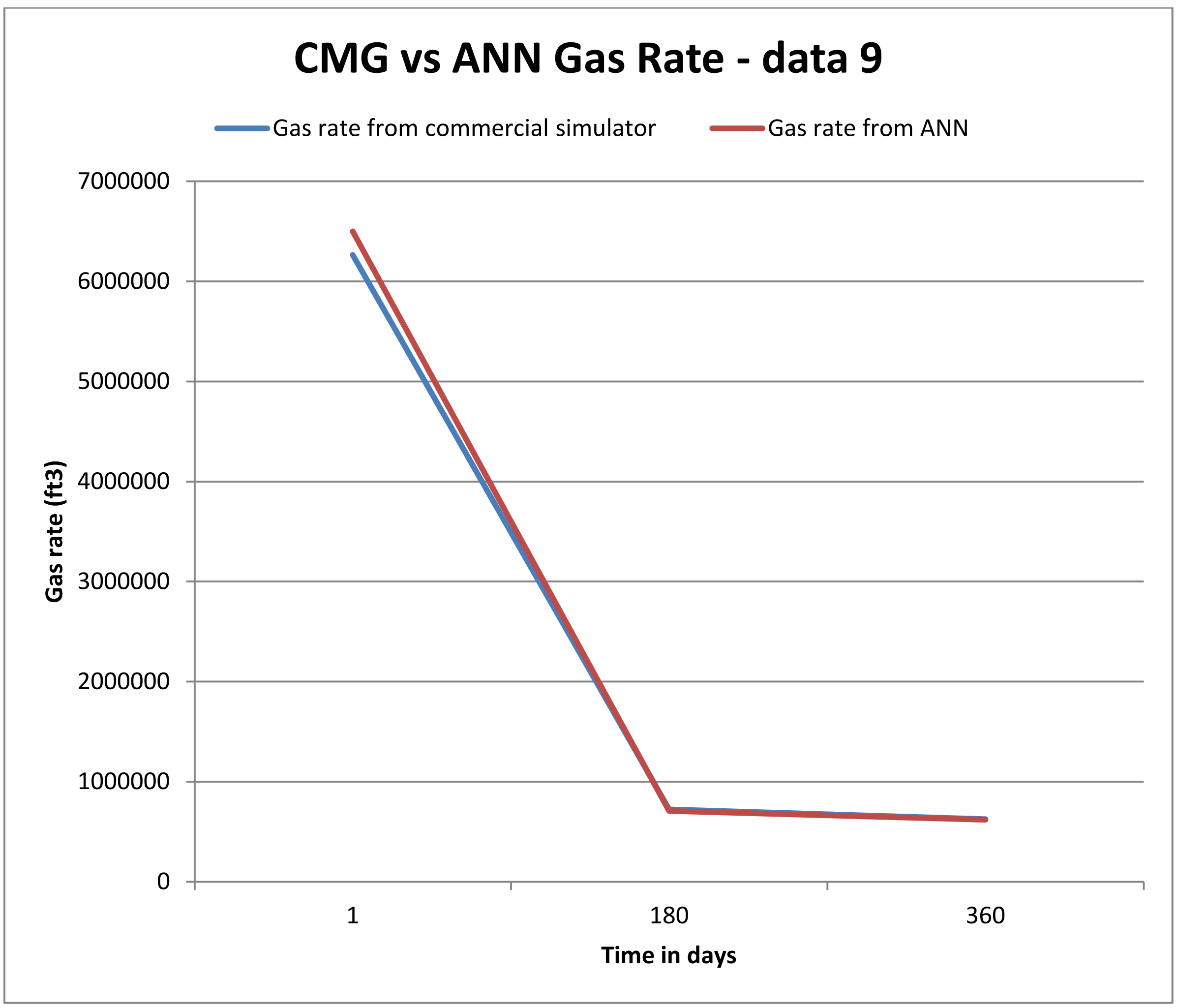

Figure 5-6–Commercial simulator vs. ANN gas rate results from data 9 (1-360 days)

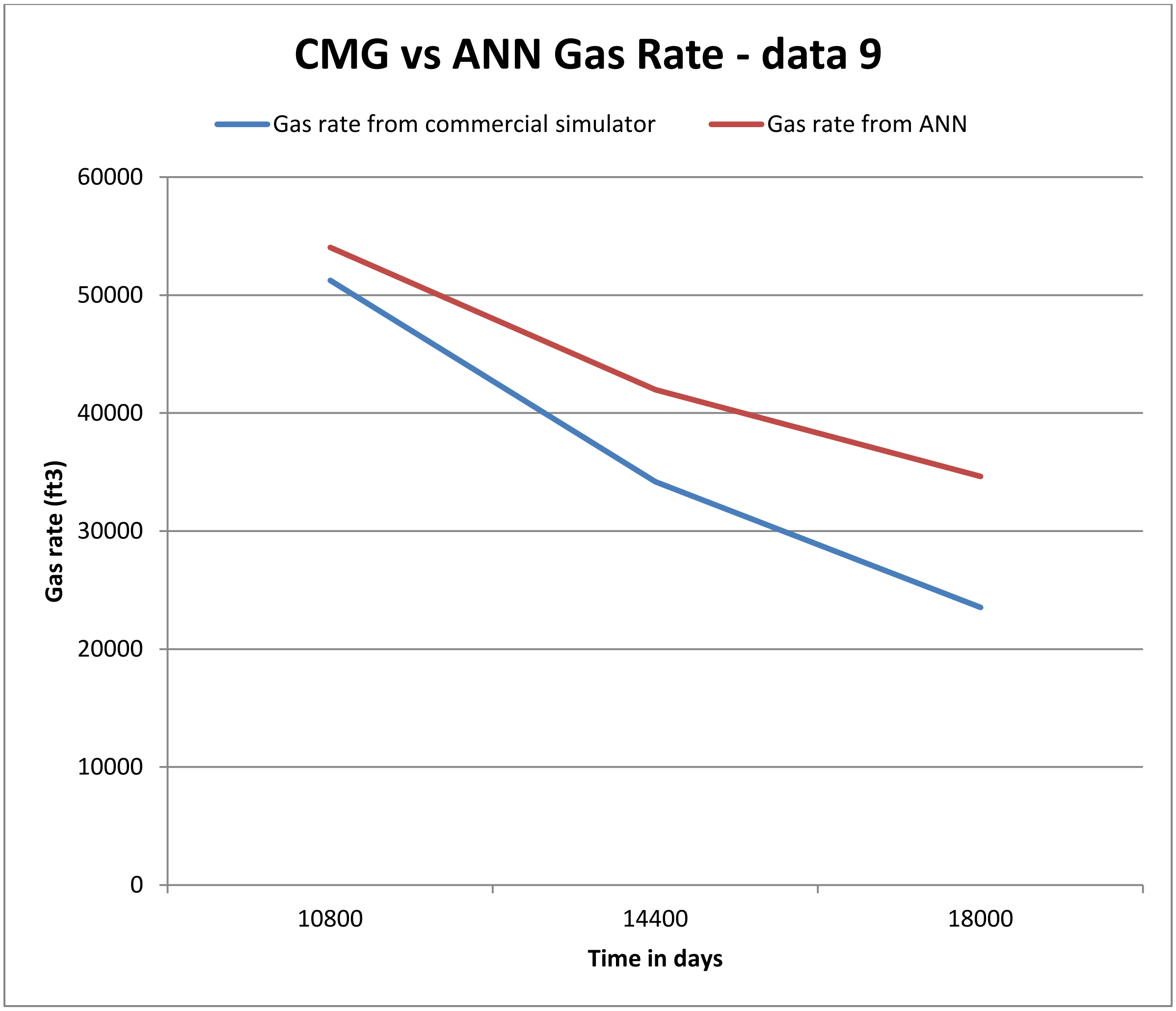

Figure 5-7–Commercial simulator vs. ANN gas rate results from data 9 (10,800-18000 days)

In order to quantify at what time (days) the network is able to predict results better, a graph of the average errors predicted from 30 test sets is show below in Figure 5-7.

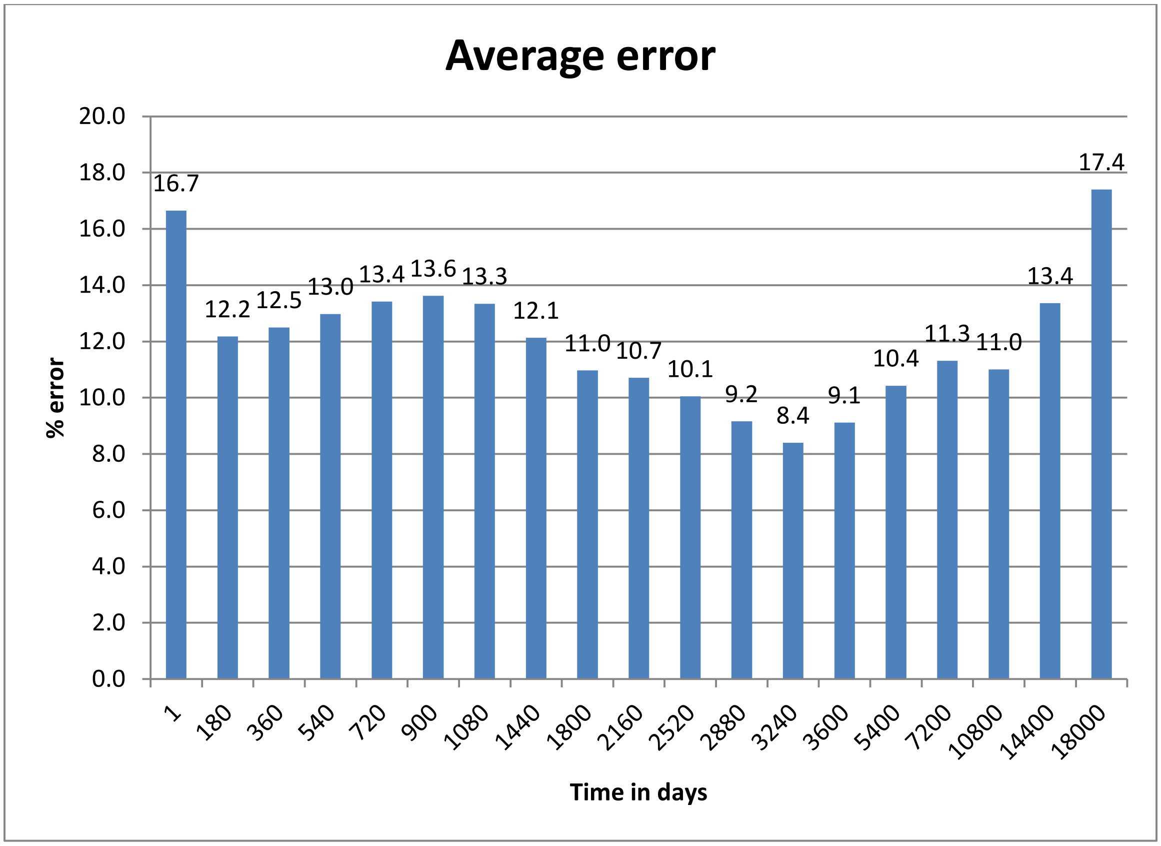

Figure 5-8– Average error of all testing set over 50 years

Figure 5-7 indicates that the network's best prediction time is around 2880-3600 days; this may be due to the fact that gas rates are more stable at this time period, while late time predictions may be affected if the reservoir is depleted. Therefore we can conclude from Figure 5-7 that the network seems to be the most adept at predicting gas rate after 3/4th of its production life has passed and least adept at predicting the first and last gas rates. The overall average error histogram is shown below in Figure 5-8.

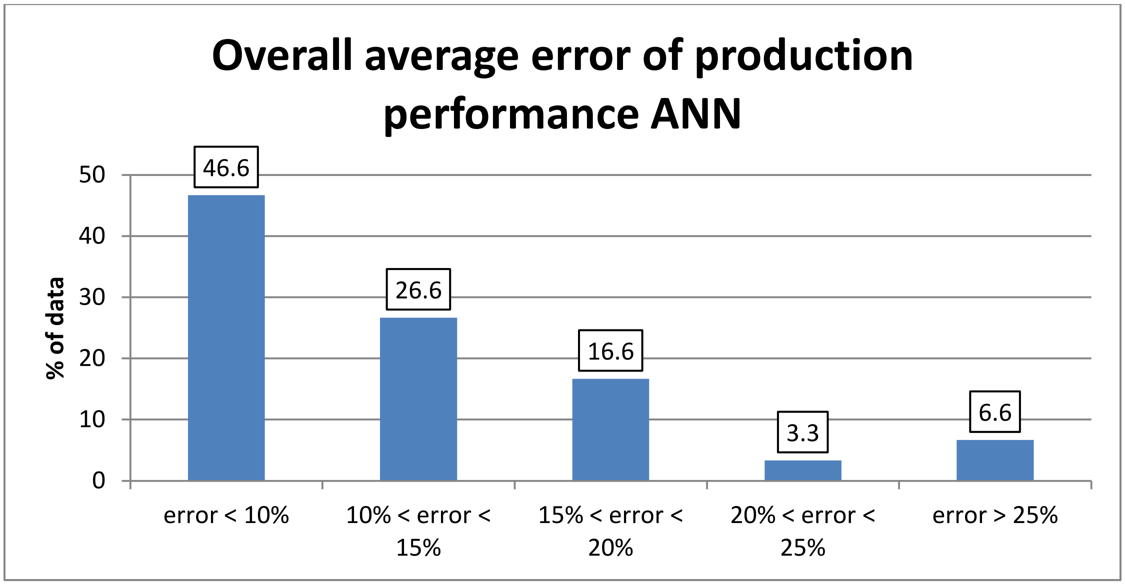

Figure 5-9 – Overall average error of production performance ANN

Figure 5-8 summarizes all the errors from the entire 30 test runs used in this performance ANN. Each histogram represents a percentage of the testing sets that falls within that range. For example, 46.6% of the testing sets have an overall average error of less than 10%. With an overall average error of all testing set at just 12.03% and more than 70% of the test sets falling in the less than 15% error category, we can safely say that the prediction capabilities of this ANN is considerably accurate.

Equivalency ANN

In the analysis of the equivalency ANN results, the first issue that must be addressed is the existence of non-unique matches.

Non-Unique Matches

When two or more matches with the same production profile, while containing a different transverse fracture design parameters are encountered during the crushed zone – transverse fracture pairing process described in Chapter 4 (Figure 4-8), they are called non-unique matches. As can be seen in Figure 5-4 below, two non-unique transverse fracture matches were encountered while attempting to match their cumulative production with the respective crushed zone model. In this figure, the dotted dark green line refers to the transverse fracture model from data 2 shown in Figure 5-5, while the yellow curve is represented by the model from data 14 shown in Figure 5-6.

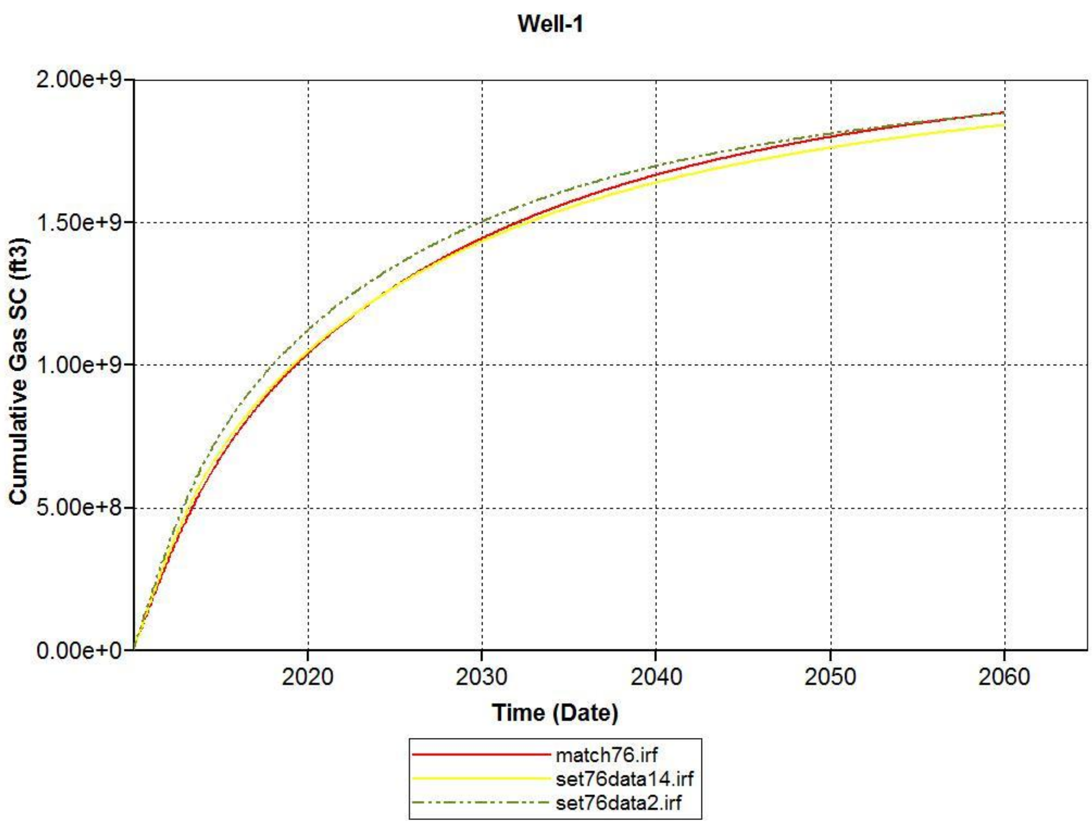

Figure 5-10–None-unique matches in data 76

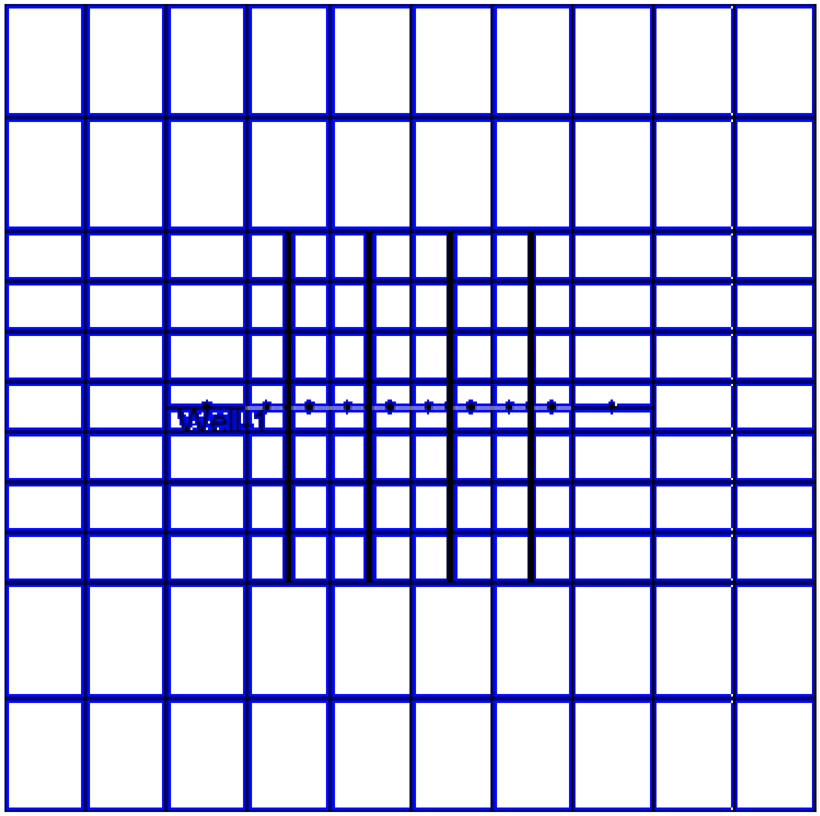

Figure 5-11– Commercial Simulator Model of data 2

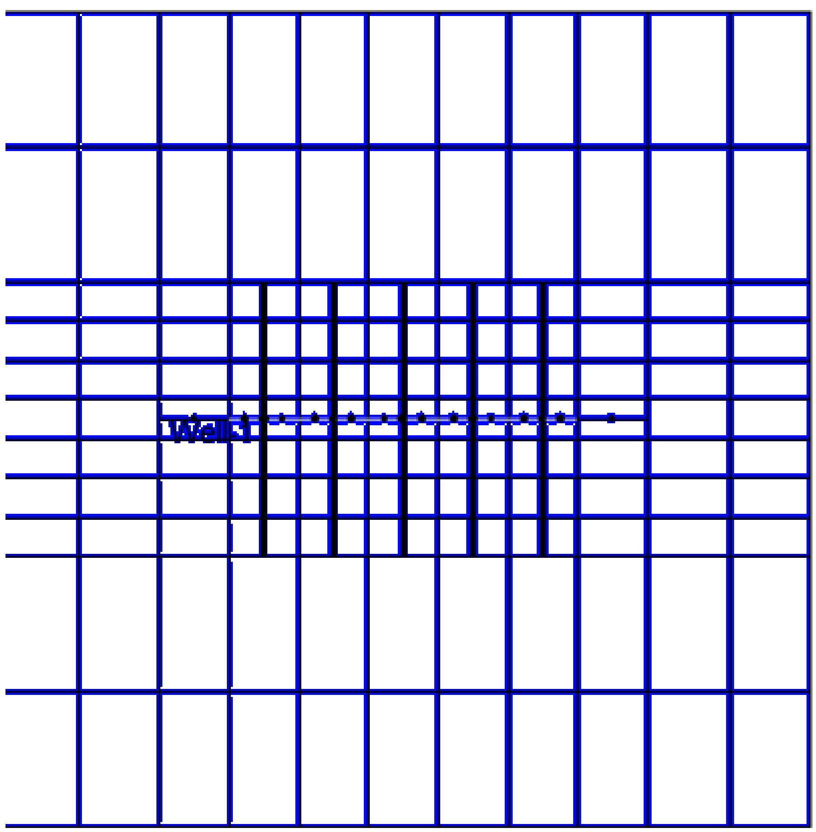

Figure 5-12–Commercial Simulator Model of data 14

Figure 5-6shows that data 14 contains5 transverse fractures while Figure 5-5shows that data 2 only has 4 fractures. Even though both matches have very similar gas rates, ~2% difference, the design characteristics are quite different as shown in Table 5-1:

	Hydraulic Fracture Spacing (ft)	Frac Half Length (ft)	Hydraulic Frac Permeability (mD)
Data 14	108.1057	212.253755	6000.446
Data 2	126.1233	273.951965	19228.82

Table 5-1– Transverse Fracture Design Characteristics of data 14 and data 2

Unfortunately, none-unique matches are ever-present during the matching process and a future study is required in order to uniquely identify which transverse fracture design is truly the equivalent of the crushed zone design used in each data set.

Establishing Equivalency ANN Analysis

From observing non-unique matches like data 76, even though data 14 has a higher number of hydraulic fracturing strips (due to lower HFsp), data 2 has a higher cumulative production due to having a longer fracture half length (xf). Although data 2 also has a higherk_{hf}, observation from other runs indicate that the k_{hf}has the least influence due to the fact that each HF strip is only 0.05 ft wide. Thus we can rank the importance of each design characteristic accordingly:

xf>hf_s>k_f

Desired accuracy of 15% cumulative production error, calculated as follow:

$$CGP_{error} = \frac{CGP - CGP_{ANN}}{CGP} \times 100$$

Where CGP is the cumulative gas production of the commercial simulator transverse model run. CGP_{error} is the cumulative gas production error in percentage and CGP_{ANN} is the cumulative gas production generated from ANN prediction using transverse design characteristics. Samples of some of the results are shown below:

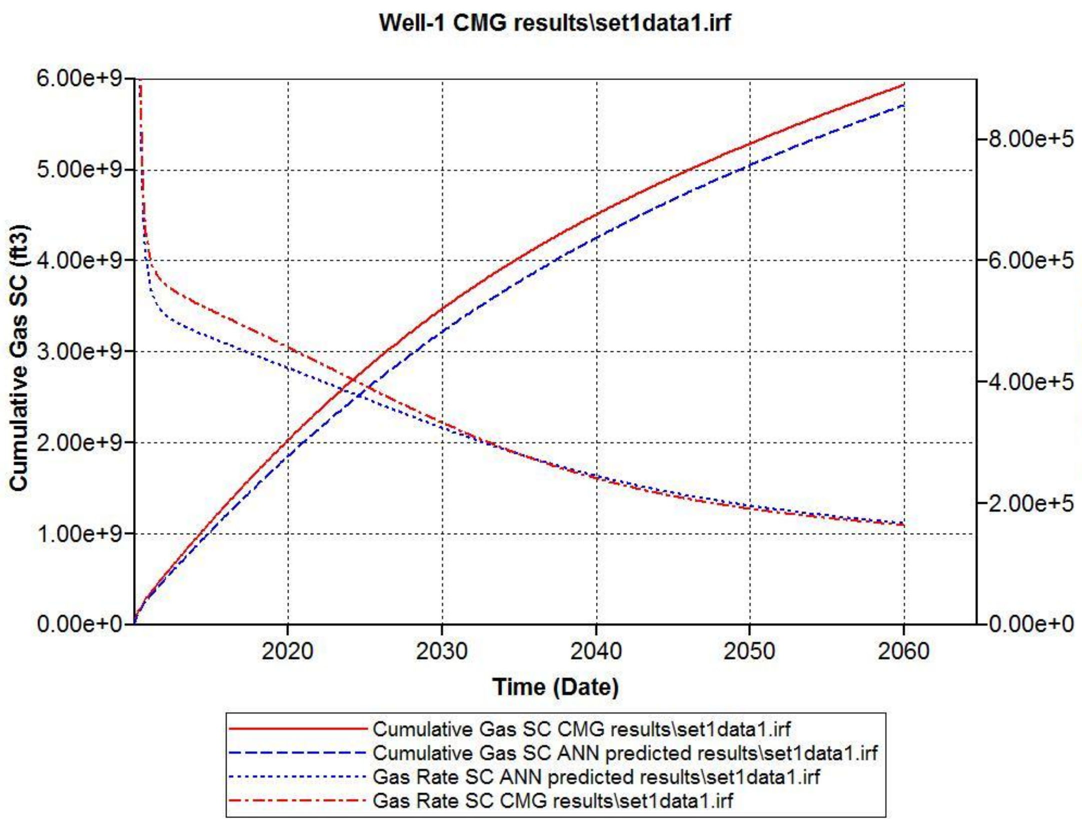

Figure 5-13–Equivalency ANN Result – data 1

Figure 5-7 shows a typical equivalency ANN result, with the red curve representing the commercial simulator data and blue dashed curve representing ANN prediction. In this figure, the most pronounced error is in the early time period, where the ANN under-predicted the initial gas rate either through an insufficiently high permeability or excessive hydraulic fracture spacing.

However, after approximately 30 years, the gas rate starts to stabilize and the gas rate prediction is near-perfect. Due to the early time discrepancies in gas rate, the final cumulative production error of this data set is 3.78%.

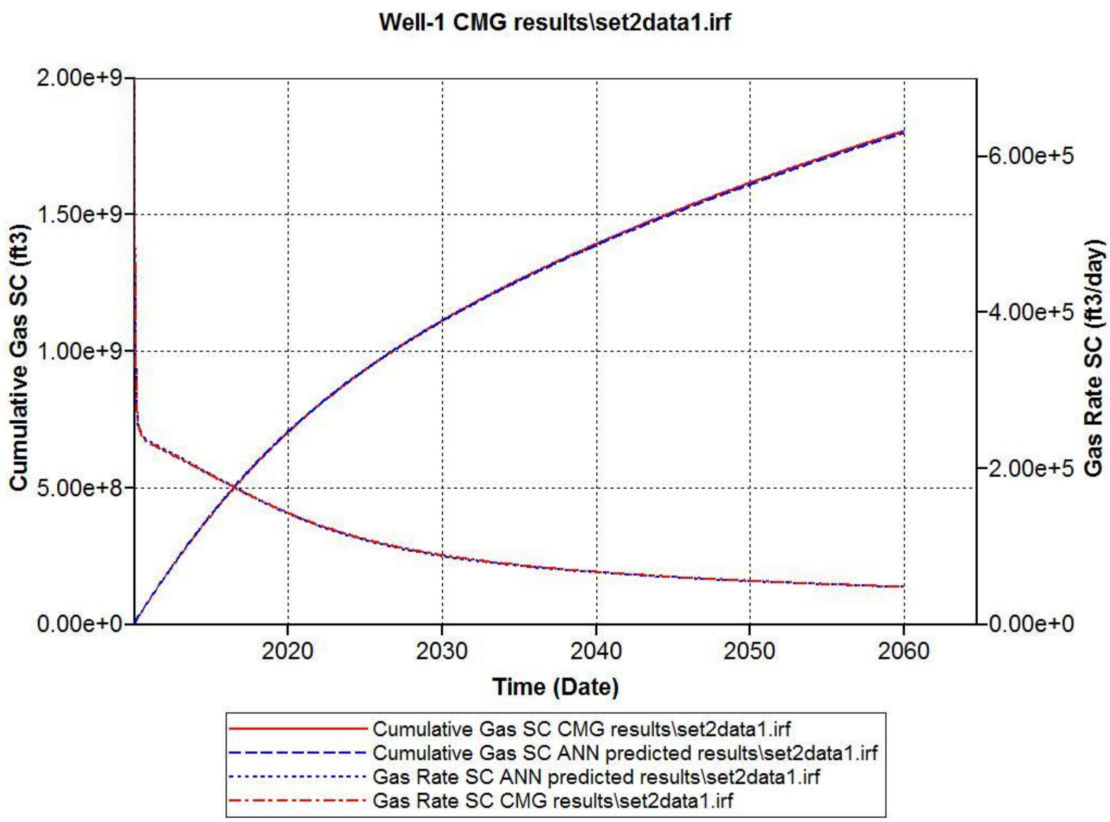

Figure 5-14–Equivalency ANN Result – data 2

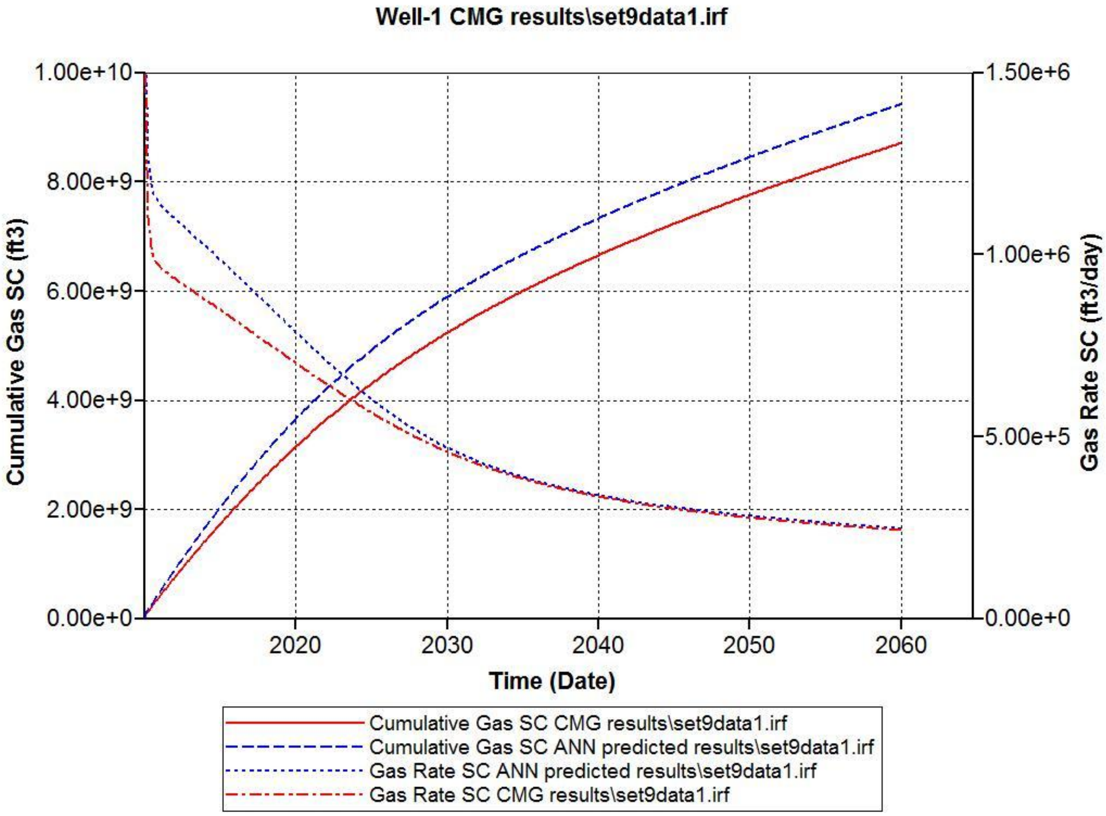

Figure 5-15–Equivalency ANN Result – data 9

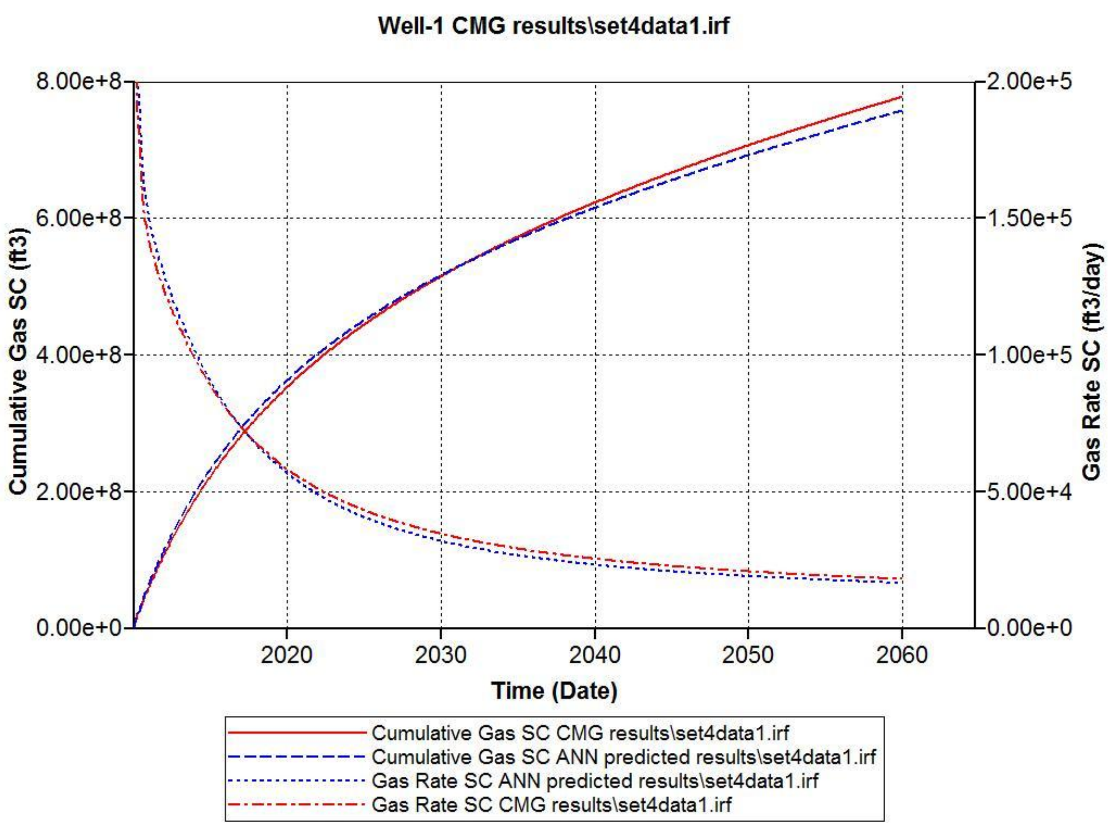

Figure 5-16–Equivalency ANN Result – data 4

Figures5-8, 5-9 and5-10 showcases the variety of results from the equivalency ANN, with Figure 5-8 representing an ideal result with both gas flow rates and cumulative production matching each other almost flawlessly. Figure 5-9 shows a reversed trend to the result from figure 5-7 where the ANN over-predict instead of under-predict the early gas rates and ends up with a final cumulative production error of 8.2%. Finally, Figure 5-10 shows a curve crossover as the ANN initially over predicts during early time before switching to under predicting the late time gas rates. This set has a final cumulative production error of just 2.5%

A histogram of the final cumulative production errors of all 16 testing sets are shown below in Figure 5-11:

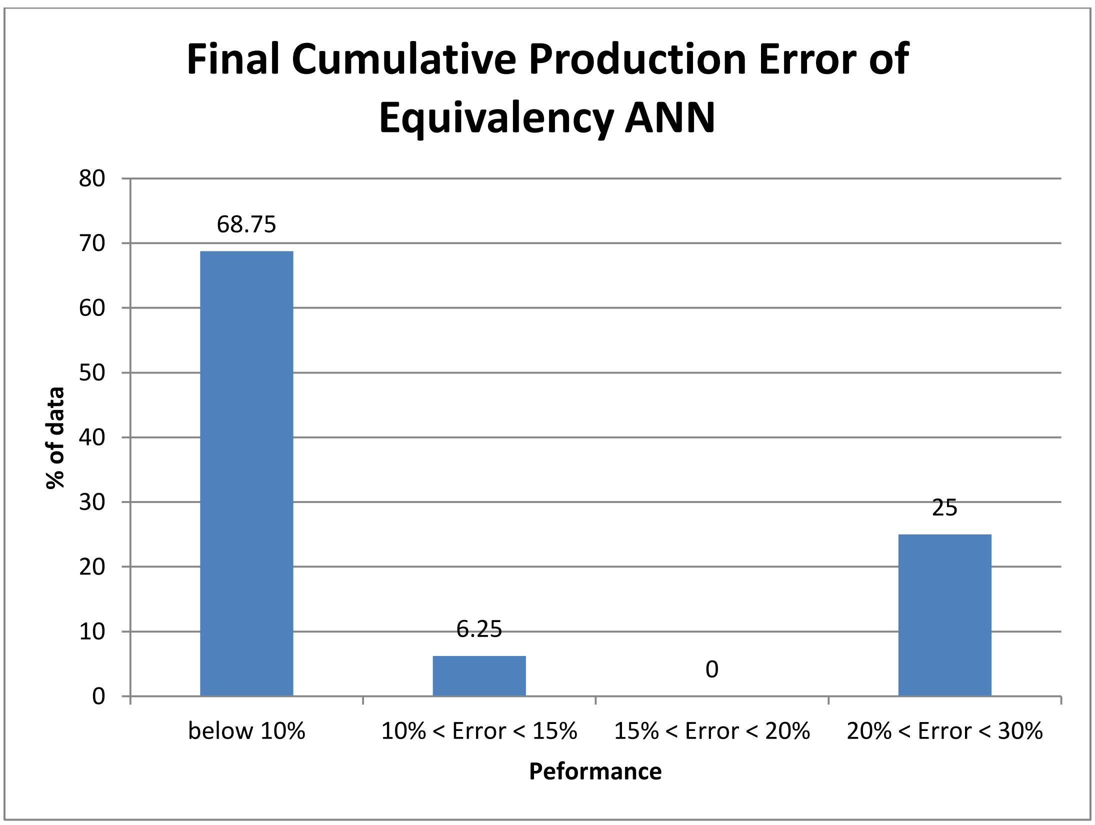

Figure 5-17–Final Cumulative Production Error of Equivalency ANN

Figure 5-11shows the ability of the equivalency ANN to predict the final cumulative production by grouping data sets into four groups consisting of: below 10%, 10% < error < 15%, 15% < Error < 20% and 20% < Error < 30%. With approximately 75% of the test sets displaying a final cumulative production error of less than 15%, we can conclude that this equivalency ANN performs within our expectation.

Even though the analysis of the final cumulative production is important because late time gas rates are generally more meaningful as they are used for estimating recoverable reserves, they are not the only indicator of the equivalency ANN's capabilities. The average cumulative production error at every time interval must be also analyzed as well. Another histogram is produced Figure 5-12, showcasing the average cumulative production error for the entire period of 50 years.

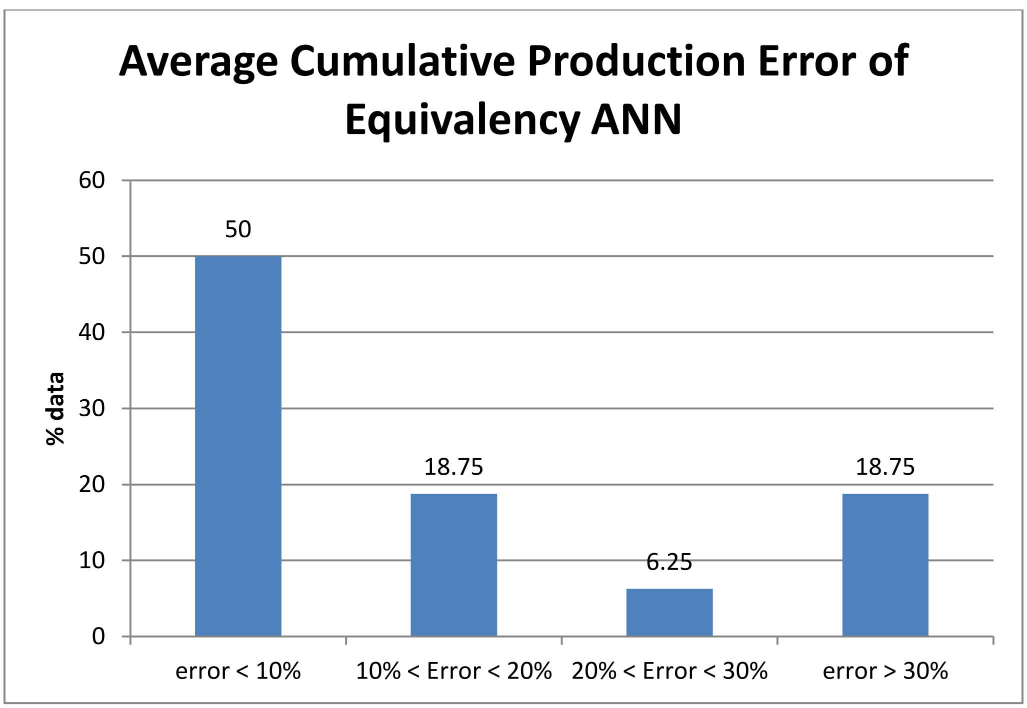

Figure 5-18–Average Cumulative Production Error of the Equivalency ANN

Figure 5-12 shows the average cumulative production error of the equivalency ANN. With around 50% of the error below 10% and 70% below 20% this capability of this ANN also falls within the desired range.

Error Filter

The error filter created in this thesis was, as discussed in Chapter 4, meant to only be a preliminary study of error filter and possibly give a slight boost to the accuracy of the equivalency ANN. With only 16 data sets to utilize, many configurations were attempted and the final configuration shown in Chapter 4 ended up performing admirably. Figure 5-13 shows the production profiles of ANN vs. Adjusted ANN vs. CMG Cumulative production. With the error-filter adjustments, the new production profile under-predicts the cumulative production initially, but over predicts during the late time period. The final cumulative production decreased from 20.02% to 6.88%.

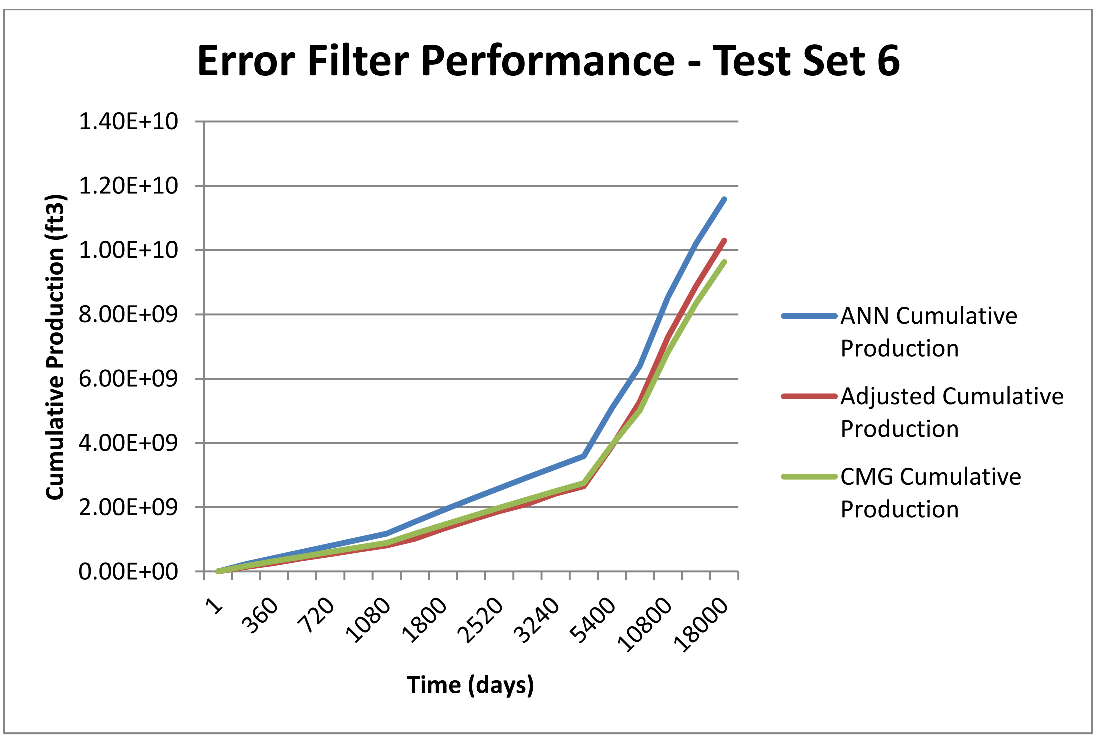

Figure 5-19–Error Filter Performance – Test Set 6

In order to gauge the capabilities of the error-filter ANN, another testing set was analyzed. However, with a total of 16 data sets available and only 5% were randomly picked as a testing set, with a minimum of at least 1 testing set, the network had to be retrained so that a new testing set can be picked randomly by MATLAB. We ended up with test set 7 as shown in Figure 5-14:

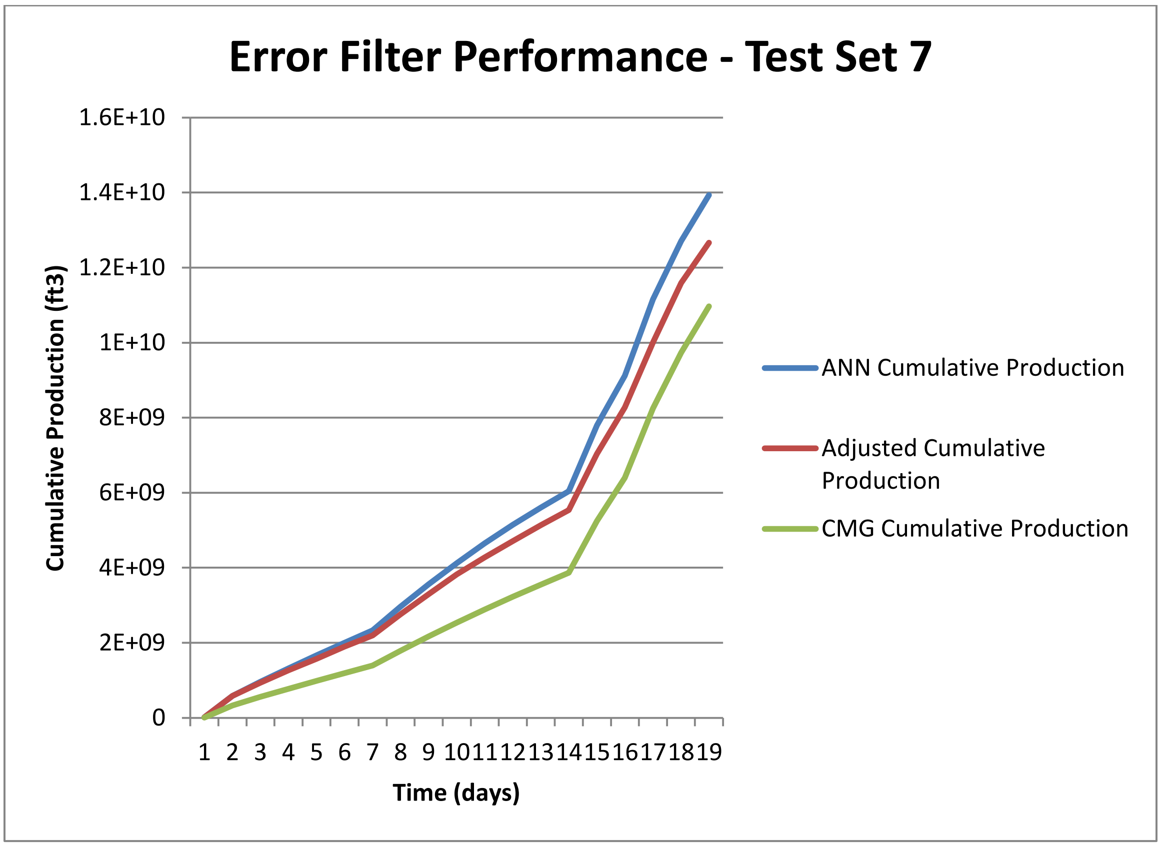

Figure 5-20–Example of Matching using the commercial simulator's graphical display program

Similar, albeit not as significant improvements were seen in this result graph in Figure 5-14, but even with the error filter, it is evident that early gas rates is extremely hard to predict. Using these results, we can estimate roughly that the error filter would be able to decrease the average and final cumulative production errors by about 40%. These estimates are applied and show in figures below:

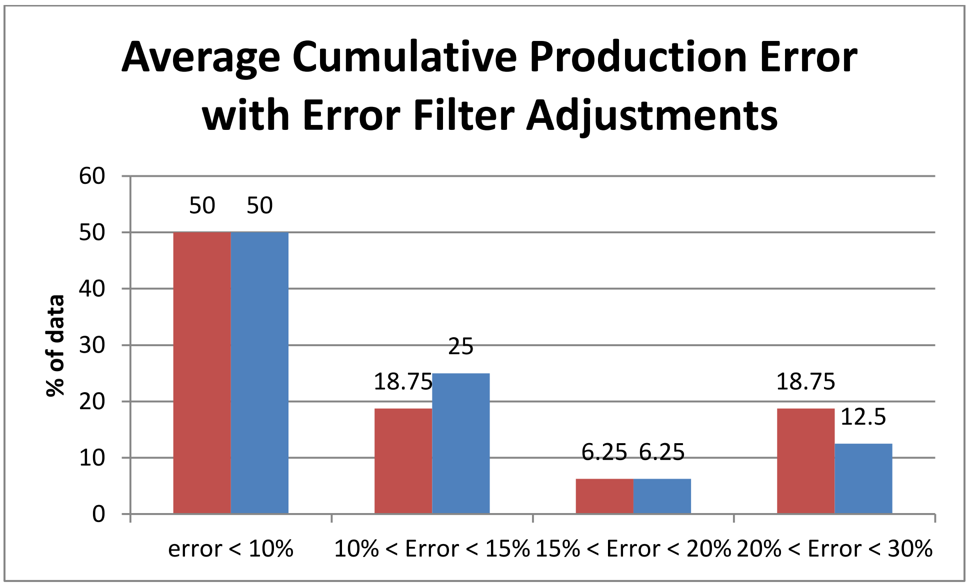

Figure 5-21–Average Cumulative Production Error with Error-filter Adjustments

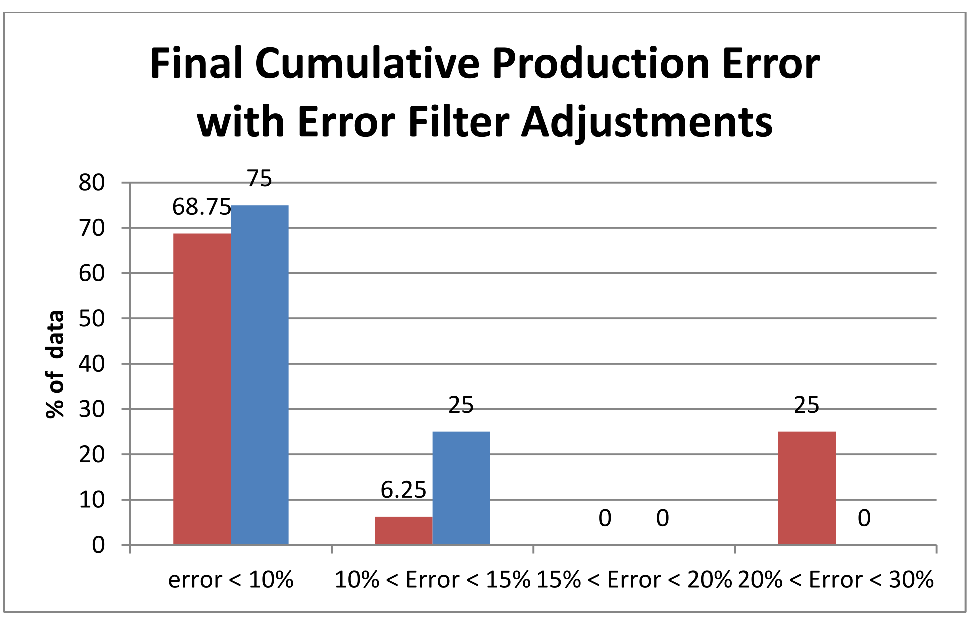

Figure 5-22–Final Cumulative Production Error with Error-filter Adjustments

Figure 5-15 and 5-16 shows the comparison bar chart between the % of data that falls into each error range of the equivalency ANN and the Error-filtered equivalency ANN. Note that the error filter used here is only meant as a study into applying error filters for equivalency ANNs. In order to obtain a significantly powerful error filter, more data sets must be used and additional network optimization may be required.

Chapter 6

Conclusions

The objective of this study is to create two ANNs capable of predicting shale gas rates and predicting the equivalent transverse fracture representation from the crushed zone model. The results indicate that this has been achieved, along with the aid of the error filter. The performance ANN enables rapid gas rate predictions for any arbitrary shale gas field that has its parameters within the range specified in chapter 4. The equivalency ANN enables quick approximation of an equivalent transverse fracture that is useful for service companies when designing hydraulic fracturing projects. The error filter improves the accuracy of the equivalency ANN, giving it a boost in credibility.

The following are observations and conclusions drawn from this study:

- Since late time results are often good, overall accuracy may improve if production time increased to 60 or 70 years
- Functional links are absolutely essential in training a successful ANN
- Eigen values of parameters are some of the most effective functional links
- The production performance ANN performs best at predicting near-late time gas rates. Early-time and late-time gas rates are slightly more problematic
- Non-unique results may require further study to identify parameters that are capable of distinguishing them
- This study, along with various other studies on ANN contributes towards the main objective of finding ways to effectively utilize ANN in the petroleum industry

References

1.) S.Polczer, Calgary Herald, Shale expected to supply half of North America's Gas, http://www.calgaryherald.com/business/Shale+expected+supply+half+North+America/1483245/story.html April, 2009

2.) U.S. Energy Information Administration: "Annual Energy Outlook 2011 with Projections to 2035." U.S. Department of Energy. Washington, DC. 2011.

3.) U.S. Energy Information Administration: Shale Gas Plays in Lower 48 States of the USA. "Review of Emerging Resources: U.S. Shale Gas and Shale Oil Plays", July 2011

4.) MathWorks.Matlab Neural Network User Guide, 2011

5.) Kulga, I. B.: "Development of an Artificial Neural Network for Hydraulically Fractured Horizontal Wells in Tight Gas Sands." Master's Thesis, The Pennsylvania State University, 2010.

6.) Thararoop, P.: "Development of a Multi-Mechanistic, Dual-Porosity, Dual-Permeability Numerical Flow Model for Coalbed Methane Reservoirs Accounting for Coal Shrinkage and Swelling Effects." Ph.D. Dissertation, The Pennsylvania State University, 2010.

7.) Ramgulam et al.: "Utilization of Artificial Neural Networks in the Optimization of History Matching." SPE 107468. Buenos Aires, Argentina. 15-18 April 2007.

8.) ESG Solutions. Frac System Schematic, https://www.esgsolutions.com/english/view.asp?x=741

9.) ESG Solutions. Multi-well multi-stage hydraulic fracture, https://www.esgsolutions.com/english/view.asp?x=870

10.) Siripatrachai, N: "Alternate Representations for Numerical Modeling of Multi-Stage Hydraulically Fractured Horizontal Wells in Shale Gas Reservoirs." Master's Thesis, The Pennsylvania State University, 2011.

11.) Neuroshell. *Neuroshell 2 Tutorial*. Ward Systems, Inc., Federick, Maryland. 1998.

12.) Artun, E.F.: "Optimized Design of Cyclic Pressure Pulsing in Naturally Fractured Reservoirs Using Neural-Network Based Proxy Models." Ph.D. Dissertation, The Pennsylvania State University, 2008.

13.) G.R. King, SPE-020730-MS: "Material Balance Techniques for Coal Seam and Devonian Shale Gas Reservoirs", 1990.

14.) Remner, D. J., T. Ertekin, W. Sung, G. R. King. A Parametric Study of the Effects of Coal Seam Properties on Gas Drainage Efficiency. *Reservoir Engineering* 1(6): 633-646 (November 1986).

15.) Westbroek, G. "Rock Types", Utah State Office of Education, 2005

16.) Obsidian Energy Company, LLC. Oil and Gas Evaluation Report, 2011

17.) AGM Inc., Horizontal wells shown in Recon's 3D view, 2010

18.) Cole, B. Horizontal well in Marcellus shale, Geology.com, http://geology.com/articles/marcellus-shale.shtml

19.) CGGVeritas, Real-Time Microseismic Monitoring, 2011 http://www.cggveritas.com/default.aspx?cid=4490

20.) Morten, M. A small Artificial Neural Network, 2009 http://www.mattmorten.co.uk/blog/tag/neural-networks/

21.) F.P. Wang and R.M. Reed: "Pore Networks and Fluid Flow in Gas Shales", SPE – 124253, 2009

Appendix A

Graphical User Interface User Manual

Introduction

The purpose of this manual is to guide the user through the GUI (Graphical User Interface) for Shale Gas Toolbox, crushed zone model section. The transverse fracture section is available in a separate manual. Note that this version is only compatible with MATLAB version 2010b pre-installed on the computer.

Starting the GUI

1) Start MATLAB by double clicking on the MATLAB executable (.exe)
2) Change the current directory to the folder where the GUI is located
3) Right click on Run_ANN_ToolBox.m and click run

Main Screen

4) The follow main GUI screen should pop up, click on the "Crushed Zone Representation" tab (note that the GUI window can be resized to fit the screen)

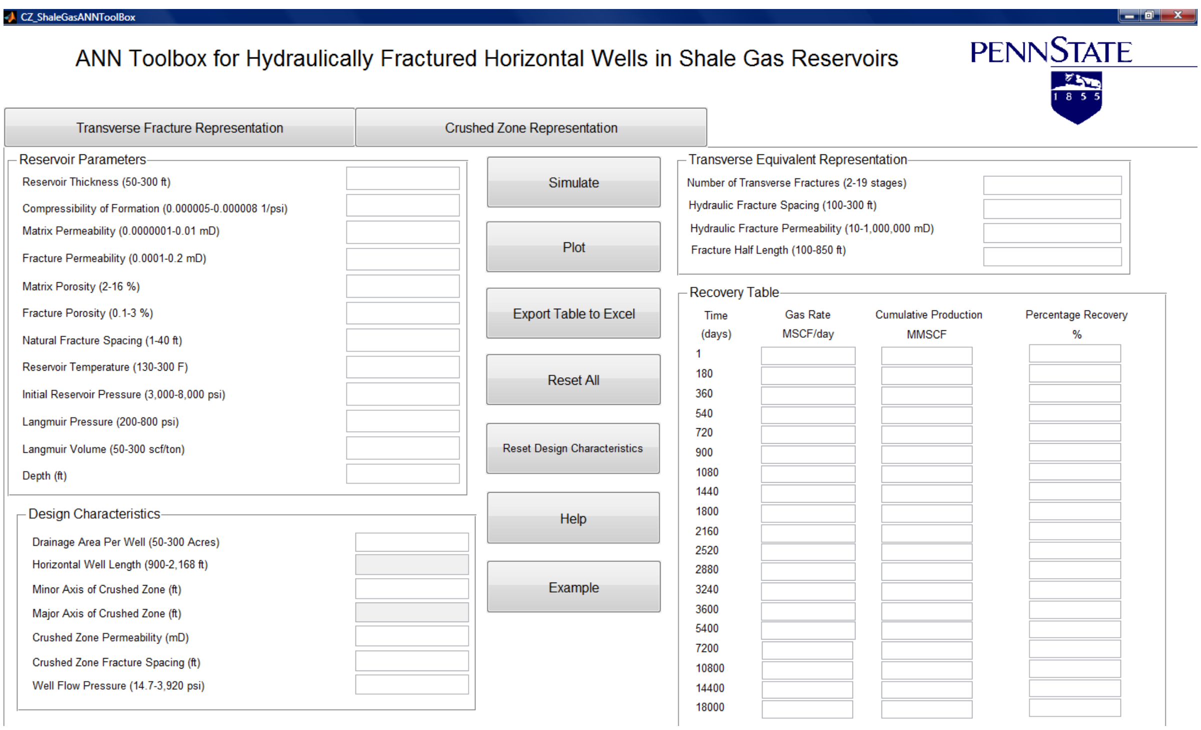

Figure A-1: Main GUI Window

5) Insert reservoir parameters and design characteristics into the relevant boxes or click on the Example button to allow the GUI to give out a pre-determined set of values

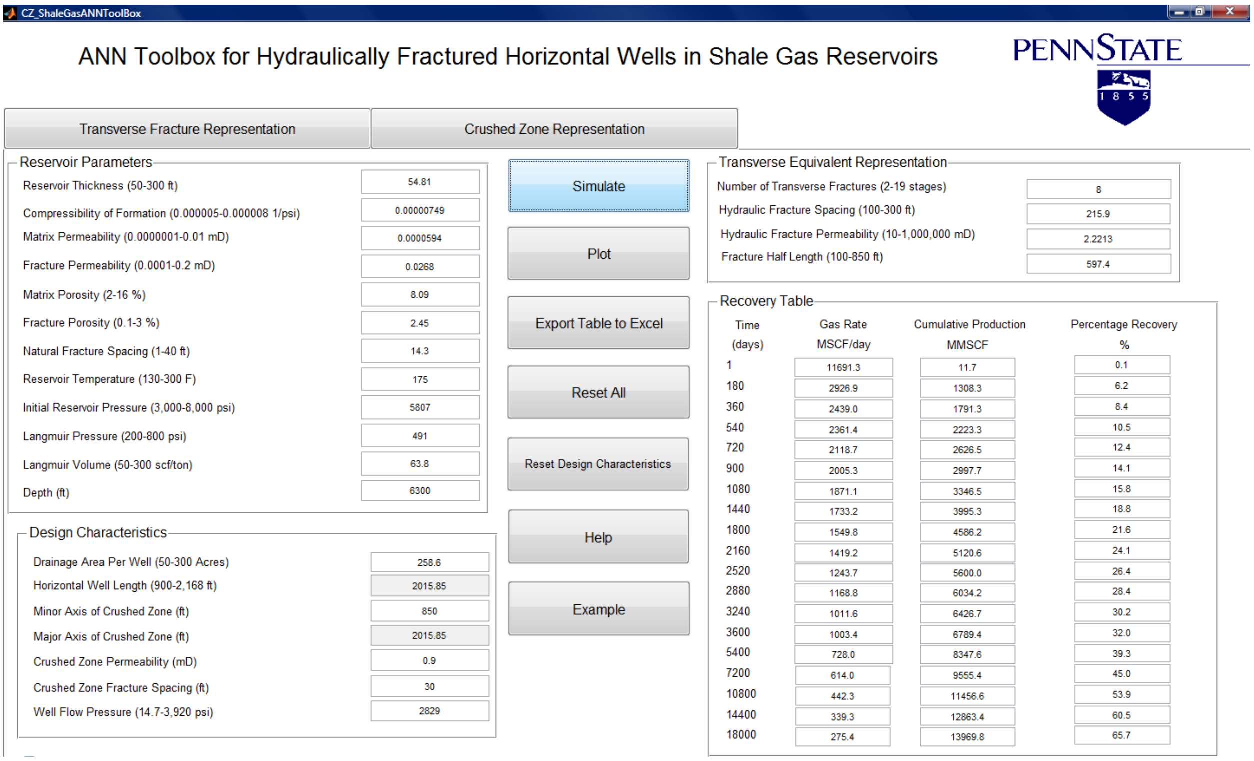

Figure A-2: Main GUI Window after pressing the Example button

6) Grayed out boxes indicate that these values are automatically calculated from parameters entered such as:

-Horizontal Well Length is always fixed at 60% of the reservoir length

-Major Axis of Crushed Zone is always equal to the Horizontal Well Length

7) Once all parameters are inserted within the acceptable range (listed in brackets besides the parameter name), click on Simulate to start ANN (Artificial Neural Network) calculation. Equivalent parameter s will then be shown in the Transverse Equivalent Representation while the Gas Rate, Cumulative Production and the Percentage Recovery are shown in the Recovery Table.

8) Click on the Plot button to plot Production Rate, Cumulative Production, Crushed Zone Representation and an Equivalent Transverse Fracture Representation on another pop-up window as shown in Figure A-3 below

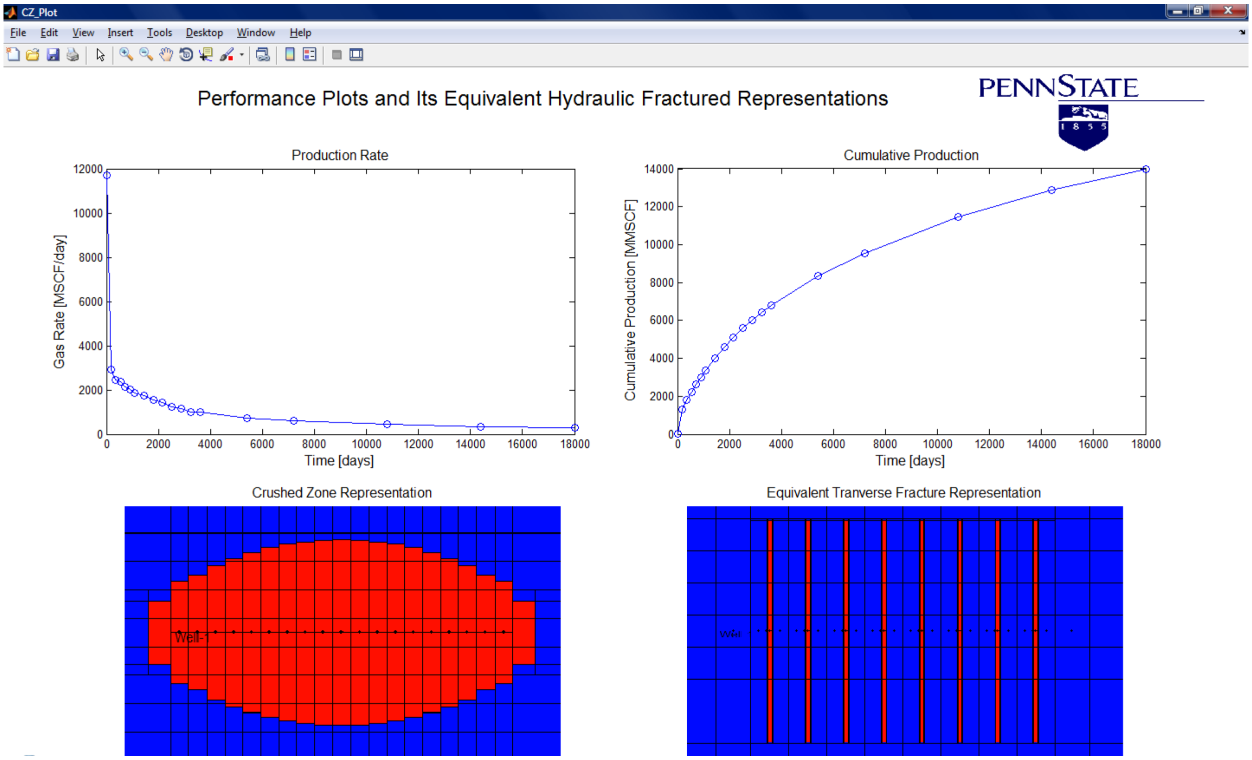

Figure A-3: Plot and Graphical Representation Figure

9) To export data to excel click on the "Export Table to Excel" button. This will create a new excel spread sheet called "CZ_ANN_Output" as shown in Figure A-4 below

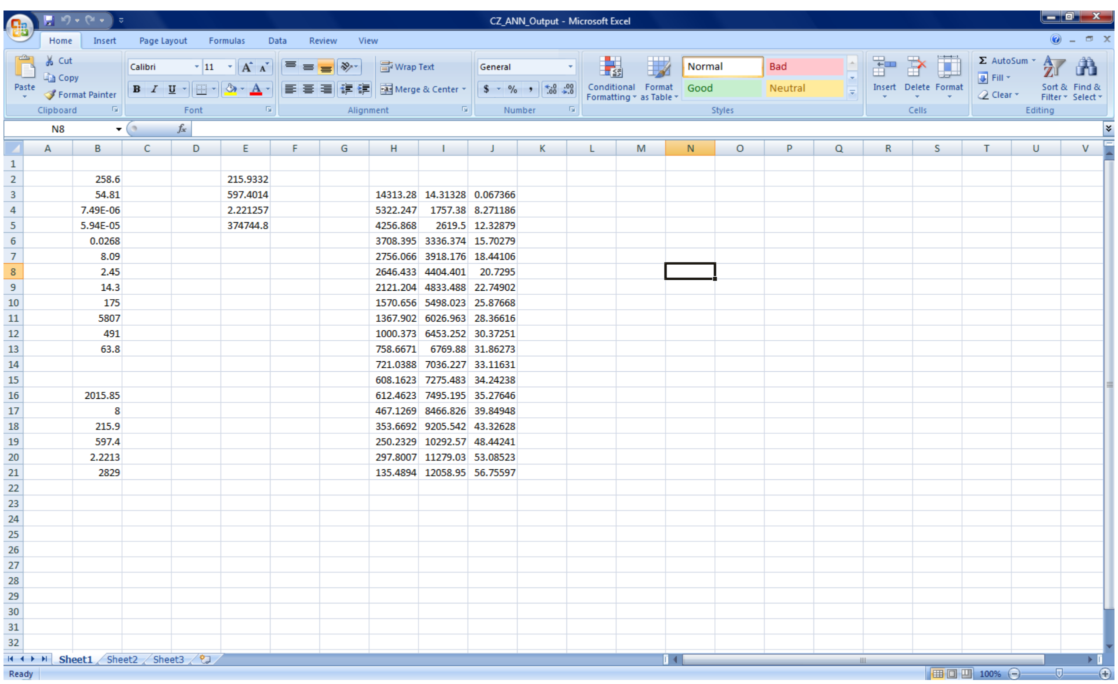

	A	B	C	D	E	F	G	H	I	J
1										
2		258.6			215.9332					
3		54.81			597.4014			14313.28	14.31328	0.067366
4		7.49E-06			2.221257			5322.247	1757.38	8.271186
5		5.94E-05			374744.8			4256.868	2619.5	12.32879
6		0.0268						3708.395	3336.374	15.70279
7		8.09						2756.066	3918.176	18.44106
8		2.45						2646.433	4404.401	20.7295
9		14.3						2121.204	4833.488	22.74902
10		175						1570.656	5498.023	25.87668
11		5807						1367.902	6026.963	28.36616
12		491						1000.373	6453.252	30.37251
13		63.8						758.6671	6769.88	31.86273
14								721.0388	7036.227	33.11631
15								608.1623	7275.483	34.24238
16		2015.85						612.4623	7495.195	35.27646
17		8						467.1269	8466.826	39.84948
18		215.9						353.6692	9205.542	43.32628
19		597.4						250.2329	10292.57	48.44241
20		2.2213						297.8007	11279.03	53.08523
21		2829						135.4894	12058.95	56.75597

Figure A-4: Exported excel sheet

10) To reset all data, click on the Reset button. To reset only the design characteristics, click on the Reset Design Characteristics button.

11) Click on the Help button to open this user manual, which is attached as an appendix to the Thesis report. The report is useful for providing background information on this project.

12) Note that warnings may pop up if an error occurs, such as when the input parameters are out of range or at the extreme end of the range which may result in an illogical output

Appendix B

MATLAB Codes

The MATLAB Codes for Generating data sets are shown here:

```
% %%%%  Data Input Generation for CMG
clear
clc
loadInput.txt

length_input = length(Input);

fori=1:length_input
number = num2str(i);
%% Number of Cases  for CMG
n = 20;
%% 1) edge  l = Edge  Length
for run=1:n
edge_l(1,run) = Input(i,1);
end
%% 2) h = Reservoir Thickness
for run=1:n
h(1,run) = Input(i,2);
end
%% 3) k_m = Matrix Permeability
for run=1:n
k_m(1,run) = Input(i,3);
end
%% 4) k_f = Fracture Permeability
for run=1:n
k_f(1,run) = Input(i,4);
end
%% 5) phi_m  = Matrix Porosity
for run=1:n
phi_m(1,run)  = Input(i,5);
end
%% 6) phi_f = Fracture Porosity
for run=1:n
phi_f(1,run) = Input(i,6);
end
%% 7) Ti  = Initial Temperature
for run=1:n
Ti(1,run) = Input(i,7);
end
%% 8) Pi  = Initial Pressure
for run=1:n
Pi(1,run)  = Input(i,8);
end
%% 9) Depth = Depth of reservoir
```

```
for run=1:n
Depth(1,run) = Input(i,9);
end
%% 10) C = Compressibility of Formation
for run=1:n
C(1,run) = Input(i,10);
end
%% 11) Lang_P = Langmuir Pressure
for run=1:n
Lang_P(1,run) = Input(i,11);
end
%% 12) Lang_V = Langmuir Volume
for run=1:n
Lang_V(1,run) = Input(i,12);
end
%% 13) nfrac = Number of Fractures

nfracbad = zeros(1,n);

%% 14) Length of Horizontal Wellbore

for loop=1:n
HW_l(1,loop)  = edge_l(1,loop)*0.6;
end

%% 15) First and  Last  Grid  Length on X Direction
x = (edge_l - HW_l)/4;

%% 16) Number of Grids on X Direction
badGrid =  zeros(1,n);

Length = zeros(1,n);


%% 18) Distance Between Fractures on Well

dummy18 = zeros(1,n);


%% 19) gamma = Specific Gravity
gamma = unifrnd (0.6  , 0.9 , [1,n]);
%% 20) Psf  = Pressure Specified (production pressure)
for run=1:n
Psf(1,run) = Input(i,15);
end
%% 21) Total Number of Blocks in x-direction
Grid = zeros(1,n);

%% 22) Fracture_S = Fracture Spacing
Fracture_S = unifrnd(100,200,[1,n]);
%% 23) frac_w = Width of Fracture
for loop=1:n
```

```
frac_w(1,loop) = 0.05;
end
%% 24) frac_l = Fracture Half Length

frac_l = unifrnd(edge_l/5,edge_l/4,[1,n]);


%% 25) First and Last Grid Length on Y Direction
y = (edge_l - frac_l)/2;
%% 26) frac_k = Permeability of Fracture

frac_kk = unifrnd(log10(1000),log10(1000000),[1,n]);

for mm=1:n
frac_k(1,mm) = 10^(frac_kk(1,mm));
end

%% 27) j_WellStart = Starting block for well (j-direction)

j_WellStart = round(Grid/2);


%% 28) i_WellStart = Starting block for well (i-direction)
dummy28 = zeros(1,n);
%% 29) i_WellEnd = Ending block for well (i-direction)

i_WellEnd = zeros(1,n);
% i_WellEnd = i_WellStart + HW_l;

%% 30) Length of Horizontal Well (in blocks)


Well_Blocksbad = zeros(1,n);


%% 31) Number of Fractures controlled by fracture spacing

for whatever=1:n
nfrac(1,whatever) = round(HW_l(1,whatever)/Fracture_S(1,whatever))-1;
end

%% 32) Number of Grids on X Direction
xGrid = nfrac + 5;

%% 33) Length of Horizontal Well (in blocks)
for whatever=1:n

Well_Blocks(1,whatever) = nfrac(1,whatever)+2;
end

%% 34) Starting Block for Well
```

```
forsmth=1:n
i_WellStart(1,smth) = ((nfrac(1,smth) + 5) - HW_l(1,smth))/2;
end

%% 35) Distance Between Fractures on Well
% Also known as WELL BLOCK SIZE!!!!

m = HW_l./(nfrac+1);

%% 36) Natural Fracture Spacing

for run=1:n
nat_frac_s(1,run)  = Input(i,14);
end
%% data = Compilation of All Parameters
indata=[edge_l;h;k_m;k_f;phi_m;phi_f;Ti;Pi;Depth;C;Lang_P;Lang_V;nfracb
ad;HW_l;x;badGrid;Length;dummy18;gamma;Psf;Grid;Fracture_S;frac_w;frac_
l;y;frac_k;j_WellStart;dummy28;i_WellEnd;Well_Blocksbad;nfrac;xGrid;Wel
l_Blocks;i_WellStart;m;nat_frac_s];
%
input=[A;h;k_m;k_f;phi_m;phi_f;Ti;Pi;Depth;C;Lang_P;Lang_V;Crushed;HW_l
;gamma;Psf ];
%% Exporting  Files
% save input.txt input -ASCII
% fOut = sprintf('indata%d',number);
indata_name = ['indata',number,'.txt'];
%
save(indata_name,'indata','-ASCII')
% save indata.txt indata -ASCII -append

end
```

MATLAB Code for Training the ANN is shown here:

```
function net = ANN_Kanin(inputs,targets)
%ANN_Kanin Creates and trains a fitting neural network.
%
%  NET = CREATE_FIT_NET(INPUTS,TARGETS) takes these arguments:
%    INPUTS - RxQ matrix of Q R-element input samples
%    TARGETS - SxQ matrix of Q S-element associated target samples
%  arranged as columns, and returns these results:
%    NET - The trained neural network
%
%  For example, to solve the Simple Fit dataset problem with this
function:
%
%    load simplefit_dataset
%    net = create_fit_net(simplefitInputs,simplefitTargets);
%    simplefitOutputs = sim(net,simplefitInputs);
%
%  To reproduce the results you obtained in NFTOOL:
```

```
%
%    net = create_fit_net(Input,Output);

%% Number of Data Set
r=596;

%% Load data
loadInput.txt
loadOutput.txt
loadtime.txt

Input = Input';
Output = Output';


%% Eigenvalue Calculations
lambda1 = zeros(length(Input(1,:)),1);
lambda2 = zeros(length(Input(1,:)),1);
lambda3 = zeros(length(Input(1,:)),1);
lambda4 = zeros(length(Input(1,:)),1);
lambda5 = zeros(length(Input(1,:)),1);
fori=1:length(Input(1,:));
A1 = [log10(Input(15,i)) Input(14,i); Input(10,i) log10(Input(4,i))]; %
Crushed Perm, Crushed Zone Minor Axis Length, Psf, k_f
A2 = [Output(1,i) Input(22,i); Input(10,i) log10(Input(4,i))]; % q1,
Cumulative Gas Production, Psf, k_f
A3 = [Output(1,i) log(Input(15,i)); Input(14,i) Input(22,i)]; % q1,
Crushed Perm, Crushed Zone Minor Axis Length, Cumulative Gas Production
A4 = [Input(7,i) Input(8,i); Input(12,i) Input(13,i)]; % Ti, Pi,
Langmuir Pressure, Langmuir Volume
A5 = [log10(Input(15,i)) Input(14,i);Input(12,i) Input(13,i)]; %
Crushed Perm, Crushed Zone Minor Axis Length,Langmuir Pressure,
Langmuir Volume
lambda1(i) = max(abs(eig(A1)));
lambda2(i) = max(abs(eig(A2)));
lambda3(i) = max(abs(eig(A3)));
lambda4(i) = max(abs(eig(A4)));
lambda5(i) = max(abs)eig(A5)));
end
lambda1 = transpose(lambda1);
lambda2 = transpose(lambda2);
lambda3 = transpose(lambda3);
lambda4 = transpose(lambda4);
lambda5 = transpose(lambda5);


%% Input & Output
% [column_In,row_In]=size(Input);
% [column_Out,row_Out]=size(Output);
%
%
% Input(:,[column_In,row_In])=Input(:,[row_In,column_In]);
% Output(:,[column_Out,row_Out])=Output(:,[row_Out,column_Out]);
```

```
inputs =
[Input(1:3,1:r);log10(Input(4:5,1:r));Input(6:14,1:r);log10(Input(15,1:
r));Input(16:19,1:r);lambda1;lambda4;lambda5;Input(20:22,1:r)];
targets = [Output(1:19,1:r);lambda2;lambda3]; % Trying without
Cumulative Production functional links
%*** functional links into targets(outputs)*****
% edge_length/qi, km*h, kf*h, porosity*h, Pi*A, A*Length,
Crushed_Perm*Crushed_Size, Pi/Psf, k/(visocity*c) <---[hydrualic
diffusivity]




%% Training
P = inputs;
T = targets;
%Normalizing the data
%Pn stands for normalized input and Tn stands for normalized output
[Pn,ps] = mapminmax(P,0,1); % gives all values between -1 & 1
[Tn,ts] = mapminmax(T,0,1); % gives all values between -1 & 1
% [Tn,ts] = mapminmax(T,-1,1); % gives all values between -1 & 1
[mi,ni] = size(Pn);
[mo,no] = size(Tn);
%defining some variables required in the network
N_in = mi; % number of inputs in the network
N_out = mo; % number of outputs in the network
Tot_in = ni; %total no. of simulations
% N_train = 215;
% % N val = 50;
% N_test = 43;
%seperating training, testing & validation data when random
%selection command is available through higher version dividing random
[Pn_train,Pn_val,Pn_test,trainInd,valInd,testInd] =
dividerand(Pn,0.90,0.05,0.05);
[Tn_train,Tn_val,Tn_test] = divideind(Tn,trainInd,valInd,testInd);
val.T = Tn_val;
val.P = Pn_val;
test.T = Tn_test;
test.P = Pn_test;

% Create Network


NNeu1 = 25;
NNeu2 = 25;
NNeu3 = 25;
NNeu4 = 25;
net =
newff(Pn,Tn,[NNeu1,NNeu2,NNeu3,NNeu4,mo],{'tansig','tansig','tansig','t
ansig','purelin'},'trainscg','learngdm','msereg');
```

```
% net =
newcf(Pn,Tn,[NNeu1,NNeu2,NNeu3,NNeu4,mo],{'tansig','tansig','tansig','l
ogsig','logsig'},'traincgf','learngdm','msereg');
% net.divideParam.trainRatio = 70/100;  % Adjust as desired
% net.divideParam.valRatio = 15/100;  % Adjust as desired
% net.divideParam.testRatio = 15/100;  % Adjust as desired

%setting training parameters for the network
net.trainParam.goal = 0.0001; %accuracy within this range
net.trainParam.epochs = 15000; % number of iteration sets
net.trainParam.show = 1;
net.trainParam.max_fail = 100000;
net.trainParam.mem_reduc = 60; %

% Train and Apply Network
% [net,tr] = train(net,inputs,targets);
[net,tr] = train(net,Pn_train,Tn_train,[],[],test,val);


% Plot
plotperf(tr)
% plotfit(net,inputs,targets)
% plotregression(targets,outputs)


% pause
%|||||||||||||||||||||||||{
%|||{getting data from the trained network ||||||||-
%|||||||||||||||||||||||||{
Tn_train_ann = sim(net,Pn_train);
Tn_test_ann = sim(net,Pn_test);
%denormalizing the data sets obtained
%output reversal
T_train = mapminmax('reverse',Tn_train,ts);
T_test = mapminmax('reverse',Tn_test,ts);
T_train_ann = mapminmax('reverse',Tn_train_ann,ts);
T_test_ann = mapminmax('reverse',Tn_test_ann,ts);
%input reversal
Pn_train = mapminmax('reverse',Pn_train,ps);
Pn_val = mapminmax('reverse',Pn_val,ps);
Pn_test = mapminmax('reverse',Pn_test,ps);



%% Gas Rate and Cumulative Production Error Errors
% *** Gas Rate Error at Various Times ***
error_q1 = abs((T_test(1,:) - T_test_ann(1,:))./T_test(1,:))*100;
error_mean_q1 = mean(error_q1);
error_q2 = abs((T_test(2,:) - T_test_ann(2,:))./T_test(2,:))*100;
error_mean_q2 = mean(error_q2);
error_q3 = abs((T_test(3,:) - T_test_ann(3,:))./T_test(3,:))*100;
error_mean_q3 = mean(error_q3);
error_q4 = abs((T_test(4,:) - T_test_ann(4,:))./T_test(4,:))*100;
```

```
error_mean_q4 = mean(error_q4);
error_q5 = abs((T_test(5,:) - T_test_ann(5,:))./T_test(5,:))*100;
error_mean_q5 = mean(error_q5);
error_q6 = abs((T_test(6,:) - T_test_ann(6,:))./T_test(6,:))*100;
error_mean_q6 = mean(error_q6);
error_q7 = abs((T_test(7,:) - T_test_ann(7,:))./T_test(7,:))*100;
error_mean_q7 = mean(error_q7);
error_q8 = abs((T_test(8,:) - T_test_ann(8,:))./T_test(8,:))*100;
error_mean_q8 = mean(error_q8);
error_q9 = abs((T_test(9,:) - T_test_ann(9,:))./T_test(9,:))*100;
error_mean_q9 = mean(error_q9);
error_q10 = abs((T_test(10,:) - T_test_ann(10,:))./T_test(10,:))*100;
error_mean_q10 = mean(error_q10);
error_q11 = abs((T_test(11,:) - T_test_ann(11,:))./T_test(11,:))*100;
error_mean_q11 = mean(error_q11);
error_q12 = abs((T_test(12,:) - T_test_ann(12,:))./T_test(12,:))*100;
error_mean_q12 = mean(error_q12);
error_q13 = abs((T_test(13,:) - T_test_ann(13,:))./T_test(13,:))*100;
error_mean_q13 = mean(error_q13);
error_q14 = abs((T_test(14,:) - T_test_ann(14,:))./T_test(14,:))*100;
error_mean_q14 = mean(error_q14);
error_q15 = abs((T_test(15,:) - T_test_ann(15,:))./T_test(15,:))*100;
error_mean_q15 = mean(error_q15);
error_q16 = abs((T_test(16,:) - T_test_ann(16,:))./T_test(16,:))*100;
error_mean_q16 = mean(error_q16);
error_q17 = abs((T_test(17,:) - T_test_ann(17,:))./T_test(17,:))*100;
error_mean_q17 = mean(error_q17);
error_q18 = abs((T_test(18,:) - T_test_ann(18,:))./T_test(18,:))*100;
error_mean_q18 = mean(error_q18);
error_q19 = abs((T_test(19,:) - T_test_ann(19,:))./T_test(19,:))*100;
error_mean_q19 = mean(error_q19);

% *** Cumulative Production Error ***
Error_GPC = abs((T_test(20,:) - T_test_ann(20,:))./T_test(20,:))*100;
Error_mean_GPC = mean(Error_GPC);
%% Error Analysis
% *** Error for Each Test at Various Times ***
Error_each_test = [error_q1; error_q2; error_q3; error_q4; error_q5;
error_q6; error_q7; error_q8; error_q9; error_q10; error_q11;
error_q12; error_q13; error_q14; error_q15; error_q16; error_q17;
error_q18; error_q19];
% *** Overall Error for Each Test ***
Error_overall = mean(Error_each_test);
Error_mean_overall = mean(Error_overall);




%% Saves the ANN tool
saveperf.mat
```

Appendix C

Data Sets

This appendix includes some of the sample data sets used for training and testing the the ANNS.

Table C-1– Data Set Sample Crushed Zone Set 1

data	edge_l	h	k_m	k_f	phi_m	phi_f	Ti	Pi	Depth	C	Lang_P	Lang_V
2	3176.089	149.01	3.99E-06	0.000723	0.114681	0.002736	208.4519	4583.23	11195.02	0.001148	596.939	155.3986
12	3058.332	141.3744	0.000134	0.000533	0.150312	0.003336	217.8293	1041.33	13097.75	0.001191	200.6532	196.3506
31	1615.73	89.72445	2.06E-07	0.001705	0.133094	0.001448	200.205	7257.869	8785.711	0.004099	423.1904	190.5232
32	2823.659	117.0855	1.62E-06	0.001324	0.069715	0.007091	236.7821	7655.017	9558.019	0.003407	624.5636	136.4409
39	2455.841	121.7643	1.21E-06	0.004571	0.099776	0.001084	261.762	1800.809	11911.39	0.002252	465.9502	147.2377
53	1860.093	73.45076	0.000147	0.00407	0.126002	0.008889	269.862	1076.679	9775.323	0.002475	292.6342	129.4264
64	1371.391	224.5893	2.51E-05	0.003016	0.159057	0.003257	230.9481	1344.138	9692.992	0.002544	375.6102	138.5095
66	2443.031	89.41479	3.29E-07	0.005021	0.058508	0.001748	230.7806	3241.468	4455.354	0.000554	725.5837	65.29194
77	2660.349	62.10668	5.59E-05	0.002314	0.138369	0.00393	290.8217	1396.782	7312.283	0.000325	215.7736	131.6207
79	1819.896	231.3723	1.95E-05	0.000983	0.137257	0.027318	236.3187	1020.73	5962.581	0.002717	346.0296	61.85754
88	2287.838	52.04458	1.31E-06	0.000131	0.067017	0.001592	178.2994	1448.412	8870.312	0.004888	266.4786	129.8536
92	3448.255	67.5025	0.000821	0.00226	0.059372	0.003583	282.3501	5315.282	7248.937	0.003627	682.4796	68.90375
93	3053.859	85.67198	1.03E-06	0.00638	0.134817	0.004339	235.2087	1859.432	13766.71	0.003431	505.898	128.7461
103	3345.339	66.23017	0.000185	0.001123	0.142906	0.01996	153.3381	1662.2	5405.906	0.002299	725.7528	184.7103
118	3402.373	60.06134	0.000431	0.000696	0.03322	0.00999	175.6108	3938.581	6535.712	0.002125	311.2706	81.95791
125	2852.432	213.8286	0.000148	0.000966	0.050746	0.01543	290.7843	1313.688	8962.366	0.003204	372.7029	89.44672
149	2738.351	104.337	2.87E-06	0.005538	0.155703	0.006275	202.2919	6578.507	14397.44	0.00176	285.0775	53.66123
162	2934.451	126.5759	0.000136	0.002229	0.095378	0.025908	197.0501	1285.65	13437.61	0.004409	396.9613	90.425
165	3226.068	118.7532	4.82E-06	0.004546	0.029194	0.003631	209.2843	1465.435	3536.686	0.003639	410.1773	72.91773
167	2890.961	91.63687	8.42E-06	0.007916	0.036386	0.02357	207.3857	1380.524	1438.407	0.004521	203.6927	54.70706
171	2820.537	87.11906	1.09E-07	0.000399	0.112621	0.022255	152.103	1191.581	1695.595	5.14E-05	588.8604	184.7464
176	1985.741	72.61448	8.29E-06	0.00061	0.132737	0.003189	292.37	4334.899	6024.109	0.004761	277.7712	181.1473
195	2354.274	52.16712	3.67E-06	0.005488	0.070137	0.004642	226.9565	3495.389	11760.93	0.00218	373.5102	86.29568
199	1587.818	180.8824	3.55E-06	0.003002	0.027342	0.004126	195.1748	1685.051	4327.422	0.001225	617.8146	101.7072

201	3513.654	133.0947	5.73E-05	0.002282	0.131956	0.019026	181.8568	1672.171	2900.533	0.003296	694.4896	139.2298
211	2219.363	258.4258	2.86E-05	0.001713	0.04353	0.026989	183.5061	1031.132	1244.723	0.003284	497.523	191.092
215	1949.221	83.5621	8.77E-07	0.000119	0.0542	0.013642	141.6051	3695.907	8193.906	0.002622	560.2445	162.631
226	1702.11	244.8708	4.19E-07	0.004414	0.034183	0.001294	253.23	6260.686	6297.268	0.000894	342.5068	159.3571
229	3465.426	81.99567	1.32E-07	0.000109	0.063652	0.002626	273.3053	1814.034	12259.31	0.004342	426.7088	103.3114
244	2465.666	51.0741	1.11E-07	0.002563	0.093126	0.001707	194.397	6334.983	2960.329	0.003819	467.9579	198.5585
256	2752.848	195.2233	4.74E-05	0.00049	0.041378	0.005123	262.2913	1782.33	6558.787	0.002778	432.8228	65.77116
260	3212.165	79.43024	8.33E-07	0.001543	0.099837	0.019586	148.7254	1266.086	1469.018	0.003431	450.4911	92.58762
266	3518.287	98.78752	1.05E-06	0.007201	0.05573	0.001261	293.8295	6554.472	7662.008	0.001112	292.9493	139.4239
269	1499.828	104.351	4.98E-05	0.000829	0.027826	0.007323	149.8564	2665.947	3660.389	0.002003	466.3234	133.5858
278	2076.655	114.9673	0.000147	0.002034	0.034945	0.002852	233.2531	1700.274	8387.972	0.001708	362.0148	194.9883
285	3543.084	286.5619	5.11E-05	0.000784	0.031502	0.026558	150.7131	1815.85	3291.389	0.003013	545.9816	146.986
288	3483.115	127.5173	6.01E-05	0.002274	0.114899	0.009788	151.6069	1628.669	7247.714	0.00461	439.0379	193.7263

Table C-2– Data Set Sample Crushed Zone Set 2

data	edge_l	h	k_m	k_f	phi_m	phi_f	Ti	Pi	Depth	C	Lang_P	Lang_V
16	1830.122	163.4494	8.15E-07	0.000503	0.022696	0.0074	268.3761	1759.055	5647.851	0.004168	736.0846	98.37224
17	2553.253	158.0979	9.83E-06	0.00235	0.031742	0.001038	282.7355	1252.798	12756.49	0.001023	479.492	196.422
19	3273.32	70.86745	1.99E-05	0.001151	0.111189	0.005132	186.836	4970.011	12595.01	0.004375	496.6738	60.92462
22	1465.215	147.7345	2.21E-05	0.000468	0.037083	0.005021	249.3513	5637.613	13318.37	0.004499	373.1392	188.3507
27	3187.291	181.719	4.4E-05	0.001308	0.068721	0.014997	221.818	1211.891	6317.745	0.00235	593.3667	173.1125
31	3120.704	122.996	0.000119	0.000178	0.150206	0.002982	145.8081	7230.254	3195.31	0.000666	323.1088	85.23897
38	2309.49	99.5296	8.65E-06	0.000824	0.116071	0.02311	165.4399	1463.121	10912.15	0.003612	232.2946	189.8455
39	3536.133	172.4219	0.00024	0.000303	0.145109	0.001213	207.3442	2928.02	3010.926	0.001698	717.3125	153.1479
58	2365.898	82.0036	9.92E-06	0.001207	0.0985	0.01383	221.2539	1247.964	4556.11	0.000331	414.0235	62.6387
60	2068.14	92.78027	6.04E-06	0.000118	0.124863	0.001962	189.0864	3854.111	10835.42	2.67E-05	266.0291	130.8966
69	1852.902	89.10124	4.66E-06	0.00023	0.113592	0.002413	196.8188	2537.769	7067.918	0.000346	471.6935	88.05772
75	3502.409	170.5055	4.63E-07	0.000212	0.157327	0.028736	299.9112	1413.667	13017.63	0.000605	620.3477	155.885
82	3339.466	122.6102	1.79E-07	0.000287	0.096882	0.001035	199.2681	3578.456	11707.03	0.003704	462.1597	94.66928
84	2822.827	116.3202	0.000547	0.003425	0.100746	0.021289	223.1826	1120.208	1795.385	0.003343	374.5162	108.2534
90	2858.902	76.94225	3.93E-06	0.004288	0.151199	0.023085	210.0298	1661.42	13838.79	0.004378	538.9977	85.41938
92	1534.085	269.9134	1.33E-07	0.004257	0.138872	0.017706	137.3764	1100.535	13418.43	0.000711	361.887	197.6673
96	1792.67	55.62815	2.15E-06	0.001868	0.15069	0.015628	152.7427	1477.263	10754.01	0.003357	219.5795	75.03346

110	3196.196	129.8999	2.97E-07	0.000695	0.140981	0.012388	141.4279	1597.785	13583.18	0.00108	233.1883	193.3844
119	1621.044	76.4073	0.000187	0.000339	0.040843	0.021864	288.4712	1515.17	5774.91	0.000453	350.2057	182.1271
124	3243.259	116.6179	1.22E-05	0.001906	0.126762	0.004367	275.3374	3068.739	13032.72	0.000551	785.8007	72.88071
149	1955.829	200.5426	2.36E-07	0.000149	0.081391	0.002781	179.8726	1864.506	2197.731	0.00491	677.385	190.2671
161	3252.572	93.9686	3.34E-05	0.000189	0.092151	0.018988	221.5622	2975.436	13549.74	0.002762	312.0557	64.39175
163	2116.53	168.3715	2.11E-07	0.000231	0.153128	0.006006	258.3875	1254.979	1197.303	0.002941	232.5133	172.9263
170	1555.455	279.3561	1.5E-06	0.009305	0.042946	0.007667	275.7187	1948.347	7068.088	0.003151	399.1985	55.05377
177	3015.63	220.8408	8.3E-05	0.000308	0.10836	0.015831	167.2782	1205.326	1498.268	0.000804	286.3705	133.5246
178	3166.954	186.6483	6.75E-05	0.00039	0.140305	0.002758	185.3871	4695.179	13407.29	0.003336	710.3646	156.8038
179	3013.057	156.4322	0.000134	0.002293	0.156391	0.022045	146.3114	1224.51	4457.179	9.45E-05	402.7218	123.1866
186	1954.68	227.3204	2.24E-06	0.001469	0.088853	0.014114	292.7823	1334.511	9307.888	0.001218	633.7061	89.42912
188	2971.179	79.84906	9.23E-05	0.000146	0.144283	0.004186	190.6056	1144.326	10347.55	0.004069	307.2967	143.4386
194	2584.33	137.5545	0.000157	0.00593	0.13461	0.010044	151.3412	1491.495	10106.43	0.001897	731.5547	92.59085
195	2608.159	215.5024	8.66E-05	0.000812	0.144073	0.009452	269.807	1484.953	13003.24	0.003162	328.3022	142.3089
223	2571.917	141.454	6.67E-07	0.000158	0.074095	0.001955	246.1421	7288.634	1386.806	0.00343	266.5221	173.5556
224	1958.458	240.8762	2.22E-07	0.000954	0.128578	0.002562	293.5594	6099.108	13588.19	0.002334	425.126	171.5922
256	2968.207	54.89441	8.92E-06	0.002892	0.140942	0.006619	272.9847	3081.48	3453.352	0.000254	322.1024	58.37725
259	2429.782	117.5676	1.24E-06	0.000626	0.035122	0.002136	227.2807	3180.328	4766.149	0.003735	232.1451	113.262
269	1813.545	144.3489	3.17E-07	0.003259	0.057999	0.020689	235.795	1004.611	4761.973	0.002661	770.0204	196.4947
273	2709.099	131.8914	4.93E-06	0.00882	0.126804	0.007722	215.0848	1295.774	10532.59	0.002581	284.6899	89.1497
291	1952.974	183.516	1.67E-05	0.002692	0.141364	0.02166	157.0381	1243.437	8944.021	0.004988	661.9603	93.05221
292	2111.818	72.48767	5.47E-07	0.005157	0.076949	0.001484	170.2696	3049.821	14562.89	0.002589	697.7485	104.288

Table C-3– Data Set Sample Crushed Zone Set 10

match number	data	edge_l	h	k_m	k_f	phi_m	phi_f	Ti	Pi	Depth	C	Lang_P	Lang_V
1	20	3497.58	66.26193	0.000459	0.002751	0.103286	0.0185	248.0842	7108.437	5386.36	2.19E-05	592.2644	96.23728
2	22	1460.43	158.6095	2.87E-06	0.001488	0.037269	0.002093	280.0221	6698.355	7639.609	0.003827	572.991	170.0194
3	30	1901.073	84.32981	3.15E-06	0.003502	0.123361	0.001553	175.1698	5829.548	10660.58	0.000409	447.9854	135.2804
4	32	1445.838	73.51681	1.12E-07	0.000551	0.083306	0.010039	182.6788	1782.243	2068.076	0.003388	409.2532	91.64353
5	40	1455.685	175.8126	1.21E-05	0.000858	0.076395	0.006759	152.7565	3722.513	3461.128	0.004757	638.8154	124.4592
6	45	1945.657	61.66898	0.000152	0.000406	0.138842	0.026369	203.8201	1392.268	5873.156	0.004596	607.6764	123.716
7	47	2571.817	109.2685	1.21E-07	0.001062	0.122117	0.006746	251.8961	6743.276	7514.937	0.001097	622.0512	55.59744
8	51	2181.82	227.7216	0.000832	0.001141	0.042617	0.008572	236.0292	2632.674	6554.322	0.001886	296.9764	66.12737

9	60	2046.817	98.29291	2.93E-05	0.00052	0.114464	0.009766	205.2783	7596.821	11290.97	0.000444	222.3542	154.3478
10	92	1527.176	72.58816	0.000705	0.001384	0.122411	0.00382	261.7151	2642.882	6424.412	0.004951	483.1452	194.3428
11	94	3203.353	83.71021	0.000323	0.001408	0.033425	0.001154	172.6135	4506.143	10794.85	0.004167	420.686	123.6918
12	99	1368.405	86.42597	1.58E-06	0.008896	0.147753	0.002942	290.8583	1953.941	6231.825	0.000342	746.3219	135.8446
13	100	2329.882	64.1938	7.37E-05	0.000838	0.085092	0.02331	220.3485	1235.007	6916.226	0.003977	207.8665	156.3634
14	113	2060.566	177.6432	4.52E-05	0.000445	0.074008	0.004449	164.8879	6812.235	2730.049	0.001463	729.5752	180.4051
15	119	1611.564	188.9187	0.000107	0.000235	0.117035	0.00247	205.1318	3356.887	8410.639	0.003883	208.3914	191.194
16	123	1339.055	110.2163	2.29E-07	0.000644	0.085781	0.005836	254.3621	1944.905	9997.932	0.002908	788.9709	68.26268
17	135	1825.831	55.07591	1.01E-05	9.27E-05	0.098555	0.004589	208.0101	5840.178	3992.253	0.001269	336.222	147.7791
18	136	1797.252	80.0063	0.000388	0.00306	0.033987	0.010358	260.4053	4104.042	5905.115	0.003517	508.4806	196.694
19	146	1604.053	62.88782	0.000348	0.001558	0.079078	0.013825	152.2672	3227.701	12541.56	0.004601	396.9506	197.3374
20	147	2089.387	168.4968	3.26E-07	0.00521	0.15712	0.008166	138.3288	2199.704	11445.29	0.00113	449.3793	181.865
21	150	2089.482	100.3186	0.00043	0.00282	0.108015	0.016721	229.4744	6536.398	9497.79	0.004992	608.7174	192.363
22	152	1511.721	96.37732	2.73E-05	0.000192	0.113322	0.010165	135.1917	1744.921	9284.879	0.001439	330.9559	186.7686
23	153	3407.683	61.23658	2.17E-06	0.000101	0.024281	0.007619	222.0053	2216.345	1407.719	0.000803	715.7401	197.4908
24	154	3474.52	203.4475	0.00051	0.002981	0.097601	0.021429	284.4952	1104.696	6382.802	0.004603	702.2792	116.7057
25	160	1719.954	157.844	9.17E-05	0.003745	0.050512	0.005112	181.8806	2857.901	7150.56	0.004052	569.6708	128.3824
26	165	1672.421	115.8706	1.45E-05	0.001038	0.054611	0.013861	173.9781	5767.085	8868.936	0.004961	765.9017	171.5386
27	166	1784.752	101.0307	1.93E-06	0.000723	0.024799	0.005693	145.2976	3251.707	3568.891	0.000947	414.5338	138.3224
28	170	1547.903	100.4341	4.16E-06	0.002896	0.150468	0.005603	154.6121	6255.475	11855.86	0.000593	518.4788	130.2404
29	174	1382.322	85.08987	1.88E-06	0.000414	0.024847	0.015645	209.5004	3669.664	10199.79	0.003052	508.3576	52.84247
30	175	1487.549	90.95051	0.000206	0.006378	0.141798	0.00163	140.1089	6953.605	1740.597	0.004677	771.8301	173.8969
31	203	3258.199	134.491	0.000296	0.000415	0.091296	0.006496	256.5107	7728.386	3482.375	0.004656	620.1325	80.02032
32	212	2244.125	180.5957	4.61E-05	0.000125	0.14534	0.008675	234.3885	1570.144	7184.834	0.002346	283.8965	192.5101
33	227	2557.501	101.1472	2.27E-06	0.002583	0.11962	0.007886	192.1766	7949.828	8011.831	0.00443	304.0589	175.3091
34	234	3085.21	227.7042	2.15E-06	0.002191	0.116778	0.001589	234.0673	2294.146	13821.1	0.004235	739.1959	96.80431
35	236	1739.596	95.20658	0.000139	0.000676	0.092536	0.004613	277.1221	1948.224	3444.151	0.002941	633.7263	97.72013
36	241	1636.274	265.786	1.51E-06	0.001969	0.135163	0.004182	161.4332	4328.554	5217.17	0.000111	335.07	141.1986
37	244	1435.925	63.90105	6.98E-05	0.000499	0.085284	0.015729	275.2544	4042.545	12843.04	0.001897	262.9582	180.9674
38	249	2082.488	73.40892	0.000451	0.000613	0.127632	0.023446	228.7525	5758.842	4600.049	0.003588	629.6327	52.68311
39	255	2662.291	122.3632	0.000209	0.00327	0.144924	0.005162	256.2605	1991.534	7021.994	0.003178	647.6717	143.3946
40	257	3027.832	122.5786	7.01E-06	0.001162	0.147746	0.001583	245.8621	4756.341	7628.9	0.001795	494.9017	174.5569
41	261	1467.999	202.4568	9.53E-06	0.001495	0.100722	0.002186	264.2811	4084.134	13241.55	0.002987	604.5369	182.367
42	267	2325.735	77.19701	0.000131	0.000363	0.095349	0.007044	226.9688	1394.03	12667.7	0.001522	689.1857	107.4795
43	280	1976.149	120.1145	0.000316	0.008865	0.031713	0.00427	246.4322	5821.194	14130.97	0.001226	454.4182	185.9516

44	296	1891.677	63.31965	0.000498	0.008126	0.076757	0.010401	137.7368	3436.381	9701.595	0.004815	572.9657	95.53883
45	304	1588.57	77.48484	0.000161	0.000724	0.029052	0.011277	207.2885	6789.292	11544.58	0.00482	546.1742	103.142
46	309	3105.034	230.7916	0.000823	0.000868	0.098174	0.023788	234.2454	2840.577	11255.19	0.004655	269.2068	113.9545
47	320	1788.416	194.506	0.000365	0.002045	0.131229	0.018275	176.4238	1072.689	4770.288	0.003558	779.233	97.69651
48	334	3535.777	75.14552	0.000353	0.008819	0.032552	0.007362	163.1794	1982.645	6150.933	0.001616	399.9267	186.2713
49	335	1889.483	121.5759	0.000186	0.003832	0.039053	0.00288	213.3856	5999.329	2356.845	0.002205	720.0892	177.4087
50	336	1704.031	107.9695	3.34E-06	0.000286	0.070872	0.006628	144.2619	7610.758	6111.071	0.003984	419.8104	165.1276
51	338	1977.003	72.9597	5.53E-05	0.000148	0.089853	0.009442	234.9364	4923.331	13733.94	0.0022	349.2864	149.5172
52	343	1522.612	120.9769	6.15E-06	0.002788	0.033705	0.007272	132.4631	7311.54	1216.272	0.003699	666.7284	60.19842
53	351	2244.633	77.34121	2.7E-07	0.001455	0.121494	0.004974	175.0831	3065.729	13844.56	0.004877	251.1413	95.22266
54	353	3004.639	95.99059	1.83E-06	0.004421	0.030952	0.001408	137.4507	7851.803	12565.16	0.001046	498.2672	106.2641
55	354	2763.507	114.8829	8.88E-07	0.000338	0.085107	0.016328	213.3014	1648.674	6337.009	0.00308	747.3512	108.5286
56	360	1900.885	59.93631	3.6E-06	0.003065	0.132387	0.018223	176.9809	4239.007	5993.945	0.003473	363.6791	62.31935
57	364	3009.795	197.3657	7.12E-05	0.000302	0.154028	0.006015	161.9929	1314.756	3290.924	0.004406	488.161	165.9588
58	376	1749.604	178.4902	3.54E-07	0.001709	0.117794	0.01987	283.7754	1238.606	11372.6	0.001687	673.7433	105.5404
59	378	2053.153	202.6239	0.000252	0.001764	0.062457	0.004944	255.7769	6222.281	14769.8	0.004326	446.304	101.0621
60	379	2438.782	81.35997	0.000725	0.006625	0.094614	0.001897	136.1097	6360.215	10563.94	0.001115	412.1116	88.48875
61	389	2851.027	265.3014	1.67E-07	0.000856	0.07288	0.01689	152.2578	1342.285	9190.42	0.001978	212.0632	145.5743
62	402	1665.131	91.90369	2.6E-05	0.001718	0.083812	0.001686	283.3127	3779.518	2309.021	0.003801	239.8018	65.80587
63	405	3058.039	68.75875	5.91E-07	0.001714	0.115719	0.00306	150.2294	2339.1	9893.702	0.00313	297.5797	68.91704
64	409	1579.461	147.5242	2.78E-05	0.000297	0.155966	0.004981	290.8086	2098.556	8909.836	0.004476	366.5433	65.12494
65	413	2489.805	89.67215	1.07E-05	0.000455	0.08555	0.017058	156.5266	7893.949	2448.623	0.002484	567.1736	138.1068
66	423	1653.911	122.814	3.23E-06	0.000253	0.048107	0.001719	154.4507	1462.583	1341.914	0.004904	321.0824	73.78381
67	440	1576.643	234.3355	1.89E-07	0.001305	0.022023	0.001329	188.0839	7473.542	5735.235	0.000143	218.6635	74.89896
68	460	1460.621	59.77512	1.07E-05	0.000153	0.070286	0.002516	241.3239	7978.858	6162.174	0.003797	450.269	99.16085
69	463	2630.454	79.84488	9.59E-08	9.55E-05	0.059084	0.004096	139.7335	5858.145	7108.899	0.003716	697.3908	177.6914
70	467	1959.301	146.7314	0.000815	0.002334	0.13205	0.004268	242.9046	7511.224	11717.87	0.000631	402.3112	130.9509
71	474	2210.38	274.8273	1.97E-07	0.000853	0.08339	0.026653	198.4911	1490.922	7339.264	0.004774	455.8405	87.28395
72	475	1654.87	90.24297	4.07E-05	0.002424	0.139799	0.006564	206.1216	1540.163	5641.511	0.00068	599.3458	178.4713
73	485	2006.689	212.0885	1.24E-05	0.000125	0.086841	0.003145	218.9783	4880.509	2438.258	0.002718	571.4348	113.8194
74	491	2599.597	127.1827	0.00027	0.007943	0.11616	0.001211	197.5089	2099.162	4513.882	0.000511	745.1146	73.37512
75	495	2996.752	172.3528	1.46E-06	0.000323	0.112828	0.028723	200.6346	1024.17	3010.174	0.002101	752.8628	57.58255
76	496	2508.485	203.5587	3.71E-06	9.93E-05	0.110923	0.001277	194.5183	5503.371	14224.22	0.000132	490.0734	176.7244
77	499	2132.185	65.40452	3.34E-06	0.000484	0.095588	0.003019	268.6681	4734.017	6381.4	0.004475	728.9757	160.0354

Table C-4– Sample Crushed Zone Design Characteristics

Crushed Zone Minor Axis Length	Crushed_Perm
419.7096	9.488204
380.9817	4.906837
456.2576	5.373469
188.5875	0.66494
465.8191	7.588374
544.7841	0.297503
447.2726	4.52429
523.6367	6.20356
227.4242	1.388977
398.3938	1.073029
640.6707	1.869771
237.9835	4.753738
652.367	0.265888
268.7695	6.493852
420.4079	2.349305
321.3732	3.445172
365.1662	0.123551
215.6702	1.474441
415.8656	8.173929
232.1541	0.279959
454.2352	9.565221
483.7506	0.160229
817.8438	0.129449
643.4296	0.283157
299.1224	0.113047
200.6905	2.633445
310.3916	0.289993
247.6645	0.548329
240.4038	8.536211
476.0158	0.304773
390.9839	3.142337
628.3549	0.110911
667.1741	9.506696
370.2252	1.038116
426.854	9.858823
159.5473	0.150034

249.8985	6.446185
493.0168	0.222304
363.3399	1.781185
326.2219	1.138113
344.5534	0.862542
171.8391	0.636629
630.559	8.331648
411.8514	4.23518
405.0044	1.590152
544.3006	0.140494
565.7243	2.756334
302.3173	0.143168
515.7398	2.471179
397.2031	8.544417
292.7782	0.38966
961.4845	2.587176
240.305	0.179259
228.1062	0.103427
601.9591	0.11034
194.4005	8.107466
380.2135	4.15797
541.9515	1.207979
342.1233	0.111243
506.7791	1.654112
489.2863	8.86958
379.0705	0.547266
398.3688	4.847895
287.6367	8.981666
274.1988	2.489079
381.0316	0.600532
343.1027	2.152508
313.4881	1.587179
480.5173	0.152311
330.974	7.960276
445.931	3.838382
727.8871	2.704554
887.9265	0.200762
327.1937	0.181502
255.8622	0.189166
346.4159	7.898967

395.5758	0.183309
234.481	8.409818
207.6922	5.003497
263.7098	3.33848
793.8912	0.17767
222.0106	3.269874
505.5375	0.640875
344.2877	2.660071
302.5214	6.595868
261.2903	1.027182
369.452	0.259721
171.7655	0.973134
380.6968	1.732838
617.3598	0.355967
168.3475	2.79786
405.489	7.864672
238.0892	4.808375
300.7514	4.305161
265.8342	0.26014
513.7111	2.466138
315.2791	2.871254
342.4891	0.622907
222.574	6.882082
188.5257	0.740407
310.5323	0.766205
735.4554	0.211975
346.7762	0.939588
371.3832	0.574139
725.0576	0.190873
530.6282	6.462058
535.7559	0.202833
611.0979	7.430285
453.3302	0.740444
312.3604	0.241933
625.4531	0.915027
893.1922	3.497607
338.6167	1.197121
359.2964	3.808107
577.6775	0.179193
656.0638	8.339433

281.824	0.800198
238.4502	0.258468
360.1336	4.675714
185.4362	0.128745
357.8872	4.723832
209.8477	0.278938
272.586	0.146606
767.5924	0.211202
281.5486	1.123605
679.8784	0.971278
506.5463	7.156871
262.5317	1.383993
288.7266	0.225892
648.9789	1.211201
188.7908	0.14503
460.3233	0.169881
263.2559	0.200941
523.9134	5.402725
346.3845	0.579142
331.1192	0.423681
681.9758	1.092014
169.3332	2.612963
181.1788	6.04908
424.9328	4.137999
1078.652	2.19356
815.2903	0.433655
238.6734	6.690846
963.9907	0.948091
615.1105	3.480205
599.294	0.527671
397.1329	5.367218
613.7268	2.21924
103.6395	0.034622
329.151	0.007652
335.9156	0.022056
530.247	0.018703
951.164	0.004803
639.228	0.020959
374.153	0.007904
510.636	0.047752

851.231	0.013117
99.7118	0.009927
168.961	0.013771
492.092	0.029716
125.826	0.023612
177.359	0.015819
312.856	0.011347
563.653	0.011064
346.921	0.000552
127.242	0.005043
695.627	0.044707
263.434	0.040270
156.138	0.007073
144.357	0.046120
252.151	0.018914
105.132	0.014172
532.463	0.007327
1034.3	0.013768
535.02	0.046591
356.174	0.006459
893.834	0.027401
559.624	0.010655
213.663	0.010983
128.144	0.018448
544.189	0.016105
158.79	0.006260
698.375	0.006195
249.089	0.009763
125.777	0.001562
459.056	0.017885
464.499	0.029188
387.088	0.013405
656.877	0.003610
338.016	0.040758
74.8236	0.016558
567.662	0.020334
402.727	0.003671
802.674	0.008835
625.443	0.009335
260.016	0.003652

316.599	0.004831
478.493	0.012034
312.196	0.019419
206.308	0.018012
153.431	0.033848
500.536	0.002289
227.742	0.046199
716.603	0.028017
390.092	0.011532
418.858	0.009801
1180.95	0.039702
779.395	0.005737
512.55	0.011366
489.507	0.004080
802.064	0.003408
207.305	0.004816
886.279	0.004272
225.333	0.007997
797.037	0.002114
808.178	0.048022
253.002	0.001672
318.261	0.007711
529.485	0.001296
286.418	0.001363
756.636	0.007819
968.933	0.004504
174.906	0.001912
226.218	0.025087
890.792	0.001408
541.824	0.048571
277.345	0.001938
61.2104	0.027916
249.008	0.046618
542.708	0.047330
865.578	0.042783
210.918	0.007565
976.11	0.006140
853.026	0.014593
255.406	0.002217
584.066	0.003162

944.098	0.016558
96.0563	0.018999
340.27	0.049260
358.158	0.014487
542.07	0.045279
235.484	0.003275
680.041	0.029389
388.63	0.019211
961.275	0.002119
578.253	0.024807
740.344	0.006272
420.801	0.006918
522.387	0.010284
515.269	0.004268
283.3499	0.138058
660.4529	0.154205
582.882	0.106316
520.6506	0.232692
756.3703	0.120623
295.0067	0.548674
421.6622	0.18565
428.0505	0.430258
620.1134	0.187441
274.0911	0.456495
616.0714	0.724579
345.3587	0.630116
1048.425	0.105471
173.3489	0.561758
935.0195	0.105095
430.6995	0.10683
510.5417	0.138602
344.3678	0.11884
267.7472	0.200535
273.5783	0.675152
724.5121	0.11908
551.9751	0.122683
408.1911	0.454162
320.3538	0.113033
240.1162	0.162765
224.8866	0.685257

402.3869	0.504079
265.1637	0.315134
716.5065	0.143798
522.2501	0.664187
367.0183	0.237585
805.6375	0.290831
267.992	0.100386
477.3052	0.167632
866.9018	0.111294
547.4755	0.189538
496.5867	0.693755
214.4609	0.32212
622.6445	0.322063
428.5438	0.345883
580.5519	0.135542
570.7006	0.404095
209.8418	0.377315
403.3952	0.472938
483.9938	0.313432
874.5059	0.25078
391.86	0.176317
529.0951	0.210765
651.3397	0.224006
291.2054	0.192014
292.0111	0.251746
410.3922	0.676367
379.8039	0.128121
189.4018	0.107348
746.3756	0.197484
357.2383	0.376149
790.389	0.113161
393.0792	0.135611
670.0976	0.102961
596.3696	0.101042
315.2756	0.173527
225.4097	0.644285
357.2698	0.603722
606.8064	0.22481
476.9685	0.265548
273.6957	0.309732

Table C-5– Sample Transverse Design Characteristics

Hydraulic Fracture Spacing	Frac Half Length	Hydraulic Frac Permeability
209.8548	567.6027	965.4364
125.1797	361.7726	1691.687
103.6949	471.0038	236.3375
123.9289	295.4575	406514.9
109.1764	360.2242	32166.74
145.9243	478.2708	5682.87
118.6993	546.4589	5628.275
119.0083	482.4208	28645.75
175.4415	349.3807	49119.92
152.7176	342.38	14078.2
147.8471	546.9543	143.0394
136.8405	253.449	3924.2751
127.0845	473.8017	2207.184
154.5425	403.5185	807994.3
107.4376	365.3125	121121
133.9055	307.0891	409905.7
136.9373	434.5576	41628.05
226.9426	348.1714	45.081749
244.4268	151.7865	6219.2469
157.888	349.733	48778.458
101.3004	404.4217	8004.4606
151.1721	365.091	4769.229
142.6237	620.616	635781.25
146.7617	579.5872	850935.02
234.637	338.2509	2524.2226
144.1423	279.0272	1246.125
137.3544	367.6579	6398.7575
132.6774	347.4492	2839.904
165.8786	341.9148	35.83861
178.5059	327.5915	733.9645
150.3784	548.4129	3754.507
112.2062	519.7374	28406.11
170.5001	608.3448	16621.24
142.3943	708.5873	34048.61
117.2286	310.6897	23213.512
172.311	347.6033	1433.547

156.1866	367.9942	11598.64
284.0944	459.4784	25202.846
129.1603	447.6713	289.40887
152.705	363.1524	1330.4582
137.389	349.752	625245.9
150.1447	224.7945	55092.283
100.1312	305.6276	818.53435
119.1427	370.8418	4107.863
250.2927	752.1342	75523.598
178.8416	444.5616	84396.4
188.659	683.5441	10551.624
173.7251	249.6179	2777.0588
107.8365	335.7357	1298.934
130.5096	293.101	12434.42
216.4222	497.5207	1894.9596
163.8894	682.7356	3037.248
161.1744	233.8906	19599.559
223.7069	363.3007	162.35819
148.423	631.0481	116161.25
106.2825	299.3526	36588.087
175.9845	356.4691	3481.91
121.9391	444.6701	484144.5
265.894	618.0345	26269.914
142.7255	389.675	89207.1
264.2096	743.6112	83281.624
118.4595	382.3253	35240.08
149.3883	429.1875	528928.3
165.3911	358.5001	1053.988
135.4782	372.8888	210.93985
175.2745	317.3735	108629.5
228.7743	518.8533	17543.536
138.3145	316.4815	29.9924
165.7785	536.78	101880.8
197.174	360.4321	671548.08
109.4558	392.8176	37644.5
194.3692	649.5241	8989.6458
112.3782	614.4156	9288.746
115.7762	422.8917	48488.72
182.7587	411.1212	488392
130.2027	269.246	72751.108

170.5244	352.0951	35019.523
277.6076	285.9343	4734.7909
123.0987	403.59	772401.5
101.0888	294.9071	1829.686
124.0455	616.5506	336675
138.802	473.2561	5107.334
228.9886	487.218	207696.84
134.732	383.0741	55344.934
160.6158	316.2279	79180.427
108.871	377.4316	833752.3
188.831	472.8007	5160.05
122.6896	281.5625	61399.25
158.6237	401.4773	60623.23
177.4909	646.2554	24723.04
120.2482	281.8139	1338.142
126.7153	376.2059	862336.7
148.8057	382.7208	1063.388
125.3131	346.0657	9432.428
166.1464	361.1055	34853.23
142.6975	476.4788	34333.5
108.7713	347.5585	1191.248
183.4763	408.8963	60155.08
191.9701	466.8829	13209.57
134.6613	300.9179	56027.94
142.8449	447.5254	2983.659
103.5641	601.0316	6680.671
123.8486	354.9977	2285.67
116.0573	371.4844	248524.8
164.7858	660.0041	2086.068
180.896	636.4862	2218.246
131.5037	426.2454	7117.753
191.6625	631.0784	25068.82
169.9988	516.3834	143518.7
140.5622	352.443	711459.4
104.2422	502.0145	568958.2
146.7387	714.9251	65896.39
112.8722	383.2658	3868.899
128.3201	300.8874	859679.6
157.5484	581.8607	84636.75
115.776	586.2098	1331.35

132.105	366.1592	893870.9
154.675	364.3304	6604.511
166.6904	430.8938	4118.613
132.4544	310.9974	4404.767
109.7521	394.555	66548.44
160.8832	349.2896	20096.97
194.7043	424.585	1744.624
141.3068	525.6108	254263.3
150.8296	370.2619	59490.56
152.9726	554.2026	392228.3
106.5721	412.6686	682244.7
150.9557	374.6456	108311
154.675	364.3304	6604.511
124.3876	558.3186	117664.2
186.0938	406.5362	6702.826
96.24942	410.4601	4064.836
164.5349	376.9903	354299.3
129.1072	422.8571	526655.1
200.4082	459.1391	649888.9
190.3936	466.7509	3162.185
141.6411	537.7628	18443.54
169.3332	333.5803	1641.499
119.0604	321.8534	124828.3
144.8635	471.7552	121102.4
194.1574	789.8258	76165.55
107.1524	652.9058	3230.664
184.1195	375.669	1298.911
129.1059	686.5719	30264.99
102.5184	545.159	4278.389
179.7882	622.0526	4595.86
182.6811	579.8104	2418.059
118.0244	483.6388	1124.846
234.23	242.99	25058.58
287.30	172.58	99062.61
157.80	136.84	24.42
110.03	584.13	12.92
175.42	557.25	44.43
267.70	412.41	93456.73
214.92	281.71	436.40
172.33	371.02	12.76

275.51	631.71	596.07
281.50	115.57	6064.58
278.55	478.19	23.56
107.78	218.94	148.94
214.66	186.85	7249.90
276.73	198.63	996.71
120.64	211.51	28.31
203.08	358.91	50.56
183.09	107.63	421.72
193.67	128.16	455.22
244.75	507.51	15.22
266.57	269.04	798126.47
268.59	303.77	149470.44
169.69	153.68	42062.74
241.13	255.91	1242.98
201.05	172.38	236.36
283.26	410.50	1028.21
162.95	628.38	38.32
225.52	362.85	8624.83
165.95	245.71	6099.22
193.18	448.69	121.81
104.48	253.08	3250.71
226.77	207.93	12295.79
225.29	156.51	46378.22
161.65	359.93	303697.24
126.01	135.63	38.55
262.86	428.02	25.89
166.60	190.60	478217.21
144.88	115.42	12.34
217.21	363.87	1226.39
226.68	282.37	479.66
258.10	264.72	245.48
181.97	571.33	10.19
293.80	305.67	180546.26
208.31	121.40	1709.03
143.41	305.44	2364.87
172.09	250.97	183592.05
128.61	403.20	210.22
171.62	343.82	43919.66
110.57	113.70	453.97

108.87	118.71	16.28
125.51	297.77	88.47
194.54	273.83	229.09
286.39	293.74	5399.89
175.41	307.13	25.23
253.53	130.75	6011.31
241.18	351.59	9347.63
242.33	302.71	9196.93
125.68	201.48	27507.23
291.52	294.64	41818.82
238.05	393.18	38047.56
155.18	354.44	41737.52
289.59	380.44	230324.47
128.53	170.86	18.18
271.72	476.07	96.81
177.86	144.18	7601.25
217.14	432.33	6036.98
152.20	210.27	27.52
140.08	120.67	38.67
136.68	209.19	434.47
182.55	122.82	19.75
175.37	226.67	2052.13
106.71	128.50	3842.74
235.70	240.26	18.70
202.10	474.69	86.04
231.75	503.84	235002.46
258.25	244.59	1387.54
265.51	155.44	65904.85
281.67	499.17	50.61
278.37	270.97	1850.68
118.38	171.50	114.87
101.96	140.10	10.44
171.92	167.75	321705.76
245.50	395.31	599.66
289.42	327.28	26465.24
165.04	175.48	27387.50
116.40	478.52	25.59
163.63	380.46	138076.35
299.53	294.37	39619.79
142.82	204.24	13.99

206.25	561.42	71.31
190.39	159.95	2175.65
254.19	338.89	990148.43
140.57	122.89	10540.37
254.15	455.01	1843.05
226.45	112.31	83.44
234.08	382.90	2439.38
291.44	380.31	22.64
299.82	371.78	113622.96
205.31	291.16	477.72
151.05	501.33	10.60
190.97	205.45	8319.82
173.45	316.27	54.85
224.35	610.98	11.96
2.02E+02	4.30E+02	4.71E+05
1.98E+02	4.70E+02	4.67E+03
2.50E+02	3.83E+02	6.09E+04
2.44E+02	5.51E+02	5.69E+03
1.42E+02	4.85E+02	1.88E+03
1.84E+02	3.88E+02	1.12E+05
2.34E+02	7.44E+02	1.17E+02
2.29E+02	4.76E+02	9.23E+05
3.10E+02	2.28E+02	3.65E+05
2.06E+02	3.12E+02	1.86E+04
1.16E+02	3.89E+02	1.11E+05
1.44E+02	2.82E+02	1.32E+04
2.50E+02	7.35E+02	4.71E+03
1.73E+02	2.84E+02	1.11E+04
1.43E+02	7.57E+02	2.61E+03
2.58E+02	4.49E+02	1.20E+04
1.56E+02	3.88E+02	1.93E+05
1.29E+02	3.58E+02	4.89E+03
2.68E+02	3.37E+02	1.62E+05
2.74E+02	2.66E+02	1.45E+04
2.17E+02	3.47E+02	1.89E+05
2.37E+02	4.72E+02	4.77E+05
2.04E+02	3.52E+02	1.27E+03
1.92E+02	3.04E+02	1.59E+02
3.00E+02	2.10E+02	2.08E+05
1.25E+02	2.06E+02	4.44E+04

1.26E+02	3.96E+02	2.66E+04
1.99E+02	3.12E+02	5.42E+03
2.15E+02	5.53E+02	8.91E+03
2.18E+02	4.72E+02	3.03E+02
2.75E+02	3.52E+02	4.29E+04
1.15E+02	3.18E+02	4.71E+04
2.01E+02	2.69E+02	3.31E+04
2.39E+02	5.51E+02	3.45E+05
1.67E+02	4.90E+02	8.01E+03
2.35E+02	3.63E+02	1.66E+02
1.06E+02	3.52E+02	1.72E+05
1.79E+02	2.16E+02	3.67E+02
1.95E+02	3.79E+02	8.87E+03
2.68E+02	5.18E+02	6.57E+03
1.38E+02	3.20E+02	2.46E+05
2.38E+02	4.66E+02	2.18E+02
1.50E+02	2.89E+02	3.40E+03
1.12E+02	4.15E+02	8.35E+03
1.10E+02	4.26E+02	1.44E+02
1.17E+02	4.82E+02	8.15E+05
1.31E+02	3.80E+02	3.95E+02
1.06E+02	3.68E+02	5.02E+05
1.63E+02	5.53E+02	1.77E+03
2.08E+02	4.30E+02	6.33E+05
2.43E+02	3.36E+02	2.02E+03
1.71E+02	3.32E+02	1.43E+03
1.19E+02	3.48E+02	5.37E+03
1.58E+02	3.02E+02	1.41E+02
1.33E+02	4.42E+02	1.06E+03
1.67E+02	2.27E+02	2.00E+03
1.65E+02	6.04E+02	3.24E+04
1.64E+02	3.35E+02	7.91E+05
1.79E+02	3.28E+02	2.04E+03
1.28E+02	4.66E+02	6.50E+05
1.21E+02	3.64E+02	1.11E+04
2.11E+02	2.49E+02	1.15E+05
2.23E+02	2.48E+02	2.15E+03
2.17E+02	4.06E+02	2.63E+03
1.32E+02	3.09E+02	1.38E+05
1.47E+02	2.18E+02	8.01E+02

1.08E+02	2.12E+02	6.00E+03

Table C-6– Sample Error Filter Data Set

	edge_l	h	k_m	k_f	phi_m	phi_f	Ti	Pi	Depth	C	Lang_P	Lang_V	Psf	Fracture_S	HF_s	xf	k_HF	cz_minor_length	crushed perm
1	2046.817	98.29291	2.93E-05	0.00052	0.114464	0.009766	205.2783	7596.821	11290.97	0.000444	222.3542	154.3478	3651.416	31.14518	175.4415	349.3807	4.691258	227.4242	1.388977
2	1527.176	72.58816	0.000705	0.001384	0.122411	0.00382	261.7151	2642.882	6424.412	0.004951	483.1452	194.3428	1053.055	2.930572	152.7176	342.38	4.148547	398.3938	1.073029
3	1368.405	86.42597	1.58E-06	0.008896	0.147753	0.002942	290.8583	1953.941	6231.825	0.000342	746.3219	135.8446	159.3332	12.10116	136.8405	253.449	3.593759	237.9835	4.753738
4	2329.882	64.1938	7.37E-05	0.000838	0.085092	0.02331	220.3485	1235.007	6916.226	0.003977	207.8665	156.3634	138.7515	17.34689	127.0845	473.8017	3.343839	652.367	0.265888
5	2089.387	168.4968	3.26E-07	0.00521	0.15712	0.008166	138.3288	2199.704	11445.29	0.0113	449.3793	181.865	953.2287	35.47576	157.888	349.733	4.688228	232.1541	0.279959
6	3027.832	122.5786	7.01E-06	0.001162	0.147746	0.001583	245.8621	4756.341	7628.9	0.001795	494.9017	174.5569	1584.517	6.371145	129.1603	447.6713	2.461512	363.3399	1.781185
7	2053.153	202.6239	0.000252	0.001764	0.062457	0.004944	255.7769	6222.281	14769.8	0.004326	446.304	101.0621	2100.676	13.76899	175.9845	356.4691	3.541818	380.2135	4.15797
8	1460.621	59.77512	1.07E-05	0.000153	0.070286	0.002516	241.3239	7978.858	6162.174	0.003797	450.269	99.16085	340.0822	5.260094	175.2745	317.3735	5.035948	381.0316	0.600532
9	1987.085	185.8896	0.000209	0.000578	0.078279	0.002498	210.2353	7054.606	4383.247	0.004559	334.3523	72.84709	699.5313	15.16333	154.675	364.3304	3.819841	238.4502	0.258468
10	1608.832	239.2641	0.000334	0.009038	0.063333	0.003523	224.5535	2386.766	8153.592	0.003211	251.6678	82.0332	840.9298	36.31829	160.8832	349.2896	4.303131	209.8477	0.278938
11	3423.358	287.64	0.000356	0.000781	0.03238	0.01602	257.03	7048.43	4646	7.72E-06	633.21	136.80	3511.57	4.63	266.57	269.04	5.902072	263.43	0.040270
12	3435.615	54.81	5.94E-05	0.026882	0.08095	0.02451	174.97	5807.23	2956	7.49E-06	491.52	63.81	2829.81	14.30	278.37	270.97	3.267331	541.82	0.048571
13	2361.249	149.01	3.99E-06	0.000723	0.114681	0.002736	208.4519	4583.23	11195.02	0.001148	596.939	155.3986	1068.184	33.20701	202	430	5.673021	283.3499	0.138058
14	1713.069	52.04458	1.31E-06	0.000131	0.067017	0.001592	178.2994	1448.412	8870.312	0.004888	266.4786	129.8536	592.4676	23.12122	206	312	4.269513	274.0911	0.456495
15	1959.3	76.94225	3.93E-06	0.004288	0.151199	0.023085	210.0298	1661.42	13838.79	0.004378	538.9977	85.41938	109.4505	16.29637	131	380	2.596597	391.86	0.176317
16	2232.937	54.89441	8.92E-06	0.002892	0.140942	0.006619	272.9847	3081.48	3453.352	0.000254	322.1024	58.37725	1296.731	3.934756	223	248	3.332438	357.2698	0.603722